

Hydroxynitrile Lyases, Immobilisation and Flow Chemistry

Coloma Hurel, J.L.

DOI

[10.4233/uuid:bca1b67e-8e9b-4f48-b21a-8b3136f1d4dc](https://doi.org/10.4233/uuid:bca1b67e-8e9b-4f48-b21a-8b3136f1d4dc)

Publication date

2022

Document Version

Final published version

Citation (APA)

Coloma Hurel, J. L. (2022). *Hydroxynitrile Lyases, Immobilisation and Flow Chemistry*. [Dissertation (TU Delft), Delft University of Technology]. <https://doi.org/10.4233/uuid:bca1b67e-8e9b-4f48-b21a-8b3136f1d4dc>

Important note

To cite this publication, please use the final published version (if applicable). Please check the document version above.

Copyright

Other than for strictly personal use, it is not permitted to download, forward or distribute the text or part of it, without the consent of the author(s) and/or copyright holder(s), unless the work is under an open content license such as Creative Commons.

Takedown policy

Please contact us and provide details if you believe this document breaches copyrights. We will remove access to the work immediately and investigate your claim.

Hydroxynitrile Lyases, Immobilisation and Flow Chemistry

Dissertation

for the purpose of obtaining the degree of doctor

at Delft University of Technology

by the authority of the Rector Magnificus, prof.dr.ir. T.H.J.J. van der Hagen

chair of the Board for Doctorates

to be defended publicly on

friday 24 June 2022 at 10:00 o'clock

by

José COLOMA HUREL

Master of Food Science, Universidad Agraria del Ecuador, Ecuador

born in Guayaquil, Ecuador

This dissertation has been approved by the promotor.

Composition of the doctoral committee:

Rector Magnificus,	chairperson
Prof.dr. U. Hanefeld	Delft University of Technology, promotor
Dr.ir. P.L. Hagedoorn	Delft University of Technology, copromotor

Independent members:

Prof.dr.ir. J.G. Daran	Delft University of Technology
Prof.dr. S. Kara	Leibniz University Hannover
Prof.dr. I.W.C.E. Arends	Utrecht University
Prof.dr. F.P.J.T. Rutjes	Radboud Universiteit
Prof.dr. A. Urakawa	Delft University of Technology, reserve member

Other members:

Dr. Y.P. Guiavarc'h	University of Lorraine
---------------------	------------------------



Funding: This work was financed by the Secretary of Higher Education, Science and Technology of Ecuador (Senescyt).

Keywords: Hydroxynitrile lyases, *Granulicella tundricola*, *Arabidopsis thaliana*, cyanohydrins, styrenes, oxidative cleavage, nitroaldol, immobilisation, Celite

Printed by: Gildeprint, Enschede

Cover by: Karina Rosas / Claudia Latorre

ISBN/EAN: 978-94-6366-560-5

All rights reserved. No parts of this publication may be reproduced, stored in a retrieval system, or transmitted, in any form or by any means, electronic, mechanical, photo-copying, recording, or otherwise, without the prior written permission of the author.

To my wife and sons

Table of Contents

1.	Summary / Samenvatting	1
<hr/>		
2.	Immobilisation and flow chemistry: tools for implementing biocatalysis	9
<hr/>		
2.1	Introduction	10
2.2	Challenges for biotransformations in flow with immobilised enzymes	10
2.3	Metrics	11
2.3.1	Immobilisation metrics	12
2.3.1.1	Enzyme surface hydrophilicity/hydrophobicity	12
2.3.1.2	Ratio enzyme:carrier (mol g ⁻¹ or U g ⁻¹)	12
2.3.1.3	Leaching assay	12
2.3.1.4	Ratio of lysine concentration to carrier functionalities (mol mol ⁻¹)	13
2.3.1.5	Ratio of carrier pore size to enzyme diameter	13
2.3.2	Economic metrics	13
2.3.2.1	Space-time-yield (STY)	13
2.3.2.2	Specific rate (SR)	14
2.3.2.3	Biocatalyst productivity	14
2.4	Reaction medium	14
2.4.1	Biotransformations in organic solvents as reaction medium	16
2.4.2	Biotransformations in biphasic systems as reaction medium	25
2.4.3	Biotransformations in aqueous systems as reaction medium	28
2.5	Addressing the cofactor hurdle	32
2.5.1	Cofactors that are fully regenerated during the catalytic cycle	32
2.5.2	Cofactors that require recycling systems	34
2.6	Conclusions	39
	References	39
<hr/>		

3.	Probing batch and continuous flow reactions in organic solvents: <i>Granulicella tundricola</i> hydroxynitrile lyase (GtHNL)	45
<hr/>		
3.1	Introduction	46
3.2	Results and Discussion	47
3.2.1	Batch reactions	48
3.2.2	Continuous flow reactions	54
3.2.3	Comparison of the reactors	56
3.3	Conclusions	57
3.4	Experimental section	58
	References	63
	Supplementary information	66
4.	Immobilisation of <i>Arabidopsis thaliana</i> hydroxynitrile lyase (AtHNL) on EziG Opal	75
<hr/>		
4.1	Introduction	76
4.2	Results and Discussion	78
4.2.1	Batch reactions	78
4.2.2	Continuous flow reactions	83
4.2.3	Comparison between batch and continuous flow systems	85
4.3	Conclusion	86
4.4	Experimental section	87
	References	91
	Supplementary information	96
5.	Batch and flow nitroaldol synthesis catalysed by <i>Granulicella tundricola</i> hydroxynitrile lyase	99
<hr/>		
5.1	Introduction	100
5.2	Results and Discussion	101
5.2.1	Batch reactions	101
5.2.2	Continuous flow reactions	106
5.2.3	Comparison between batch and continuous flow systems	107
5.3	Experimental section	108

	References	113
	Supplementary information	119
6.	Oxidative cleavage of styrenes: Expanding the potential of <i>Granulicella tundricola</i> hydroxynitrile lyase (GtHNL)	121
6.1	Introduction	122
6.2	Results and Discussion	123
6.2.1	Time course reactions	123
6.2.2	Reaction optimisation	126
6.2.3	Substrate scope	128
6.2.4	Reaction mechanism	130
6.3	Conclusions	133
6.4	Experimental section	134
	References	137
	Supplementary information	142
7.	Conclusion and Outlook	143
8.	Acknowledgements	147
9.	<i>Curriculum vitae</i> and list of publications	151

1

Summary

The utilisation of flow chemistry and immobilisation in biocatalysis is gaining attention as an attractive way to overcome some of the limitations commonly reported in traditional batch systems such as mass transfer restrictions, low productivities, substrate/product inhibition and safety, among others. In **chapter 2**, the application of immobilisation and flow chemistry as important tools for the development of biocatalysis are reviewed. Important metrics related to enzyme immobilisation and flow chemistry are discussed. Enzyme immobilisation allows the utilisation of flow chemistry and buffer-saturated organic solvents as reaction medium as a viable alternative to overcome the mass transfer limitation of aqueous systems. On top of this, high substrate loading and straightforward enzyme reuse are possible. Likewise, flow chemistry improves mass transfer, safety and allows process intensification. All these advantages are only possible if the enzyme is efficiently immobilised on a suitable carrier.

Hydroxynitrile lyases are versatile enzymes that catalyse the stereoselective addition of hydrogen cyanide to prochiral aldehydes or ketones for the synthesis of chiral cyanohydrins, which are important platform molecules for the chemical, food and pharmaceutical industries. *Granulicella tundricola* hydroxynitrile lyase (GtHNL) is a manganese dependent cupin that catalyses the selective synthesis of (*R*)-cyanohydrins. In **chapter 3**, GtHNL-A40H/V42T/Q110H (GtHNL-3V) was immobilised on Celite R-633 and used in a flow-reactor for the continuous synthesis of (*R*)-mandelonitrile. This variant is more active and stable compared to the wild type enzyme. The continuous process was compared to a batch process in a rotating bed reactor in terms of conversion, stability and productivity. Methyl-*tert*-butyl ether (MTBE) saturated with 100 mM sodium acetate buffer pH 4 was used as reaction medium to ensure high enantioselectivity by suppressing the racemic chemical background reaction. Good conversion, excellent enantioselectivity and high stability were observed in both systems. However, the continuous flow approach facilitated greater process intensification compared to the rotating bed reactor. In addition, the much smaller volume of the continuous flow system improved the safety of the process.

The immobilisation of his-tagged enzymes using Ni²⁺ (or other divalent metal ions) on nitrilotriacetic acid (Ni-NTA) has been widely reported. However, the nickel induced genotoxicity, carcinogenicity and immunotoxicity still needs to be addressed.

Therefore, the development and use of carriers bearing non-toxic metal ions is desirable. **Chapter 4** deals with the immobilisation of the acid-sensitive hydroxynitrile lyase from *Arabidopsis thaliana* (*A*tHNL) on EziG Opal for the synthesis of (*R*)-mandelonitrile. This material is made of controlled porosity glass particles and contains non-toxic Fe³⁺ for the immobilisation of his-tagged enzymes. MTBE saturated with 100 mM citrate/phosphate buffer pH 5 was used as reaction medium to suppress the chemical racemic background reaction. The system was evaluated in batch and continuous flow. The batch system showed good conversion, excellent enantioselectivity and high stability (8 cycles). The continuous flow system achieved good conversion and excellent enantioselectivity at low flow rate (0.1 mL min⁻¹). Higher flow rates resulted in lower conversion and enantioselectivity due to the chemical racemic background reaction catalysed by the EziG Opal carrier material. In terms of productivity, the flow system reached a STY (mol_{product} h⁻¹ L⁻¹ g_{enzyme}⁻¹) 3.7 times higher than the batch approach showing that the flow system greatly enhanced productivity.

After the successful immobilisation of *G*tHNL-3V on Celite R-633 for the continuous synthesis of (*R*)-mandelonitrile, **Chapter 5** deals with the promiscuous activity of *G*tHNL-3V for the synthesis of chiral β-nitro alcohols using nitromethane instead of cyanide as nucleophile. *G*tHNL-3V was immobilised on Celite R-633 and evaluated in batch and flow systems for the synthesis of (*R*)-2-nitro-1-phenylethanol (NPE). MTBE saturated with 100 mM KPi buffer pH 7 was used as reaction medium to ensure optimal enzymatic activity. Good yield and excellent enantioselectivity were achieved in batch after 24 hours of reaction time. Celite-*G*tHNL-3V could be successfully recycled 5 times. By switching to a continuous flow system, 15% yield of (*R*)-NPE was achieved using a flow rate of 0.1 mL min⁻¹. The system was not stable and the yield decreased to 4% after 4 hours of reaction time. Lower flow rate (0.01 mL min⁻¹) did not improve the yield of (*R*)-NPE but allowed the continuous synthesis of (*R*)-NPE during 15 hours. Surprisingly, the batch system displayed 5 and 37 times higher STY compared to both flow rates evaluated. This can be explained by the change in polarity of the reaction medium due to the high concentration (1 M) and high polarity (log *P* = -0.27) of nitromethane. The change in polarity of the reaction mixture might not allow to maintain a constant water activity close to the surface on Celite-*G*tHNL-3V, which is required for optimal enzyme activity.

Enzyme engineering is a fascinating tool to expand the potential of biocatalysis by switching or adding enzyme activities. Remarkably, the rational design in **Chapter 6** allowed to add a peroxidase-like activity in *Granulicella tundricola* HNL using *tert*-butyl hydroperoxide (TBHP) as oxidant. The single mutations H96A and H96F were introduced in *Gt*HNL wild type and the mutation H96A was introduced in *Gt*HNL-3V. This allowed the oxidative cleavage of several styrene derivatives. The best results were obtained using α -methyl styrene as substrate and *Gt*HNL-H96A as catalyst. 41% yield of acetophenone was achieved after 24 hours of reaction time. *Gt*HNL is a Mn^{2+} dependent enzyme. The reaction mechanism was explored by electron paramagnetic resonance (EPR) studies. The expected (based on previous reports) Mn^{3+} ($S = 2$) was not detected but a higher oxidation state (Mn^{4+}) ($S = 3/2$) is possible. The addition of butyl hydroxyl toluene (BHT) as radical scavenger suppressed the reaction. This suggests a radical mechanism for the *Gt*HNL-H96A catalysed oxidative cleavage of styrene derivatives.

Samenvatting

Het gebruik van flowchemie en immobilisatie in biokatalyse begint meer aandacht te krijgen als een aantrekkelijke methode om een aantal veel gerapporteerde beperkingen van traditionele batch systemen te verhelpen. Deze beperkingen zijn onder andere de massaoverdracht limitatie, lage productiviteit en substraat/product inhibitie en veiligheid. In **hoofdstuk 2** wordt de toepassing behandeld van immobilisatie en flowchemie als belangrijke tools voor de toekomstige ontwikkeling van biokatalyse. Belangrijke parameters die gerelateerd zijn aan enzym immobilisatie en flowchemie worden behandeld. Enzym immobilisatie maakt het mogelijk om flowchemie en buffer-verzadigde organische oplosmiddelen als reactiemedium in te zetten als realistisch alternatief om de limitatie in massaoverdracht van waterige systemen te omzeilen. Bovendien is het ook mogelijk om hoge substraat concentraties te gebruiken, en is het eenvoudig om de enzymen te hergebruiken. Eveneens verbeterd flowchemie massaoverdracht en veiligheid, en staat het toe het proces te intensiveren. Al deze voordelen zijn alleen van toepassing als het enzym efficiënt is geïmmobiliseerd op een geschikte drager.

Hydroxynitril lyases zijn veelzijdige enzymen die de stereoselectieve additie van waterstofcyanide aan prochirale aldehyden of ketonen katalyseert ten behoeve van de synthese van chirale cyaanhydrines. Dit zijn belangrijke platformmoleculen voor de chemische, farmaceutische en voedselindustrieën. *Granulicella tundricola* hydroxynitril lyase (*GtHNL*) is een manganafhankelijke cupin die de selectieve synthese van (*R*)-cyaanhydrines katalyseert. In **hoofdstuk 3** wordt *GtHNL*-A40H/V42T/Q110H (*GtHNL*-3V) geïmmobiliseerd op Celite R-633 en gebruikt in een flowreactor voor een continue synthese van (*R*)-mandelonitril. Deze variant is actiever en stabiel in vergelijking met het wildtype enzym. Het continue proces is vergeleken met een batch proces in een roterend bed reactor op gebied van conversie, stabiliteit en productiviteit. Methyl-*tert*-butylether (MTBE), verzadigd met 100 mM natriumacetaat buffer pH 4, is gebruikt als het reactiemedium om hoge enantioselectiviteit te garanderen door middel van het onderdrukken van de racemische, chemische achtergrondreactie. In beide systemen zijn goede conversie, excellente enantioselectiviteit, en hoge stabiliteit waargenomen. De continue flow aanpak faciliteerde echter een betere procesintensificatie ten opzichte van de roterend

bed reactor. Daarnaast verbeterde het continue flow systeem de veiligheid van het proces vanwege het kleinere reactorvolume.

Immobilisatie van enzymen met een his-tag met behulp van Ni²⁺ (of andere divalente metaalionen) op nitriloazijnzuur (Ni-NTA) wordt veel toegepast. De door nikkel veroorzaakte genotoxiciteit, carcinogeniteit en immunotoxiciteit moet echter nog wel verholpen worden. Om deze reden is het ontwikkelen en gebruik van dragers met non-toxische metaalionen wenselijk. **Hoofdstuk 4** gaat over het immobiliseren van de zuur-gevoelige hydroxynitril lyase van *Arabidopsis thaliana* (AtHNL) op EziG Opal en te gebruiken voor de synthese van (*R*)-mandelonitril. Dit materiaal is gemaakt van glasdeeltjes met een gecontroleerde porositeit en bevat non-toxische Fe³⁺, bedoeld voor de immobilisatie van enzymen met een his-tag. MTBE, verzadigd met 100 mM citraat/fosfaatbuffer pH 5, is gebruikt als reactiemedium om de racemische chemische achtergrondreactie te onderdrukken. De methode is geëvalueerd in een batchsysteem en continue flow. Het batchsysteem vertoonde goede conversie, excellente enantioselectiviteit en hoge stability (8 cycli). Het continue flow systeem behaalde goede conversie en excellente enantioselectiviteit bij lage stroomsnelheden (0,1 mL min⁻¹). Hogere stroomsnelheden resulteerden in lagere conversie en enantioselectiviteit als gevolg van de racemische achtergrondreactie die gekatalyseerd wordt door het EziG Opal dragermateriaal. Op het gebied van productiviteit behaalde het flowsysteem een ruimte-tijd-opbrengst STY (mol_{product} h⁻¹ L⁻¹ g_{enzym}⁻¹) die 3,7 maal zo hoog was in het batchsysteem, wat laat zien dat het flowsysteem de productiviteit sterk verbetert.

Na de succesvolle immobilisatie van GtHNL-3V op Celite R-633 ten behoeve van de continue synthese van (*R*)-mandelonitril, behandelt **hoofdstuk 5** de promiscue activiteit van GtHNL-3V voor de synthese van chirale β-nitroalcoholen, gebruik makende van nitromethaan in plaats van cyanide als nucleofiel. GtHNL-3V is geïmmobiliseerd op Celite R-633 en vergeleken op gebied van synthese van (*R*)-2-nitro-1-fenylethanol (NPE) in een batch- en een flowsysteem. MTBE verzadigd met 100 mM KPi buffer pH 7 is gebruikt als reactiemedium om optimale enzymatische activiteit te garanderen. In het batchsysteem is een goede opbrengst en uitstekende enantioselectiviteit behaald na een reactietijd van 24 uur. Celite-GtHNL-3V kon 5 maal succesvol worden hergebruikt. Een opbrengst van 15% (*R*)-NPE is behaald met behulp van het overschakelen naar een continue flowsysteem met een stroomsnelheid

van 0,1 mL min⁻¹. Het systeem was niet stabiel en de opbrengst daalde naar 4% na een reactietijd van 4 uur. Een lagere stroomsnelheid (0,01 mL min⁻¹) verbeterde de (*R*)-NPE opbrengst niet, maar maakte het wel mogelijk om gedurende 15 uur continue (*R*)-NPE te synthetiseren. Verrassend genoeg, vertoonde het batchsysteem een STY van 5 en 37 maal zo hoog vergeleken met de twee stroomsnelheden van het continue systeem. Dit kan verklaard worden aan de hand van de verandering van de polariteit van het reactiemedium als gevolg van de hoge concentratie (1M) en hoge polariteit ($\log P = -0,27$) van nitromethaan. De verandering in polariteit van het reactiemengsel bemoeilijkt wellicht het in stand houden van een constante wateractiviteit dicht op het oppervlak van Celite-GtHNL-3V, wat benodigd is voor optimale enzymactiviteit.

Enzym engineering is een fascinerend gereedschap om de mogelijkheden van biokatalyse uit te breiden via het veranderen of toevoegen van enzymactiviteiten. Opmerkelijk genoeg maakte het rationeel ontwerp in **Hoofdstuk 6** het mogelijk om, met behulp van *tert*-butylhydroperoxide (TBHP) als oxidant, een peroxidase-achtige activiteit toe te voegen aan *Granulicella tundricola* HNL. De mutaties H96A en H96F zijn geïntroduceerd in het wildtype GtHNL en de mutatie H96A is geïntroduceerd in GtHNL-3V. Dit maakte de oxidatieve splitsing mogelijk van een aantal styreen derivaten. De beste resultaten zijn behaald met α -methylstyreen als substraat en GtHNL-H96A als katalysator. Een opbrengst van 41% acetofenon is bereikt na een reactietijd van 24 uur. GtHNL is een enzym dat afhankelijk is van Mn²⁺. Het reactiemechanisme is onderzocht via elektron paramagnetische resonantie spectroscopie (EPR). De verwachte Mn³⁺ (S = 2) (gebaseerd op eerdere bevindingen) was niet gedetecteerd maar een hogere oxidatietoestand (Mn⁴⁺) (S = 3/2) is mogelijk. De toevoeging van butylhydroxytolueen (BHT) als radicaalvanger onderdrukte de reactie. Dit suggereert een radicaal mechanisme voor de door GtHNL-H96A gekatalyseerde oxidatieve splitsing van styreen derivaten.

2

Immobilisation and flow chemistry: tools for implementing biocatalysis

The merger of enzyme immobilisation and flow chemistry has attracted the attention of the scientific community during recent years. Immobilisation enhances enzyme stability and enables recycling, flow chemistry allows process intensification. Their combination is desirable for the development of more efficient and environmentally friendly biocatalytic processes. In this feature article, we aim to point out important metrics for successful enzyme immobilisation and for reporting flow biocatalytic processes.

Relevant examples of immobilised enzymes used in flow systems in organic, biphasic and aqueous systems are discussed. Finally, we describe recent developments to address the cofactor recycling hurdle.

This chapter is based on

José Coloma, Yann Guiavarc'h, Peter-Leon Hagedoorn and Ulf Hanefeld

Chem. Commun., **2021**, 57, 11416–11428. DOI: 10.1039/d1cc04315c

2.1 Introduction

Most of the active pharmaceutical ingredients (API), natural products and fine chemicals are synthesised using (bio)chemical catalysts in large batch reactors. In recent years the utilisation of enzymes has facilitated the design of more environmentally friendly batch processes that fulfil 10 out of the 12 green chemistry principles.^{1,2} However, mass transfer limitation, the generation of significant amounts of waste and handling of large volumes of toxic reagents are still problems that have to be overcome. Flow chemistry solves most of these challenges. In a continuous reactor the substrates are pumped through the reactor and the product is collected continuously. This set up improves mass transfer thus increasing reaction rates and reducing reaction time. The reduced reactor volume in flow transformations minimizes energy requirements for heating and cooling (green chemistry – principle 6) and it is also of great benefit to the reduction of waste (green chemistry – principle 1).³⁻⁶ Indeed, there is an increasing interest in microreactor technology for the synthesis of high added-value products and for the development of high throughput methods at industrial scale and in academic research.⁷ In addition, the reduction in volume in continuous flow processes increases safety by avoiding handling of and thus potential exposure to large volumes of toxic compounds.^{8,9}

Soluble enzymes can be used for biotransformations in flow but reusability is difficult and the downstream processing needs to include a step for enzyme removal and its possible recycling. Immobilisation of enzymes allows straightforward reuse of the catalyst as it remains in the reactor. Moreover, in many cases increased operational stability is observed. This is an important contributor to the further development of flow chemistry.

With this feature article we aim to highlight important parameters to consider for a successful application of immobilised enzymes and for reporting continuous flow reactions. The latest applications in different reaction media will be discussed. In this context special attention will be paid to cofactors and their recycling in flow.

2.2 Challenges for biotransformations in flow with immobilised enzymes

Two main challenges have to be addressed in order to perform a successful biotransformation in flow: (i) immobilisation of the enzyme for recycling and straightforward downstream processing and (ii) suppressing the leaching of the

enzyme and/or cofactor (if applicable) into the reaction medium during operation. Overall, an enzyme can be immobilised by adsorption/deposition, ionic binding, covalent attachment to solid carrier materials, chemical cross linking or encapsulation. All of these methods have advantages and disadvantages that have to be evaluated case by case.¹⁰⁻¹⁵

As mentioned above, enzyme and/or cofactor leaching are essential aspects that need to be addressed in flow systems. Enzymes themselves or organic cofactors that remain within the enzyme active site and are fully regenerated during the catalytic cycle such as pyridoxal 5'-phosphate (PLP) or thiamin diphosphate pose a relatively small problem. Conversely, organic cofactors that are transiently fixed to the enzyme (*i.e.* nicotinamide cofactors) need to be regenerated to their given oxidative state before re-entering the enzyme. Thus, the development of an efficient cofactor regeneration system that gives freedom to the cofactor to leave the active site without losing it from the reactor is essential to allow the economic feasibility of the process for industrial applications. Also, the system must be flexible, allowing the implementation of reactions in cascade with a rapid exchange of substrates and avoiding chemical modifications of the cofactor.¹⁶ Here we do not discuss metal containing enzymes among the cofactor containing enzymes. All the aspects discussed for organic cofactors (and metal containing organic cofactors) equally apply to these enzymes. In this feature for instance *Granulicella tundricola* hydroxynitrile lyase (GtHNL) is a Mn²⁺ cofactor containing enzyme.

A number of successful cofactor recycling systems in flow have been reported, for instance by immobilising onto different carriers.¹⁷⁻²² The performance of immobilised enzymes and the different cofactor regeneration systems in flow will be discussed for organic, biphasic and aqueous conditions.

2.3 Metrics

In a recent review, key developments of continuous flow biocatalysis from 2018 to September 2020 were discussed.²³ It was found that the rise in the number of publications about this topic was not coupled to an increase in quality of reporting. Frequently, the productivity of the system as space-time-yield (STY) and the residence time were not given. This indicates that additional efforts must be made by the scientific community in order to ensure that the reproducibility and fair comparison between the results reported by different research groups is possible. This is actually

a long-standing problem, and already more than a decade ago this was pointed out.²⁴ We consider the following metrics important to achieve this goal.

2.3.1 Immobilisation metrics

2.3.1.1 Enzyme surface hydrophilicity/hydrophobicity

For enzymes of known structure, the analysis of the enzyme surface is crucial prior to the selection of the carrier for its immobilisation. Molecular visualisation software provides details of the enzyme surface, i.e. charge, hydrophilicity or hydrophobicity and allows to choose the carrier that is compatible with these properties (Fig. 1A). A mismatch between enzyme and carrier might induce adverse interactions, such as (partial) protein unfolding, resulting in enzyme deactivation.²⁵

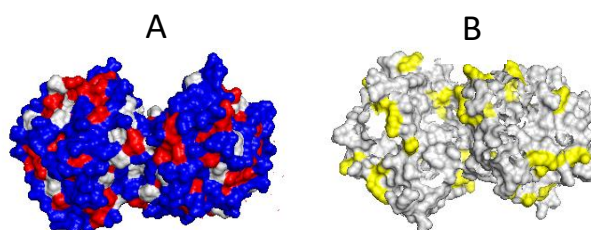


Fig. 1 Surface visualisation of dimeric A#HNL (PDB code: 3dqz). (A) Residues in blue (arg, lys, his, glu, asp, asn, gln, thr, ser, cys) are hydrophilic, residues in grey (pro, tyr, typ) and residues in red (ala, gly, val, ile, leu, phe, met) are hydrophobic; B) residues in yellow are lysines. The images were created using PyMOL molecular Graphics System.

2.3.1.2 Ratio enzyme: carrier (mol g^{-1} or U g^{-1})

This parameter is essential when the immobilisation is performed by adsorption/deposition. A sufficient amount of carrier (g) must be available for the enzyme (mol or U) immobilisation and parameters such as pore diameter, pore volume and water absorption have to be carefully evaluated. In addition, it is important to ensure that the entire enzyme solution is adsorbed during the immobilisation. A layer of enzyme solution not adsorbed onto the carrier during the immobilisation step, might lead to loss of enzyme.²⁶

2.3.1.3 Leaching assay

Once the enzyme has been immobilised, a leaching assay needs to be performed under reaction conditions to evaluate the effectiveness of the immobilisation method and the robustness of the biocatalyst. When biotransformations are performed in organic solvents, desorption of the enzyme is generally avoided due to its insolubility in the reaction medium. A straightforward method to evaluate leaching under reaction

conditions is to perform two reactions in parallel, after a certain time the immobilised enzyme is filtered off from one of the reactions. In heterogeneous catalysis, this is well established as “hot-filtration”.²⁷ The arrest of conversion immediately after removal of the immobilised enzyme demonstrates that the enzyme is not leaching from the carrier into the reaction medium under reaction conditions.

2.3.1.4 Ratio of lysine concentration to carrier functionalities (mol mol⁻¹)

Commonly, a covalent immobilisation is achieved by the interaction of lysine residues on the enzyme surface with reactive aldehydes or epoxides of the carrier. For this reason it is essential to determine the number of surface exposed lysine residues in order to choose an appropriate enzyme to support ratio. For an enzyme of known structure the number of surface exposed lysine residues can be determined using a molecular visualisation software (Fig. 1B). With these straightforward calculations the covalent attachment is more likely to be successful.²⁵ The same applies to the carboxylic acid groups of aspartic acid or glutamic acid if they are the functional groups utilised for covalent immobilisation. Similarly, the ratio of a his-tagged enzyme (or any tag) to its counterpart (Fe, Zn, Co, Ni or other) on the carrier should be calculated.

2.3.1.5 Ratio of carrier pore size to enzyme diameter

Immobilisation performed by adsorption/deposition requires that the enzyme diameter is smaller than the pores of the carrier even in the most unfavourable conformation. For this, transmission electron microscopy (TEM), nitrogen adsorption–desorption isotherms and mercury porosimetry are useful techniques to determine the pore size of the carrier.^{25,28,29} A high ratio of carrier pore size to enzyme diameter leads to high enzyme loading and minimises diffusion limitation.^{13,30,31} The distribution of enzyme molecules on a porous carrier can be modulated by the immobilisation rate. In general, higher immobilisation rates leads to undesired, more heterogeneous distributions.³²

2.3.2 Economic metrics

2.3.2.1 Space-time-yield (STY)

This parameter is frequently used to evaluate the productivity of different systems normalised to 1 liter volume (g h⁻¹ L⁻¹). It describes the amount of product formed at a certain flow rate and reaction volume as shown in eqn (1):

$$STY = \frac{[P] \cdot f}{RV} \quad (1)$$

where [P] is the concentration of product leaving the reactor in g L⁻¹, *f* is the flow rate in L h⁻¹ and RV is the reaction volume in L. Since batch and continuous flow system setups have a completely different geometry, a direct comparison based on conversion or yield is simply not possible. In contrast, the calculation of the STY enables a fair comparison between the different systems. This comparison should be made at the same level of conversion since the product formation in batch and flow follow different kinetics.²

2.3.2.2 Specific rate (SR)

This parameter enables one to establish the rate of an enzyme under given conditions and comparison of different setups. It describes the amount of product formed during a certain reaction time per unit of enzyme and is calculated according to eqn (2):

$$SR = [P] \cdot \frac{f}{M_{ENZ}} \quad (2)$$

where [P] states the concentration of product leaving the reactor in mol mL⁻¹, *f* is the flow rate in mL min⁻¹ and *M*_{ENZ} is the amount of purified enzyme used for the reaction in g. If the amount of enzyme is expressed in mmol and the SR is calculated under *V*_{max} conditions (saturating substrate concentrations), then it is equal to the *k*_{cat}. SRs are normalised to the amount of enzyme immobilised thus different setups can be compared directly. As explained for STY, the comparison of specific rates for batch and continuous flow must be made at the same level of conversion.

2.3.2.3 Biocatalyst productivity

This is a dimensionless number calculated from the amount of product synthesised per amount of enzyme used during its operational lifetime.³³

Additional important parameters related to reporting of biocatalytic reactions in flow processes are: (i) operational stability, (ii) biocatalyst loading, (iii) substrate concentration, (iv) reactor volume, (v) residence time. Details about these metrics have been extensively discussed in excellent reviews.^{33,34}

2.4 Reaction medium

The reaction medium is an important aspect to consider for biocatalytic transformations, indeed for all transformations. For details about physical properties, environmental and health impacts, flammability/explosion limits and reactivity/stability of different solvents commonly used for biocatalytic transformations the GlaxoSmithKline (GSK) solvent selection guide can be consulted.³⁵ In general the best solvent is no solvent, so reactions converting neat substrate into neat product would be the ideal. In biocatalysis this is often impossible due to inhibition effects. Overall, biocatalysis is usually performed under aqueous, biphasic or pure organic solvent conditions. Each of them has specific advantages and disadvantages. Water (buffered) is the natural reaction medium in which most bio-catalytically utilised enzymes display the highest activity.

However, the separation of water from the product can be complicated and expensive due to its high boiling point. This might affect green metric indicators such as the E factor.^{36,37} In addition, apolar substrates dissolve poorly in water. This affects parameters such as STY and consequently, the economic performance of the process is often poor. Biphasic reactions, i.e. the addition of a water immiscible solvent is a straightforward method to improve economic and environmental metrics. Here, apolar substrates are soluble in the organic solvent layer, therefore high substrate loading is possible and the product is immediately extracted from the water layer and can be obtained from the organic phase by e.g. distillation. Moreover, product inhibition and hydrolysis of water sensitive compounds are avoided.³⁸ However, the introduction of organic solvents as a second layer in a biphasic system might lead to mass transfer limitations and enzyme deactivation at the interphase.³⁹ The utilisation of non-aqueous reaction media was introduced long ago and is today fully developed. Under these conditions, equilibria can be reverted and very high substrate loading can be achieved, enhancing economic parameters (indeed, no solvent is the best solvent).^{40–43} In order to perform a biotransformation in organic solvents, the enzyme must be immobilised on an appropriate carrier to avoid it lumping together. At the same time enzymes and cofactors are generally not soluble in organic solvents, thus this is an interesting approach to avoid leaching. For flow chemistry these are therefore good conditions. Only lipases have the ability to work in pure organic solvent medium.⁴⁴ For all other enzymes, the water activity (a_w) of the system must be carefully evaluated for optimal enzymatic performance. As a rule of thumb, enzymes work well in buffer saturated organic solvents with a log P around 2, this provides the amount of water that the

enzyme requires for conformational flexibility but still suppresses undesired side reactions. Overall, if different parameters such as type of solvent ($\log P$), a_w , immobilisation method and carrier are properly studied, an enzyme in an organic solvent medium is able to perform as well as in aqueous conditions.^{42,43}

To examine the influence of all these parameters in organic solvent, biphasic and aqueous systems, cofactor or cofactor free systems on the two challenges named-above, selected examples of biotransformations performed in flow systems are presented (Table 1) and will be discussed.

2.4.1 Biotransformations in organic solvents as reaction medium

Hydroxynitrile lyases (HNLs) comprise a diverse group of enzymes that catalyse the addition of cyanide to a prochiral aldehyde or ketone to produce chiral cyanohydrins, important building blocks for synthesis.⁴⁵ They include metal containing cupins, α,β -hydrolase fold enzymes, FAD containing structures and many more. The metal containing cupins can equally well be viewed as cofactor dependent enzymes.^{11,25,26,45} A key challenge in every chiral cyanohydrin synthesis is the competing chemical, racemic background reaction. It can be suppressed by low pH values or, even better, by performing the reaction in organic solvents, as was already realised in the last century.^{11,46}

Recently, the immobilisation of *Granulicella tundricola* hydroxynitrile lyase (GtHNL; Mn²⁺ containing cupin) for the synthesis of (*R*)-mandelonitrile by using a packed bed reactor (Fig. 2) was reported.²⁶

Table 1: Selected examples of biotransformations using immobilised enzymes in flow

Biocatalyst	Immobilisation method	Reactor	Medium	STY (g h ⁻¹ L ⁻¹)	Comments	Ref.
GtHNL-A40H/V42T/Q110 H from <i>Granulicella tundricola</i> immobilised on Celite R-633.	Adsorption	PBR (6.4 cm length, 0.45 cm inner diameter, 0.39 mL reaction volume) 150 mg Celite R-633, 1 U/mg _{carrier}).	Organic, acetate buffer saturated MTBE pH 4	From 784 at 0.1 mL min ⁻¹ up to 5237 at 1 mL min ⁻¹	97% of conversion at 0.1 mL/min, excellent enantioselectivity (>99 %) at flow rates between 0.1 mL/min and 1 mL/min.	26
AtHNL from <i>Arabidopsis thaliana</i> immobilised on EziG Opal (control porosity glass beads bearing Fe ³⁺ on the surface.	Ionic	PBR (6.4 cm length, 0.45 cm inner diameter, 0.30 mL reaction volume, 150 mg EziG Opal, 10 U/mg _{carrier}).	Citrate/phosphate buffer saturated MTBE pH 5	From 1005 at 0.1 mL min ⁻¹ up to 1899 at 1 mL min ⁻¹	96% of conversion at 0.1 mL/min, excellent enantioselectivity (>99 %) at 0.1 mL/min but it decreased up to 60% at 1 mL/min.	52
MeHNL from <i>Manihot esculenta</i> and HbHNL from <i>Hevea brasiliensis</i> immobilised on amino functionalized monolith microreactor.	Covalent	Monolith microreactor (6 x 40 mm, 0.96 mL reactor volume, 260 mg silica).	Organic, citrate/phosphate buffer saturated MTBE pH 5	613 for HbHNL 1229 for MeHNL	A drastic increase in catalytic performance was observed for the flow reactions as compared to the batch system. MeHNL displayed higher operational stability as compared to HbHNL.	25
<i>E. coli</i> whole cells containing ω-transaminase and PLP immobilised on methacrylated beads.	Adsorption	PBR (1/4 in. x 4.6 mm x 10 cm, reactor volume with beads: 0.5 mL).	Organic, water saturated MTBE	n.d	Several non-natural ketones were converted with excellent enantioselectivity. The use of organic solvent as reaction medium suppressed leaching of ω-transaminase and PLP. No additional PLP was required.	74

<i>Candida Antarctica lipase B (Ca/B)</i> and <i>A#HNL</i> immobilised on Celite R-633.	Adsorption	1 st reactor - <i>Ca/B</i> : PBR (microbore column 3 mm/100 mm), 0.70 mL. 2 nd reactor – <i>A#HNL</i> PBR (microbore column 3 mm/50 mm), 0.35 mL.	Organic, Microaqueous MTBE	n.d		The system addressed the in situ safe generation of HCN. The continuous flow system proved to be more efficient as compared to the batch system (40 min vs 345 min).	51
<i>Candida Antarctica lipase B (Ca/B)</i> immobilised on amino functionalised silica microspheres (MAT540™)	Covalent	PBR, 70 mm x 4 mm; total length: 70 mm; packed length: 65 mm; inner volume: 0.816 mL	Organic, toluene (mL/min)	dry (0.1	n.d	The kinetic resolution of 5 racemic amines was achieved using 2-ethoxyacetate as acylating agent. Good conversion and excellent enantioselectivity were reached. Up to 2 times higher specific rate was observed for the flow system as compared to the batch approach.	81
Lipase from <i>Thermomyces lanuginosus</i> (TLL) immobilised on Immobead 100.	Covalent	PBR (250 mm x 4 mm), immobilized enzyme (1 g, 10 ⁴ units), residence time 40 minutes	Biphasic, 0.25 mL min ⁻¹ of <i>rac</i> cyclopropanecarboxylate ester in heptane + 0.25 mL min ⁻¹ 0.1 M Glycine-NaOH buffer pH 9	6.38		The continuous flow system showed 17% of conversion and enantioselectivity E = 58 after 5.5 minutes of resident time reaction. The batch system displayed 53% of conversion and E = 52 after 23 hours reaction time.	57
Acyl transferase from <i>Mycobacterium smegmatis</i> (MsAcT) immobilised on amino or metal functionalised monolith microreactor	Covalent bonding or electrostatic his-tag interactions with Co ²⁺ or Ni ²⁺ metals	Monolith microreactor (6 x 40 mm, 4 cm ³ g ⁻¹ total pore volume)	Biphasic, 50% phosphate buffer pH 7.5 + 50% neopentylglycol in ethyl acetate (v/v)	n.d		Almost full conversion for the synthesis of the monoester was observed after 45 seconds independently of the immobilisation method used.	60
Halo tagged alcohol dehydrogenase	Covalent binding	PBR (3 x 50 mm), column volume 3.53 x 10 ⁻⁴ L	Biphasic, NADP ⁺ in phosphate buffer + ketones	From 14 to 117 (4 different ketones)		The cofactor was efficiently recycled reaching a total turnover	16

from <i>Lactobacillus brevis</i> immobilised on HaloLink resin			in 2-propanol. Ratio 10:1		number for NADP ⁺ higher than 12000 mol mol ⁻¹	
Alcohol dehydrogenase from <i>Lactobacillus brevis</i> immobilised by encapsulation within a superabsorber polymer based carrier	Encapsulation	PBR, reactor volume 0.2 and 0.4 mL, residence time 1 h	Organic, MTBE	7.5 at 0.2 mL h ⁻¹ 5.5 at 0.4 mL h ⁻¹	The immobilised enzyme displayed 60% of conversion after 5 hours of reaction time whereas the soluble enzyme in biphasic medium reached full conversion	82
Acyl transferase from <i>Mycobacterium smegmatis</i> (MsAcT) immobilised onto agarose beads	Covalent	PBR (6.6 mm i.d.), 1.9 g of immobilised-MsAcT (1 mg/g _{agarose}), reactor volume 1.4 mL	Biphasic, 0.25 M of different alcohols in 0.1 M phosphate buffer pH 8 + pure ethyl acetate. Ratio 90:10	13.6 g day ⁻¹	5 commercially relevant esters were synthesised with conversions ranging from 65% to 96% within 5 minutes of reaction time using ethyl acetate as acyl donor. The use of EtOAc as acyl donor enables to label the products as natural.	62
Whole cells containing DERA-C47M immobilised on alginate-luffa matrix	Absorption combined with cross-linking	PBR (20 cm x 0.8 cm), 850 mg loofa sponge with the immobilized enzyme (350 or 700 mg of cells)	Aqueous, 0.1 M TEOA buffer pH 7.5	n.d	The optimised flow system enabled the synthesis of 4.5 g of lactol product per day	72
Amine dehydrogenase (AmDH) and formate dehydrogenase (FDH) from <i>Candida boidinii</i> were immobilised on Nuvia IMAC	Ionic binding	PBR (Omnifit™ EZ SolventPlus™ 10 mm x 100 mm chromatography column), 5:1 ratio of AmDH to FDH	Aqueous, 2 M ammonium formate (NH ₄ COOH) buffer pH 8.5	4.45 at 48% conversion up to 18.45 at 24% conversion	The system was able to operate for more than 5 days without or internal mass transfer limitations. The half-life of the biocatalyst was 159 h.	20

resin bearing Ni ²⁺ on the surface							
Amine dehydrogenase (AmDH) and formate dehydrogenase (FDH) from <i>Candida boidinii</i> were immobilised on EziG Amber resin bearing Fe ³⁺ on the surface	Ionic binding	PBR (5 mm I.D., 50 mm length), 150 mg EziG Amber	Aqueous, 1 M ammonium formate (NH ₄ COOH) buffer pH 9	12.5 at 68% of conversion	The system reached up to 68% of conversion at 0.2 mL min ⁻¹ without loss of productivity after 3 hours. A decrease in productivity was observed after 6 hours probably due to FDH inactivation.	78	
Lactate dehydrogenase (LDH) and formate dehydrogenase (FDH) were immobilised on carbon particles (Black pearls 2000)	Absorption	PBR (Omnifit glass column, 6.6 mm I.D and variable length). Total bed volume = 1.02 mL, reactor volume = 0.48 mL. 3 mg LDH and 3 mg of FDH were used. Flow rates between 17.2 and 51.6 μL min ⁻¹	Aqueous, 50 mM Tris-HCl buffer pH 8.	22.9	100% of conversion was achieved after 30 minutes reaction time. The system proved to be highly stable without any decrease in conversion during 30 h on stream. Higher productivity was achieved as compared to the batch system (STY = 0.23 g h ⁻¹ L ⁻¹)	83	
<i>Thermococcus kodakarensis</i> glycerol kinase (GlpK _{TK}), <i>Mycobacterium smegmatis</i> acetate kinase (AceK _{MS}), <i>E. coli</i> glycerol-3-phosphate dehydrogenase (G3PDE _{Ec}), NADH oxidase from <i>Clostridium aminovalericum</i> (NOX _{Ca}), fructose	Covalent	Three cascade steps: Phosphotransfer reaction: PBR, 25 × 15 mm ² Benchmark column to a packed bed volume of 21.2 ml. 0.25 mL/min and reaction time 84.8 min Oxidation reaction: PBR, 250 × 15 mm ² Benchmark column to a packed bed volume of	Aqueous, 0.2 M sodium citrate buffer pH 7.9	Phosphotransfer reactor: 2.79 (69.95 g L ⁻¹ h ⁻¹ g ⁻¹) Oxidation reactor: 0.86 (10.75 g L ⁻¹ h ⁻¹ g ⁻¹) Aldol reactor: 0.57 (28.58 g L ⁻¹ h ⁻¹ g ⁻¹) The system displayed a STY of 70 g L ⁻¹ h ⁻¹ g ⁻¹ for the	The system regenerate the cofactor efficiently, total turnover numbers of 16848 and 10839 for ATP and NAD ⁺ were achieved respectively.	17	

aldolase (FruA) from <i>Staphylococcus carnosus</i> were immobilised onto Sepharose beads		28.3 ml. 0.25 mL/min and reaction time 113.2 min Aldol reaction: PBR, 150 × 15 mm ² Benchmark column to a final depth of 10 cm (17.7 ml packed-bed volume). 0.1 mL/min and reaction time 177 min.			synthesis of D-fagomine	
Acid phosphatase (PhoN-SF) was immobilised on metacrylate polymeric beads. Fructose-1,6-diphosphate aldolase (RAMA) and rhamnulose 1-phosphate aldolase (RhuA) from <i>Thermotoga maritima</i> were immobilised on different epoxy functionalised carriers.	Covalent	Three cascade steps: Phosphorylation reaction: PBR, diameter = 4.6 mm, length = 33 mm, volume = 0.525 mL. PhoN-Sf (250 µL, 25 U) Aldol reaction: PBR, diameter = 4.6 mm, length = 150 mm, inner volume = 2.5 mL. 100 U of RAMA or RhuA and 100 U of PhoN-Sf Phosphorylation reaction: PBR, diameter = 4.6 mm, length = 33 mm, volume = 0.525 mL. PhoN-Sf (50 U) Flow rate = 0.03 mL min ⁻¹	Aqueous, 50 mM acetate buffer pH 6	0.747 g day ⁻¹ for the synthesis of <i>N</i> -Alloc-3-aminopropanal (RAMA) ^a .	The retroaldol reaction was inhibited by immobilisation. The aldol products were obtained from inexpensive starting materials. 0.6 g of D-fagomine precursor were synthesised by immobilised RAMA.	73

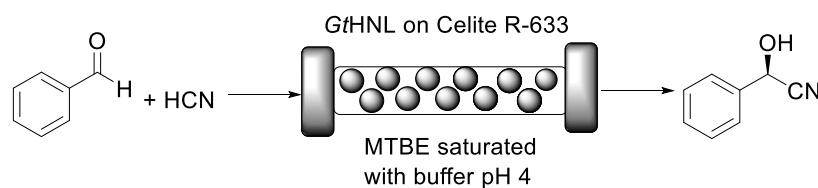


Fig. 2 GtHNL catalysed synthesis of (*R*)-mandelonitrile

GtHNL was immobilised by adsorption on Celite R-633, also known as diatomaceous earth, a siliceous material obtained from diatoms, a type of microscopic algae. As described earlier, key aspects such as carrier pore volume and water absorption capacity were carefully evaluated.⁴⁷ This carrier is: (i) environmentally friendly; (ii) the pore size is relatively large (6.5 μm), an important feature to minimise diffusion limitation; (iii) the immobilisation method is straightforward and no chemical treatment is required; (iv) it is a food grade material. All these important characteristics make Celite a green carrier for biocatalysis. However, as nothing is perfect all these advantageous features are accompanied by one main drawback: Celite also catalyses the racemic background reaction. This is suppressed by utilisation of organic solvents and by using continuous flow operation. Methyl *tert*-butyl ether (MTBE) was selected as reaction medium since other HNLs performed well in this organic solvent in batch systems^{47–49} and it is considered one of the ‘greenest’ organic solvents.³⁵ It was used buffer saturated (pH 4) to ensure full enzyme activity.⁵⁰ As expected no leaching of the enzyme was observed. Both, batch and flow produced enantiopure (*R*)-mandelonitrile. However, in batch, the STY was significantly lower than in the flow system even though otherwise identical reaction conditions were applied: 12 g h⁻¹ L⁻¹ versus 784 g h⁻¹ L⁻¹. This represents a huge improvement in productivity (65 times), enabling an important reduction in waste generated due to the reduced volume, making the flow system a ‘greener’ process as compared to the batch approach. The potential of Celite was also demonstrated for the synthesis of cyanohydrins in batch and flow using organic solvents with another (*R*)-selective HNL. The enzyme from *Arabidopsis thaliana* (AtHNL; α,β-hydrolase fold) is structurally unrelated to GtHNL. Immobilisation on Celite improved the stability of the acid sensitive AtHNL.⁴⁸ Conversion up to 96.8% and enantiomeric excess of 99.8% were reached after 45 minutes of reaction time in a batch system. Five years later, the successful synthesis of cyanohydrins with the same AtHNL preparation was compared in batch and flow systems.⁵¹ This time the safety limitation of this reaction (green chemistry – principles 3 and 12) related to the handling of toxic hydrogen cyanide (HCN) was addressed by performing the HCN

generation in situ from the cheap and less toxic ethyl cyanofornate as well as the actual cyanohydrin synthesis in flow (Fig. 3).

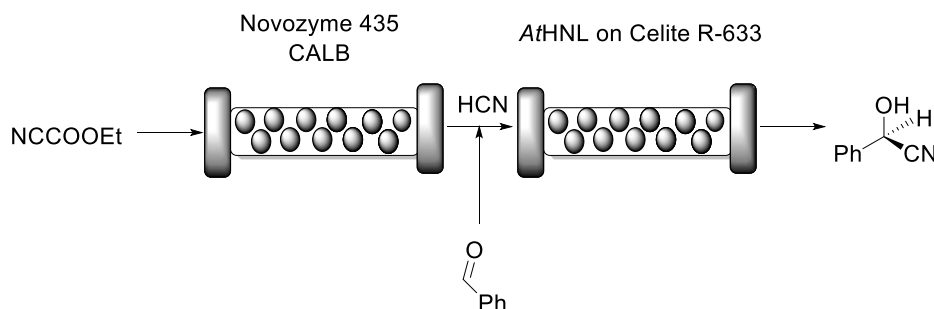


Fig. 3 Two-step synthesis of (*R*)-mandelonitrile catalysed by CALB and AtHNL.

The flow approach proved to be superior as compared to the batch system not only in terms of safety and waste reduction but also in terms of productivity: the reaction time was reduced from 345 min to 40 min by switching from batch to flow. The same AtHNL was also immobilised via the his-tag on the carrier EziG Opal.⁵² This is a controlled porosity glass carrier bearing Fe³⁺ on its surface. The availability of metal ions for the enzyme binding was guaranteed by using a molar ratio of monomeric AtHNL:Fe³⁺ of 1:5. Again buffer saturated MTBE (here pH 5 rather than pH 4 for GtHNL) was used as reaction medium. After several steps of reaction engineering, near complete conversion and excellent enantioselectivity were achieved at low flow rate (0.1 mL min⁻¹). No enzyme leached from the carrier. Although the racemic reaction was suppressed better in flow than in batch, an important decrease in enantioselectivity was observed at flow rates above 0.2 mL min⁻¹. High flow rates reduce the contact time between enzyme and substrate allowing the racemic reaction to proceed. Again the flow system proved to be more efficient with a STY of 690 mol h⁻¹ L⁻¹ g_{enzyme}⁻¹ versus 187 mol h⁻¹ L⁻¹ g_{enzyme}⁻¹ in batch.

GtHNL and AtHNL are both (*R*)-selective enzymes, however the multitude of different HNLs also offer access to the (*S*)-cyanohydrins. The (*S*)-selective *Manihot esculenta* HNL (MeHNL; α,β -hydrolase fold) and *Hevea brasiliensis* HNL (HbHNL; α,β -hydrolase fold) were therefore utilised to study siliceous monolithic micro-reactors (Fig. 4). The use of monolithic micro-reactors instead of packed bed reactors represents an interesting alternative in flow.²⁵ These reactors further reduce reaction time as consequence of the large surface to volume ratio, high thermal efficiency and improved safety.^{53,54} In addition, mass transfer is enhanced due to its hierarchical/tortuous porous structure reducing diffusion limitation.⁵⁵ Possible

disadvantages are the higher costs compared to packed bed systems and the difficulty to scale up.⁷

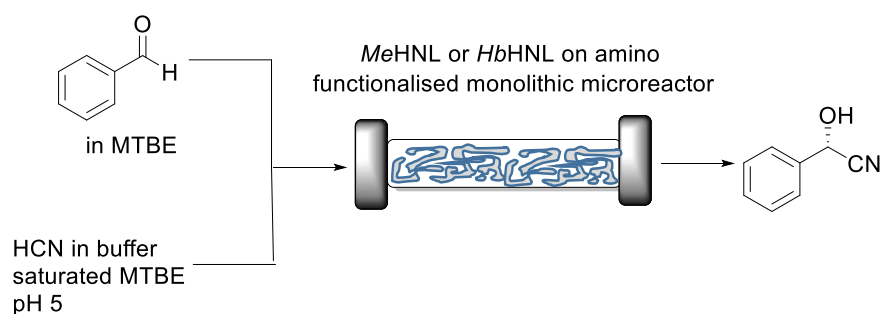


Fig. 4 *MeHNL* or *HbHNL* catalysed synthesis of (*S*)-mandelonitrile.

In this case, a careful examination of the surface characteristics of the enzymes and carriers enabled the successful covalent attachment. As explained above (Fig. 1), the most relevant parameters of *MeHNL* and *HbHNL* such as diameter, hydrophilicity, number of surface exposed lysine residues and their position related to the active site entrance were obtained by analysing the crystal structure. The pore size diameters of the carriers used for the immobilisation was estimated by transmission electron microscopy (TEM) images. Overall: (i) the carrier chosen had to be hydrophilic to avoid adverse folding effects, (ii) *MeHNL* and *HbHNL* had 36 lysine residues for covalent attachment without affecting the active site entrance and (iii) the pore size of the carriers was 2.6 to 3 times larger than the enzymes diameter even in the most unfavourable conformation which represent an internal pore volume 100 times larger as compared to the volume of either enzyme. The enzymes were covalently immobilised on carriers with the corresponding properties and probed in batch and flow reactions. In these cases the lysines were not close to the active site, independent of the carrier no extra actions needed to be taken. In other cases the lysines that obstructed the active site when covalently attached, were removed by mutations.¹³ Just as described above for the *GtHNL* and *AtHNL* catalysed cyanohydrin synthesis, the racemic background reaction was minimised in flow. Both immobilised enzymes showed very high productivity with STY of 1229 g L⁻¹ h⁻¹ and 613 g L⁻¹ h⁻¹ for *MeHNL* and *HbHNL* respectively.²⁵

Overall, buffer saturated organic solvents have been successfully applied in flow systems for the synthesis of chiral cyanohydrins. Undesired reactions, here the racemic cyanohydrin formation, were efficiently suppressed, the enzymes did not

leach from the carrier independent of the immobilisation method used, high substrate concentrations (500 mM) were employed and high STYs were achieved.

2.4.2 Biotransformations in biphasic systems as reaction medium

Biphasic systems are also widespread in biocatalysis as they enable high substrate loadings for apolar starting materials. Additionally they are ideal reaction conditions for lipases, that often display interfacial activation.⁴⁴ On the downside additional diffusion limitation and partitioning occur which needs to be overcome by strong stirring in batch systems. In flow good mixing of the biphasic mixture before entering the reactor might be required, however with the monolith reactor mentioned above the mixing occurs in situ. The lipase mediated kinetic resolution of the *rac*-cyclopropanecarboxylate ester for the synthesis of (1*R*,2*S*)-2-(3,4-difluorophenyl) cyclopropan-1-amine generates the stereocentres for ticagrelor, one of the most important drugs for the treatment of acute coronary syndrome and stroke.⁵⁶

A comparison of batch and flow systems under biphasic conditions revealed the potential of the flow approach.⁵⁷ Lipase from *Thermomyces lanuginosus* (TLL) was covalently attached to Immobead 100 and used as catalyst (Fig. 5).

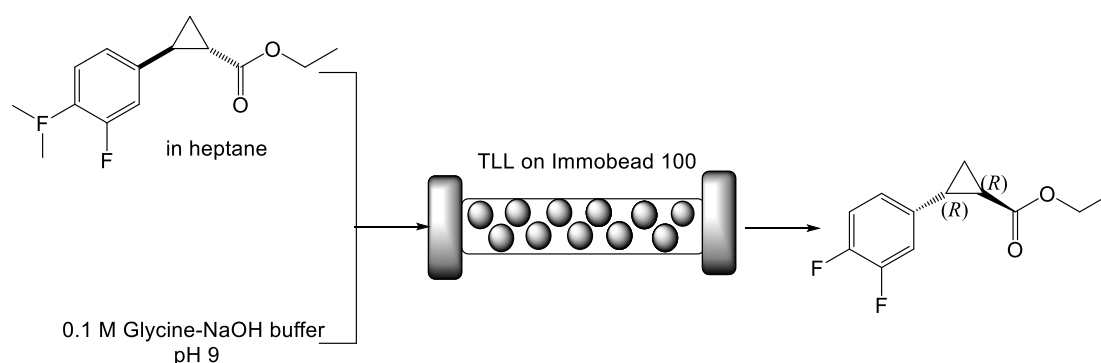


Fig. 5 TLL catalysed kinetic resolution of *rac*-cyclopropanecarboxylate ester yielding (1*S*,2*S*)-2-(3,4-difluorophenyl) cyclopropan-1-acid. The unaltered (1*R*,2*R*) ester is converted into the desired amine.

In batch, 53% conversion and enantioselectivity $E = 52$ were achieved after 23 hours of reaction time. Alternatively, when the reaction was performed in flow in a packed bed reactor (250 x 4 mm) at a total flow rate of 0.5 mL min⁻¹ (0.25 mL min⁻¹ of substrate in heptane + 0.25 mL min⁻¹ 0.1 M Glycine–NaOH buffer pH 9), 17% of conversion with slightly better enantioselectivity $E = 58$ were reached after only 5.5 minutes of residence time. In regard of productivity, the flow reactor displayed a STY of 28.2 mmol h⁻¹ L⁻¹ whereas the batch reactor yielded only 0.4 mmol h⁻¹ L⁻¹. Importantly, the maximum 50% of conversion would be attained (theoretically) with a residence time

of 16.5 minutes by simply reducing the flow rate or coupling multiple reactors in series to extend the reactor length. This also highlights the flexibility of continuous flow systems to scale up processes.

Transesterification reactions are commonly performed with lipases in anhydrous medium. Acyl transferase such as the one from *Mycobacterium smegmatis* (*MsAcT*) recently introduced the option of transesterification reactions under aqueous conditions.⁵⁸ After a first report showed the potential of cell free extracts of *MsAcT* to perform acylation in water in a batch system,⁵⁹ the system was transferred to flow and the acylating agent ethyl acetate was used as organic layer. The continuous transesterification of neopentylglycol (NPG) with immobilised *MsAcT* on siliceous monolith micro-reactors was performed in a biphasic 50/50% system and the enzyme was immobilised either by covalent bonding or his-tag interactions (Fig. 6).⁶⁰

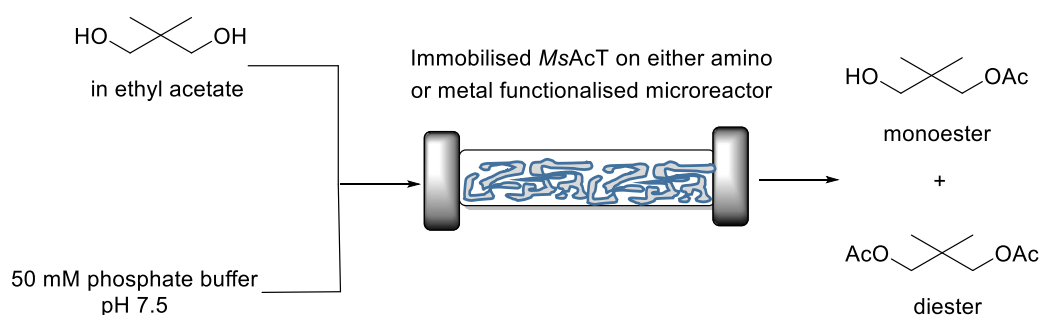


Fig. 6 Continuous *MsAcT* catalysed transesterification of neopentylglycol in a biphasic system

An excess of either glutaraldehyde in the case of covalent binding or metal ions (Co^{2+} or Ni^{2+}) when the his-tag was used, were available to ensure binding. The system displayed an exceptional performance for the synthesis of the mono-ester independent of the immobilisation method used: almost full conversion after just 45 seconds. The ratio of mono- to di-ester could be influenced with the flow rate, however full conversion to di-ester was not achieved. This represents a huge improvement over the batch system reported earlier, where full conversion of NPG was not even completed after 7 hours.⁵⁹

The substrate scope of *MsAcT* for transesterification reactions in water revealed that different acyldonors such as vinyl acetate and phenyl acetate can be used and aliphatic and aromatic secondary alcohols are converted, while *tert*-alcohols are no substrates.⁶¹ This has opened up new possibilities for the synthesis of natural flavour compounds in a more sustainable fashion.

Recently an application of *MsAcT* for commercially relevant materials was reported.⁶² The successful immobilisation of *MsAcT* onto agarose (Fig. 7.) enabled improved STY in flow. Here, the goal was the synthesis of esters utilising exclusively natural substrates (obtained from nature or by biotechnological approaches). Thus, the natural but less reactive ethyl acetate was used as acyl donor instead of non-natural vinyl acetate. A drawback of performing the transesterification of alcohols and ethyl esters is the negative impact of ethanol on *MsAcT*. This was circumvented by the above mentioned immobilisation on agarose. The immobilised enzyme retained >75% of its activity after 24 hours of incubation in 500 mM ethanol whereas the free enzyme retained less than 60% of its original activity after only 2 hours of incubation. High conversions were reported for the acylation of 2-phenyl ethanol (75%), cinnamyl alcohol (76%) and *n*-hexanol (95%) with immobilised *MsAcT* (1 mg g_{agarose}⁻¹) in batch after 1, 2 and 0.5 hours respectively. By switching to a packed bed reactor and segmented flow (diameter = 6 mm and reactor volume = 1.4 mL) with immobilised *MsAcT* (1.9 g with enzyme loading of 1 mg g_{agarose}⁻¹) a drastic increase in productivity was observed. Five commercially relevant esters were synthesised with conversions ranging from 65% to 96% within 5 minutes of reaction time. The batch reaction achieved a STY of 23 g L⁻¹ h⁻¹ whereas the continuous flow system reached 318 g L⁻¹ h⁻¹.

Overall, several successful examples of biotransformations in flow using biphasic systems have been reported. The enhanced mass transfer commonly observed in flow, including segmented flow, helps to circumvent the diffusion limitation of biphasic batch reactions and enables higher substrate loadings as compared to aqueous systems.

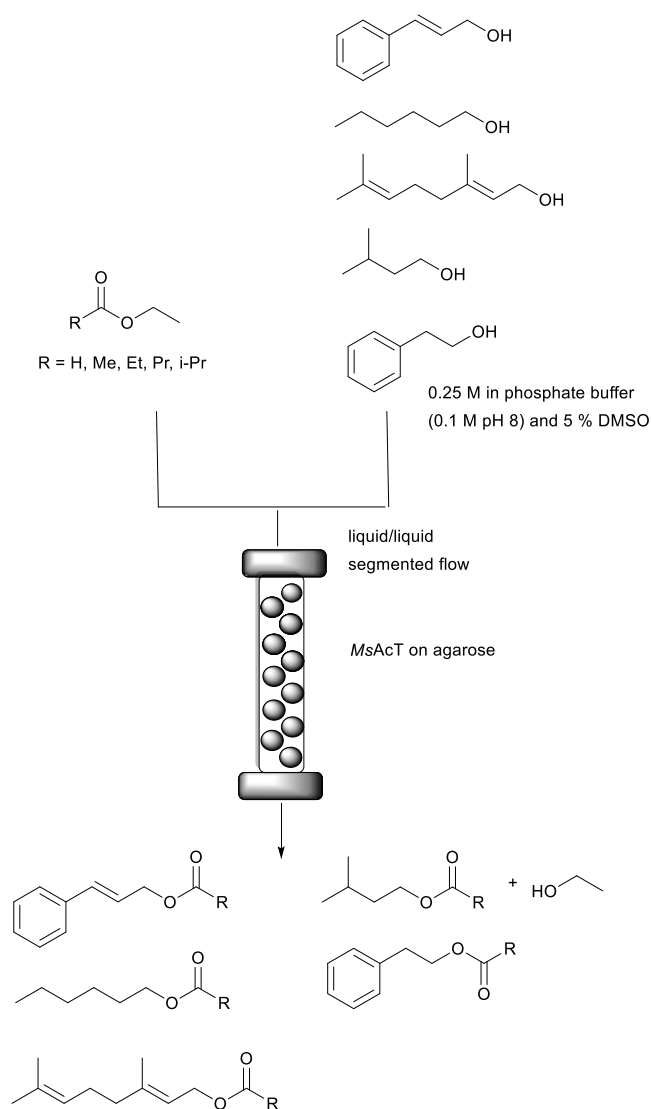
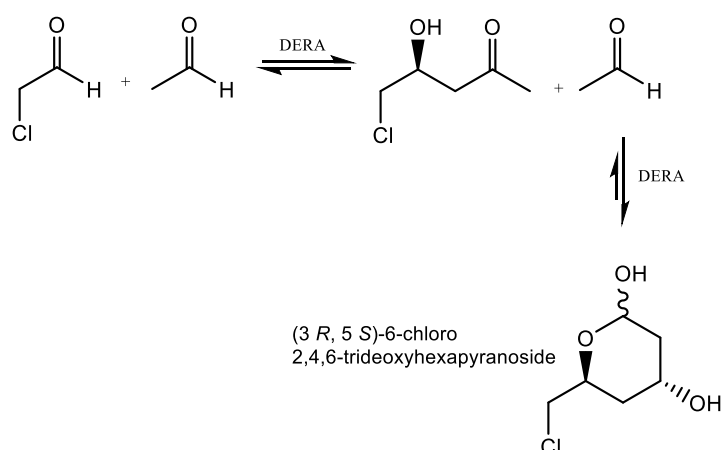


Fig. 7 Continuous *MsAcT* catalysed transesterification of primary alcohols in a biphasic system with segmented flow.

2.4.3 Biotransformations in aqueous systems as reaction medium

2-Deoxy-D-ribose-5-phosphate aldolase (DERA) is a very versatile enzyme for the synthesis of aldol products using acetaldehyde as donor. The sequential aldol condensation catalysed by DERA is one of the most efficient routes for the synthesis of the side chain of HMG-CoA reductase inhibitors called statins, important cholesterol lowering drugs (Scheme 1).^{63–65}



Scheme 1: Sequential aldol condensation catalysed by DERA for the synthesis of a chiral statin precursor.

However, the main limitation for an economically efficient industrial application is the enzymes sensitivity towards aldehydes, in particular acetaldehyde. Promising results with protein engineering techniques and reaction engineering were reported.^{66–70} The DERA from *Lactobacillus brevis* (*Lb*DERA) already naturally displays high stability to acetaldehyde.⁷¹ The introduction of a single amino acid substitution, *Lb*DERA-E78K, improved the enzyme stability even further. This made the synthesis of a chiral precursor of statins, (3*R*,5*S*)-6-chloro-2,4,6-trideoxyhexapyranoside, in a batch system possible, with an notable space-time-yield of 792.5 g L⁻¹ d⁻¹.

As demonstrated above for organic solvents and biphasic mixtures immobilisation and continuous flow are two important techniques to consider for improved enzyme stability for aqueous systems, too. Recently, DERA was utilised in a continuous flow approach in aqueous medium for the coupling of acetaldehyde and its chloro-derivative (Fig. 8).⁷²

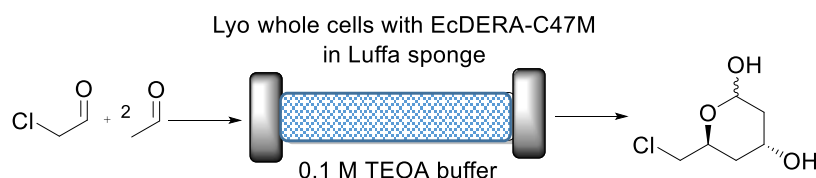


Fig. 8 Continuous *Ec*DERA-C47M catalysed aldol reaction for the synthesis of (3*R*,5*S*)-6-chloro-2,4,6-trideoxyhexapyranoside in aqueous medium.

For this, lyophilised whole cells of *E. coli* BL21(DE3) expressing *E. coli* DERA-C47M, a variant more stable towards acetaldehyde,⁶⁸ were immobilised inside an alginate matrix by encapsulation and fibrous material obtained from the fruit of the Egyptian Luffa plant, commonly known as the luffa bathroom sponge, was used as support to

increase the surface area. From the green chemistry perspective, alginate and luffa sponge are excellent materials for biocatalysis. They are non-toxic, renewable and biodegradable. An enzyme loading of 700 mg led to 80% of conversion of chloroacetaldehyde after *circa* 100 min at a flow rate of 0.1 mL min⁻¹ and the enzyme was stable for more than 5 hours of continuous reaction. No enzyme leaching occurred. The productivity of the system was reported as 4.5 g of product per day but unfortunately different enzyme loadings and substrate concentrations were used for the continuous and batch systems making a reliable comparison of the two systems impossible. This once again emphasised the importance of reporting all metrics. On the other hand the DERA reactor is part of a plug-and-play system in which reactors with different catalysts are combined. The power of this is demonstrated in the next example.

Dihydroxyacetone phosphate (DHAP) dependent aldolases require a much more complex reaction system than DERA, as the unstable DHAP needs to be generated in situ. This multistep procedure of phosphorylation, aldol reaction and dephosphorylation lends itself ideally to the plug-and-play approach. While the modules for phosphate chemistry can remain the same, different aldolases can be plugged in. The successful continuous flow synthesis of different carbohydrate analogues by immobilised *Shigella flexneri* acid phosphatase (*SfPhoN*) and two aldolases (RAMA, rabbit muscle aldolase or RhuA from *Thermotoga maritima*) demonstrates this (Fig. 9).⁷³ The three step cascade reaction starts with the *SfPhoN* to phosphorylate dihydroxyacetone (DHA). The resulting DHAP then, is converted by the desired aldolase, here either RAMA or RhuA, with different aldehydes and finally in the third step *SfPhoN* dephosphorylates the aldol product yielding the desired carbohydrate analogue.

SfPhoN was immobilised on methacrylate polymeric beads whereas the immobilisation of RAMA and RhuA was performed on different epoxy carriers. The stability of soluble and immobilised RAMA was evaluated after 24 hour cycles in batch under reaction conditions. Soluble RAMA was unstable with a 50% decrease of conversion after 3 cycles and the enzyme was completely inactive after 5 cycles. Immobilisation demonstrated to be a suitable technique to improve enzyme stability.

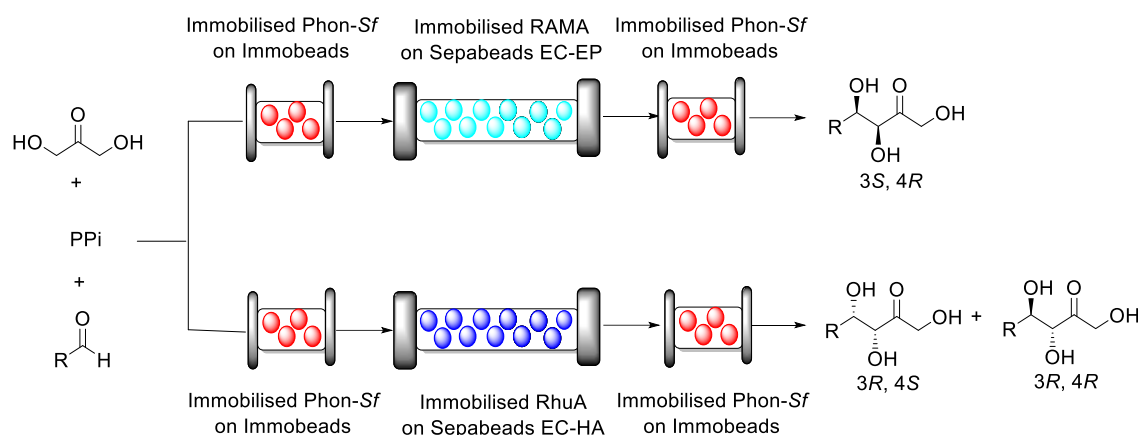


Fig. 9 Aldol cascade synthesis catalysed by *SfPhon* and either RAMA or RhuA in a plug-and-play system in aqueous medium.

The best results were observed when RAMA was immobilised on Sepabeads EC-EP or Relyzyme EP403 (rigid methacrylic polymeric beads). The enzyme was fully active after 6 cycles. Remarkably, immobilisation completely suppressed the retroaldol reaction. This might be explained by internal diffusion limitation or a modification of the equilibrium of the reaction. RhuA was also immobilised on epoxy carriers. Complete binding and high activity were observed when RhuA was immobilised on Sepabeads EC-HA. Having established suitable carriers for immobilisation, the cascade reaction was performed in flow with packed bed reactors (Fig. 9). The synthesis of various aldol products in good yield was possible, however higher conversion was observed with RAMA. 68% conversion was observed for the coupling of DHAP to propanal during the first day but this dropped to 51% after 5 days. Higher conversion (80%) was observed for 4-pentenal during the first day, unfortunately the conversion decreased to 7% after 5 days. Finally, 70% of conversion was observed for *N*-alloc-3-aminopropanal, an important starting material for the synthesis of D-fagomine (antidiabetic piperidine iminosugar drug) during the first day with a decrease to 10% after 5 days. Due to the covalent immobilisation methods chosen no leaching occurred.⁷³

Aqueous systems are the most widely used reaction media in biotransformations. Here enzymes normally display their highest activity. However, the poor solubility of apolar substrates and unwanted side reactions are the main drawbacks for a wider industrial use. Special attention must be taken to avoid leaching of immobilised enzymes into the reaction media. Here this was achieved by covalent linking or the use of whole cells that do not leach easily.

2.5 Addressing the cofactor hurdle

Today, enzymes are used as biocatalysts with good success at an industrial scale. Conversely, cofactor recycling remains a hurdle for industrial scale application of cofactor dependent enzymes. The main differentiation in the type of cofactor is:

- The cofactor is fully regenerated during the catalytic cycle and does not leave the active site; for example PLP or thiamin but also metal cofactors.
- The cofactor transiently binds to the enzyme, it has to leave the active site for regeneration. It requires a cofactor regeneration system very often involving a second enzyme and cofactor mobility is essential; NAD(P)H/NAD(P)⁺ are the prime examples.

The simplest system to approach the cofactor recycling hurdle is the use and immobilisation of whole cells as they have the metabolic pathways to regenerate their cofactors. Then, the problem is limited to avoid the leaching of the cofactor to the reaction medium. The use of organic solvents as reaction medium seems to be a good choice because of the often poor solubility of the cofactor in organic solvents.

2.5.1 Cofactors that are fully regenerated during the catalytic cycle

In line with the above the continuous flow synthesis of chiral amines by using a packed bed reactor and water saturated MTBE as reaction medium was reported.⁷⁴ For this, *E. coli* cells containing both ω -transaminases (ω -TA) and PLP were immobilised on methacrylate beads, most probably via hydrogen bonding between the peptidoglycan layer of the *E. coli* cell wall (containing amide, alcohol and ether functional groups) and the polymeric carrier. PLP is fully regenerated during the catalytic cycle of the enzyme within the enzyme, therefore a regeneration system is not required. The conversion of several non-natural ketones (from 67% to 94%) with excellent enantioselectivity (> 99%) and residence times between 30 and 60 min without leaching of *E. coli* cells, ω -TA and PLP was achieved (Fig. 10).

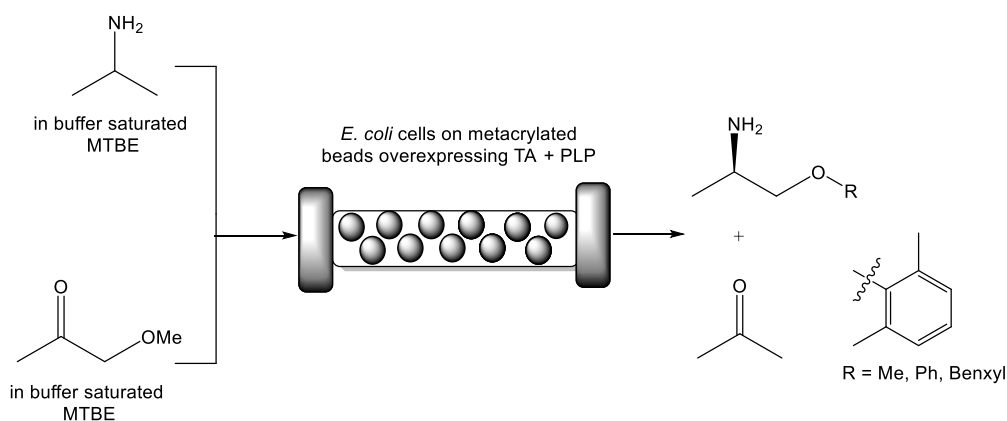


Fig. 10 Stereoselective amine synthesis catalysed by immobilised *E. coli* cells and PLP on metacrylate beads.

Importantly, no quenching or purification was required and the system was operated for 10 days for the synthesis of mexiletine, a drug used to treat abnormal heart rhythms, chronic pain, and some causes of muscle stiffness.

An essential breakthrough for cofactor application in flow was their attachment to ionic carriers.⁷⁵ Any ionic material that can act as counter ion to phosphate moieties present in most cofactors will transiently bind the ionic cofactors. When a buffer of low ionic strength is used as reaction medium the cofactor will remain on the carrier and will be available for the enzyme, even when it needs to be recycled outside the enzyme active site. This principle was demonstrated with Flavin (FAD), PLP and also NAD^+ .²¹ The enzymes were attached to porous carriers and polyethyleneimine (PEI), which is an amine, was the counter ion. For PLP and TA this was fully developed.⁷⁶ Purified ω -TA from *Halomonas elongate* (*HeTA*) and PLP were successfully co-immobilised on porous methacrylate carriers for the continuous synthesis of optically pure amines in aqueous conditions. The beads were functionalised with different reactive groups (cobalt-chelates, epoxides and positively charged amines such as PEI) to allow the electrostatic interaction with his-tagged ω -TAs and PLP. The continuous enantioselective deamination of α -methylbenzyl amine gave > 90% conversion for up to 50 column volumes at 1.45 mL min^{-1} without leaching of the cofactor to the reaction medium. The synthesis reaction of cinnamylamine required a doubling of the reaction time. After an initial decrease in activity it remained stable at 60% for at least 20 column volumes; equiv. to 40 min (Fig. 11).

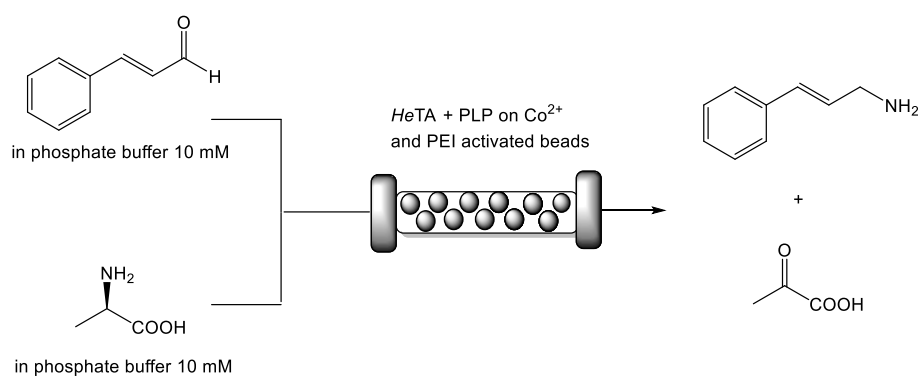


Fig. 11 Synthesis of cinnamylamine in continuous flow. Enzyme and PLP are immobilised via ionic interactions. The *HeTA* via Co^{2+} on the carrier and a his-tag, the PLP via PEI attached to the carrier.

The initial loss of activity might be due to some PLP leaching, induced by the amine donor. An intriguing covalent immobilisation of the FAD containing phenylacetone monooxygenase (PAMO) via its cofactor was described. The cofactor was attached to agarose via a tether and then the apo enzyme from *Thermobifida fusca* was added.⁷⁷ The immobilised enzyme displayed similar activity as compared to its free form but higher thermostability after 1 h of incubation at 60 °C. However, a recyclability study showed low enzyme stability with a decrease of *circa* 40% after 3 cycles.

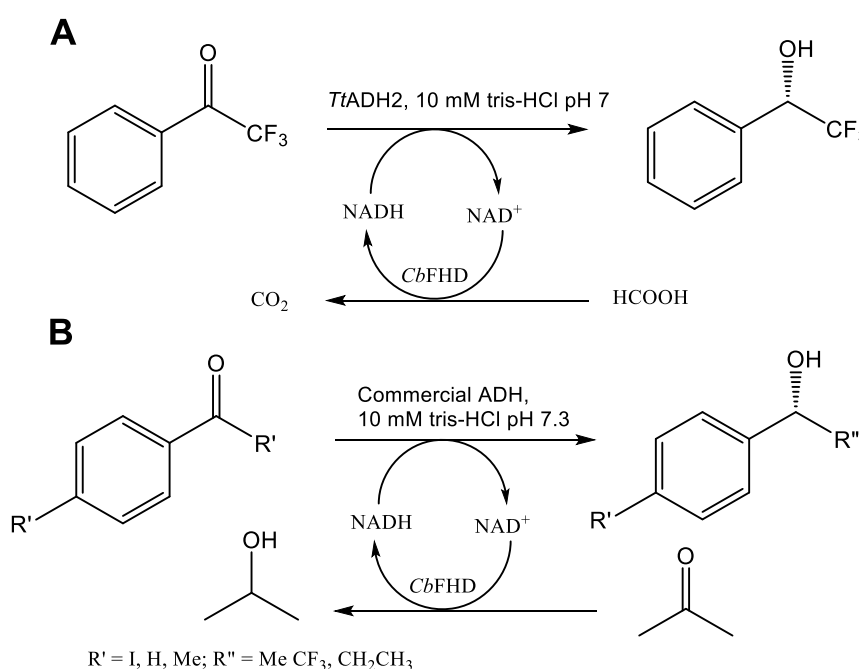
Cofactors that do not require a recycling system and remain in the active site can readily be used in flow systems. Both organic solvents that suppress solubility or aqueous systems with ionic carriers at low buffer concentrations prevent leaching of enzyme and cofactor.

2.5.2 Cofactors that require recycling systems

The application of pure enzymes and cofactors reduces side reactions and it is therefore also preferred in systems which apply cofactors that need to be recycled. The above mentioned immobilisation via ionic interactions was of equal success here.²¹ Commercial porous carriers were coated with PEI to allow the co-immobilisation of enzymes and phosphorylated cofactors such as NAD^+ . The cofactor adsorption is dynamic and allows to establish an association–dissociation equilibrium without leaving the porous carrier. It thus is available for the enzyme performing the desired reaction, here alcohol dehydrogenase from *Thermus thermophilus* (*TtADH2*) and the enzyme required for cofactor recycling, here formate dehydrogenase from *Candida boidinii* (*CbFDH*). The two enzymes and the cofactor were co-immobilised on an anionic exchanger and tested in the continuous asymmetric reduction of 2,2,2-trifluoro-1-phenylethan-1-one (Scheme 2A). Full conversion with a productivity of 250

mM min⁻¹ and a TTN of 85 for immobilised NAD⁺ after 107 hours on stream in continuous flow with less than 10% NAD⁺ loss were achieved.

The system was further improved by applying a commercial ADH that can accept isopropanol as co-substrate. This makes the second enzyme redundant and the cofactor does not have to leave the active site.²² Enzyme and NADPH were coimmobilised on porous agarose beads coated with PEI. The system displayed STYs between 97 and 112 g L⁻¹ day⁻¹ for a range of ketones and the immobilised cofactor reached a TTN of 1076 for 120 hours. During this time, neither the enzyme nor the cofactor were inactivated or leached (Scheme 2B).



Scheme 2. (A) Asymmetric reduction of 2,2,2-trifluoro-1-phenylethan-1-one catalysed by *TtADH2* with external cofactor recycling by *CbFDH*; (B) asymmetric reduction of ketones with internal cofactor recycling.

This can directly be compared to a recent,¹⁶ successful NADPH cofactor regeneration system for the synthesis of chiral alcohols based on a membrane liquid/liquid extractor for continuous flow. The cofactor remained in the aqueous layer and was recycled (Fig. 12).

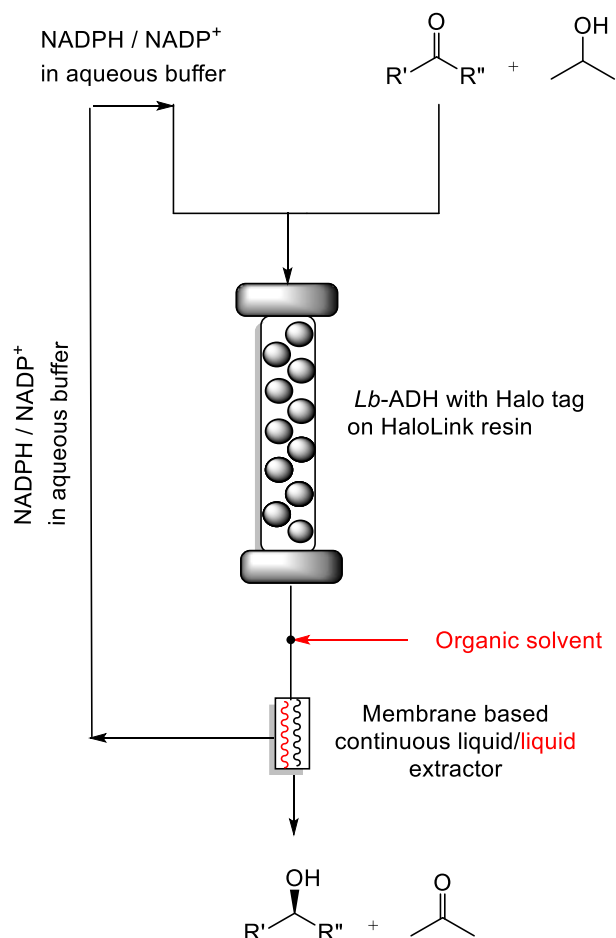


Fig. 12 Synthesis of chiral alcohols catalysed by immobilised *Lb*ADH with cofactor recycling rather than immobilisation.

The organic phase was added after the reaction mixture passed through the immobilised enzyme. This regeneration system without any chemical modification of the cofactor enabled the reduction of four different ketones with STYs from $14 \text{ g L}^{-1} \text{ h}^{-1}$ to $117 \text{ g L}^{-1} \text{ h}^{-1}$, cofactor turnover numbers ranging from 128 to 2023 mol mol^{-1} and excellent enantioselectivity ($> 99\%$). The reliability and robustness of the system was demonstrated with the continuous synthesis of ethyl (*S*)-4-chloro-3-hydroxybutanoate over 32 hours without any loss in performance displaying a STY of $121 \text{ g L}^{-1} \text{ h}^{-1}$. A longer run (123 h) exhibited an astonishing cofactor turnover number of 12855 mol mol^{-1} which represents a step forward compared to previous reports.^{17–19}

Amine dehydrogenases (AmDH) enable the synthesis of chiral amines from cheap ammonium salts as amine donors. Unfortunately, this reaction is commonly hampered by substrate and product inhibition. Immobilisation and continuous flow helps to address these problems, as was recently shown.²⁰ The asymmetric reductive amination of 5-methyl-2-hexanone was achieved by co-immobilisation of an amine

dehydrogenase (AmDH) and FDH onto Nuvia IMAC (immobilised metal affinity chromatography) resin from BioRad (Fig. 13).

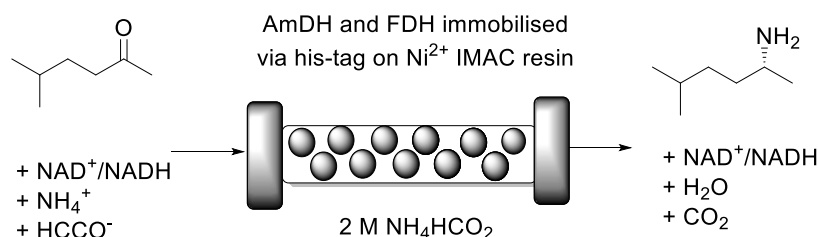


Fig. 13 Reductive amination of 5-methyl-2-hexanone with cofactor regeneration catalysed by immobilised AmDH and immobilised FDH in aqueous ammonium formate buffer. Ratio ketone to NAD⁺ 10:1

By immobilising both his-tagged enzymes to Ni²⁺ on the surface of the carrier, the synthesis of (*R*)-5-methyl-2-aminohexane in a packed bed reactor became possible. This setup displayed a STY of 107 g L⁻¹ day⁻¹ at 48% of conversion moving up to 443 g L⁻¹ day⁻¹ at 24% of conversion. Remarkably the flow system remained operational for more than 120 hours.

Earlier the continuous synthesis of 4-fluoroamphetamine under aqueous conditions catalysed by co-immobilised AmDH and FDH was reported.⁷⁸ EziG Amber, a controlled porosity glass carrier with Fe³⁺ on the surface for his-tag binding was used in a packed bed reactor. This system displayed a STY in the same range (300 g L⁻¹ day⁻¹), however a rapid enzyme deactivation was observed after 6 hours. In both examples low cofactor concentrations could be used and it was recycled during the reaction. Nonetheless, the cofactor was not immobilised and thus finally lost.

Recently, the cofactor regeneration problem in flow was beautifully addressed by applying an enzyme engineering approach.¹⁷ A three step cascade was employed for the conversion of glycerol to a precursor of *D*-fagomine (Fig. 14). In each step one enzyme reaction is performed by multi-enzyme modules. The modules consist of the catalytically active enzyme, if required the recycling enzyme and an esterase (Est) that reacts with the carrier to covalently immobilise the multi-enzyme modules.

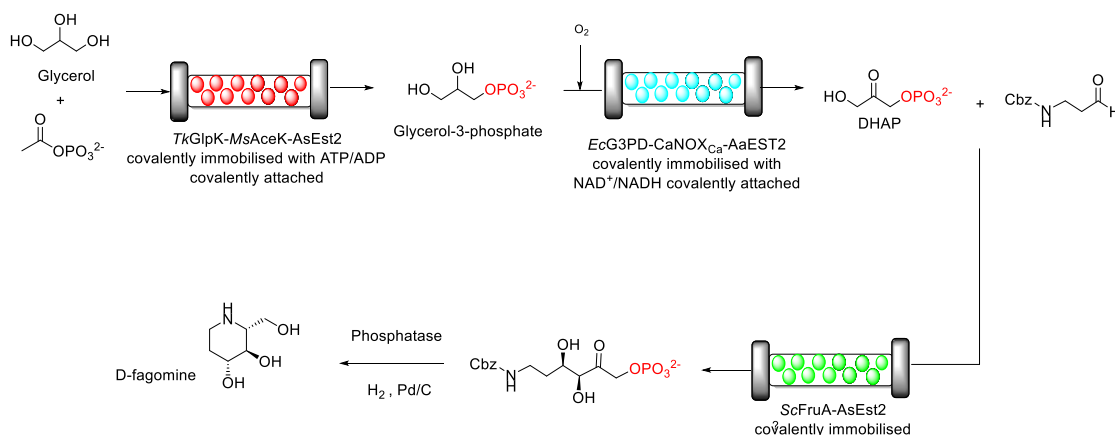


Fig. 14 Cascade synthesis of D-fagomine in continuous flow in aqueous medium. The cofactors were covalently attached to the catalysts via a specific thiol group. The modules of two or three enzymes are attached to the carrier via a covalent linker between AaEST2 and the carrier.

Thus, two three-enzyme and one two-enzyme modules are covalently attached to the carriers, each combination in a separate reactor. The two cofactors (ATP and NAD⁺) required were functionalised for the covalent attachment to the multi-enzymes modules with a long PEG-linker at the adenine. This linker allows the movement of the cofactor between the catalytic and cofactor recycling enzymes of the respective module. Subsequently, each cofactor was tethered to the protein linker between the catalytic and the recycling enzyme via an accessible thiol group. The key distinction of this set up is that the cofactor was immobilised to a specific amino acid close to catalytic and recycling enzymes whereas in previous reports the linkage was not specific.^{79,80}

First, glycerol was phosphorylated to glycerol-3-phosphate by *Thermococcus kodakarensis* glycerol kinase (*TkGlpK*) and for the ATP regeneration *Mycobacterium smegmatis* acetate kinase (*MsAceK*) was used. Secondly, *E. coli* glycerol-3-phosphate dehydrogenase (*EcG3PD*) performed the oxidation of glycerol-3-phosphate to dihydroxyacetone phosphate (DHAP) and the cofactor NAD⁺ was regenerated by an NADH oxidase from *Clostridium aminovalericum* (*CaNOX*). Finally, an aldol reaction catalysed by a monomeric FruA from *Staphylococcus carnosus* produced the desired product, precursor of D-fagomine, with excellent STY (70 g L⁻¹ h⁻¹ g⁻¹) and astonishing high cofactor turnovers (16848 for ATP and 10839 for NAD⁺). Cofactor dependent enzymes are important biocatalysts for synthesis. When the cofactor is regenerated during the catalytic cycle such as PLP or FAD the main concern is to avoid leaching of the cofactor to the reaction media. The use of organic solvents has been reported as an important tool to circumvent this limitation. When

the cofactor is not regenerated during the catalytic cycle, the implementation of a cofactor recycling system is required. For this co-immobilisation of enzymes and cofactor is an attractive approach. However, the efficiency of this recycling system is limited ($TTN_{\text{NADPH}} = 1076$ and $TTN_{\text{NAD}^+} = 85$).^{21,22} Higher cofactor recycling efficiency has been reported by using membrane technology ($TTN_{\text{NADPH}} = 12855$).¹⁶ Nevertheless, the high cost of ultra or nanofiltration technologies impair their economic viability. Finally, the immobilisation of cofactors of either type using a protein engineering approach demonstrated to be as efficient as the use of membrane technology reaching a $TTN_{\text{ATP}} = 16848$ and $TTN_{\text{NAD}^+} = 10839$.¹⁷

2.6 Conclusions

Immobilisation and flow chemistry are important tools for the further development of biocatalysis. Process intensification, better control of the processes, reduced reactor volumes and therefore increased safety are advantages commonly reported in organic, biphasic and aqueous systems. To fully appreciate the advantages and to also probe them rigorously solid metrics are essential.

Similarly, large steps have been made to address the cofactor recycling challenge in flow. Co-immobilisation of enzymes and cofactors, membrane based separation and protein engineering techniques have allowed the development of efficient regeneration systems for challenging cascade reactions with cofactor dependent enzymes. Pronounced progress to answer the two challenges, enzyme immobilisation and prevention of leaching of enzyme or cofactor (including metals) during the flow process, have been made. Overall, the implementation of enzyme immobilisation and flow chemistry allow for more efficient, safe and thus green and environmentally friendly processes.

References

1. P. Anastas and N. Eghbali, *Chem. Soc. Rev.*, **2010**, 39, 301–312.
2. M. Santi, L. Sancineto, V. Nascimento, J. Braun Azeredo, E. V. M. Orozco, L. H. Andrade, H. Gröger and C. Santi, *Int. J. Mol. Sci.*, **2021**, 22, 990.
3. S. G. Newman and K. F. Jensen, *Green Chem.*, **2013**, 15, 1456–1472.
4. R. A. Sheldon and J. M. Woodley, *Chem. Rev.*, **2018**, 118, 2, 801–838.
5. F. Ferlin, D. Lanari, and L. Vaccaro, *Green Chem.*, **2020**, 2, 5937–5955

6. V. Sans, *Current Opinion in Green and Sustainable Chemistry*, **2020**, 25, 100367.
7. E. J. S. Brás, V. Chu, J. P. Conde and P. Fernandes, *React. Chem. Eng.*, **2021**, 6, 815–827.
8. B. Bouchaut, L. Asveld, U. Hanefeld and A. Vlierboom. *Int. J. Environ. Res. Public Health*, **2021**, 18, 1963.
9. W. J. Yoo, H. Ishitani, Y. Saito, B. Laroche and S. Kobayashi. *J. Org. Chem.* **2020**, 85, 5132–5145.
10. K. Faber, *Biotransformations in Organic Chemistry*, **2018**, 7th ed., Springer Nature: Switzerland,; pp. 224-233.
11. U. Hanefeld, *Chem. Soc. Rev.*, **2013**, 42, 6308—6321.
12. M. T. de Martino, F. Tonin, V. R. L. J. Bloemendal, U. Hanefeld, F. P. J. T. Rutjes and J. C. M. van Hest, *RSC Adv.*, 2021, 11, 21857–21861.
13. U. Hanefeld, L. Gardossi and E. Magner, *Chem. Soc. Rev.*, **2009**, 38, 453–468.
14. R. A. Sheldon and S. van Pelt, *Chem. Soc. Rev.*, **2013**, 42, 6223.
15. A. Basso and S. Serban, *Molecular Catalysis*, **2019**, 479, 110607.
16. B. Baumer, T. Classen, M. Pohl and J. Pietruszka. *Adv. Synth. Catal.*, **2020**, 362, 2894– 2901.
17. J. Hartley, C. C. Williams, J. A. Scoble, Q. I. Churches, A. North, N. G. French, T. Nebl, G. Coia, A. C. Warden, G. Simpson, A. R. Frazer, C. N. Jensen, N. J. Turner and C. Scott, *Nature Catalysis*, **2019**, 2, 1006–1015.
18. A. Šalić and B. Zelić, *RSC Adv.*, **2014**, 4, 41714–41721.
19. M. L. Contente and F. Paradisi, *Nature Catalysis*, **2018**, 1, 452–459.
20. R. D. Franklin, J. A. Whitley, A. A. Caparco, B. R. Bommarius, J. A. Champion, A. S. Bommarius, *Chemical Engineering Journal*, **2021**, 407, 127065.
21. S. Velasco-Lozano, A. I. Benítez-Mateos and F. López-Gallego, *Angew. Chem. Int. Ed.*, **2017**, 56, 771 –775.
22. I. Benítez-Mateos, E. San Sebastian, N. Ríos-Lombardía, F. Morís, J. González-Sabín and F. López-Gallego, *Chem. Eur. J.*, **2017**, 23, 16843 – 16852.
23. P. De Santis, L. E. Meyer and S. Kara. *React. Chem. Eng.*, **2020**, 5, 2155–2184.

24. L. Gardossi, P. B. Poulsen, A. Ballesteros, K. Hult, V. K. Svedas, Đ. Vasic-Racki, G. Carrea, A. Magnusson, A. Schmid, R. Wohlgemuth and P. J. Halling, *Trends in Biotechnology*, **2010**, 28, 171–180.
25. M. P. van der Helm, P. Bracco, H. Busch, K. Szymańska, A. Jarzębski and U. Hanefeld, *Catal. Sci. Technol.*, **2019**, 9, 1189–1200.
26. J. Coloma, Y. Guiavarc'h, P. L. Hagedoorn and U. Hanefeld, *Catal. Sci. Technol.*, **2020**, 10, 3613–3621.
27. R. A. Sheldon, M. Wallau, I. W. C. E. Arends and U. Schuchardt. *Acc. Chem. Res.*, **1998**, 31, 485-493.
28. L. Dettori, F. Vibert, Y. Guiavarc'h, S. Delaunay, C. Humeau, J.L. Blin, I. Chevalot, *Microporous and Mesoporous Materials*, **2018**, 267, 24–34.
29. M. C. Bourkaib, P. Gaudin, F. Vibert, Y. Guiavarc'h, S. Delaunay, X. Framboisier, C. Humeau, I. Chevalot, J.-L. Blin, *Microporous and Mesoporous Materials*, **2021**, 323, 111226.
30. H. H. P. Yiu and P. A. Wright, *J. Mater. Chem.*, **2005**, 15, 3690–3700.
31. S. Hudson, J. Cooney and E. Magner. *Angew. Chem. Int. Ed.*, **2008**, 47, 8582 – 8594.
32. J. M. Bolivar, A. Hidalgo, L. Sanchez-Ruiloba, J. Berenguer, J. M. Guisana, F. Lopez-Gallego. *Journal of Biotechnology*, **2011**, 155, 412– 420.
33. L. Tamborini, P. Fernandes, F. Paradisi and F. Molinari. *Trends in Biotechnology*, **2018**, 36, 73 – 88.
34. M. P. Thompson, I. Peñafiel, S. C. Cosgrove and N. J. Turner, *Org. Process Res. Dev.*, **2019**, 23, 9–18.
35. C. M. Alder, J. D. Hayler, R. K. Henderson, A. M. Redman, L. Shukla, L. E. Shuster, H. F. Sneddon, *Green Chem.*, **2016**, 18, 3879–3890.
36. Roger A. Sheldon, *Green Chem.*, **2017**, 19, 18–43.
37. P. Domínguez de María and F. Hollmann, *Front. Microbiol.*, **2015**, 6, 1257.
38. E. M. M. Abdelraheem, H. Busch, U. Hanefeld, and F. Tonin, *React. Chem. Eng.*, **2019**, 4, 1878–1894.
39. M. Villela Filho, T. Stillger, M. Müller, A. Liese and C. Wandrey, *Angew. Chem. Int.*, **2003**, 42, 2993 – 2996.
40. A. Zaks and A.M. Klibanov, *Science*, **1984**, 224, 1249-1251
41. E. Bourquelot, M. Bridel, *Ann. Chim. Phys.* **1913**, 145.
42. A. M. Klibanov, *Nature*, **2001**, 409, 241-246.

43. M. M. C. H. van Schie, J. D. Spöring, M. Bocola, P. Domínguez de María and D. Rother, *Green Chem.*, **2021**, 23, 3191–3206.
44. P. Bracco, N. van Midden, E. Arango, G. Torrelo, V. Ferrario, L. Gardossi and U. Hanefeld, *Catalysts*, **2020**, 10, 308.
45. P. Bracco, H. Busch, J. von Langermann and U. Hanefeld, *Org. Biomol. Chem.*, 2016, **14**, 6375–6389.
46. D. Costes, E. Wehtje, P. Adlercreutz, *Enzyme and Microbial Technology*, **1999**, 25, 384–391.
47. P. Bracco, G. Torrelo, S. Noordam, G. de Jong and U. Hanefeld, *Catalysts*, **2018**, 8, 287.
48. D. Okrob, M. Paravidino, R. V. A. Orru, W. Wiechert, U. Hanefeld and M. Pohl, *Adv. Synth. Catal.*, **2011**, 353, 2399 – 2408
49. G. Torrelo, N. van Midden, R. Stloukal and U. Hanefeld, *ChemCatChem*, **2014**, 6, 1096 – 1102.
50. M. Paravidino, M. J. Sorgedraeger, R. V. A. Orru and U. Hanefeld, *Chem. Eur. J.*, 2010, **16**, 7596 – 7604.
51. A. Brahma, B. Musio, U. Ismayilova, N. Nikbin, S. B. Kamptmann, P. Siegert, G. E. Jeromin, S. V. Ley, M. Pohl, *Synlett*, **2015**, 27, 262–266.
52. J. Coloma, T. Lugtenburg, M. Afendi, M. Lazzarotto, P. Bracco, P. L. Hagedoorn, L. Gardossi and U. Hanefeld, *Catalysts*, **2020**, 10, 899.
53. T. Yu, Z. Ding, W. Nie, J. Jiao, H. Zhang, Q. Zhang, C. Xue, X. Duan, Y. M. A. Yamada and P. Li, *Chem. Eur. J.*, **2020**, 26, 5729 – 5747.
54. Y. Zhu, Q. Chen, L. Shao, Y. Jiacef and X. Zhang, *React. Chem. Eng.*, **2020**, 5, 9-32.
55. K. Szymańska, M. Pietrowska, J. Kocurek, K. Maresz, A. Koreniuk, J. Mrowiec-Białon, P. Widłak, E. Magner, A. Jarzębski, *Chemical Engineering Journal*, **2016**, 287, 148–154.
56. K. G. Hugentobler, H. Sharif, M. Rasparini, R. S. Heath and N. J. Turner, *Org. Biomol. Chem.*, **2016**, 14, 8064–8067.
57. K. G. Hugentobler, M. Rasparini, L. A. Thompson, K. E. Jolley, A. J. Blacker and N. J. Turner, *Org. Process Res. Dev.*, **2017**, 21, 195–199
58. I. Mathews, M. Soltis, M. Saldajeno, G. Ganshaw, R. Sala, W. Weyler, M. A. Cervin, G. Whited and R. Bott, *Biochemistry*, 2007, **46**, 8969-8979.

59. L. Wiermans, S. Hofzumahaus, C. Schotten, L. Weigand, M. Schallmeyer, A. Schallmeyer and P. Dominguez de María, *ChemCatChem*, **2013**, 5, 3719 – 3724.
60. K. Szymańska, K. Odrozek, A. Zniszczoł, G. Torrelo, V. Resch, U. Hanefeld and A. B. Jarzębski, *Catal. Sci. Technol.*, **2016**, 6, 4882 – 4888.
61. N. de Leeuw, G. Torrelo, C. Bisterfeld, V. Resch, L. Mestrom, E. Straulino, L. van der Weel and U. Hanefeld, *Adv. Synth. Catal.*, **2018**, 360, 242–249.
62. M. L. Contente, L. Tamborini, F. Molinari and F. Paradisi, *J. Flow Chem.*, **2020**, 10, 235–240.
63. M. Haridas, E. M. M. Abdelraheem, U. Hanefeld, *Appl Microbiol Biotechnol*, **2018**, 102, 9959–9971.
64. X. R. Wu, J. P. Jiang and Y. J. Chen, *ACS Catal.*, **2011**, 1, 1661–1664.
65. P. Hoyos, V. Pace and A. R. Alcántara, *Catalysts*, 2019, **9**, 260.
66. M. Schürmann, *Industrial Enzymes Applications*; Wiley-VCH: Weinheim, Germany, 2019; pp. 385–403.
67. S. Jennewein, M. Schürmann, M. Wolberg, I. Hilker, R. Luiten, M. Wubbolts and D. Mink, *Biotechnol. J.*, **2006**, 1, 537–548.
68. M. Dick, R. Hartmann, O. H. Weiergraber, C. Bisterfeld, DeSantis, J. Liu, D. P. Clark, A. Heine, I. A. Wilson and C. H. Wong, *Bioorg. Med. Chem.*, **2003**, 11, 43–52.
69. G. DeSantis, J. Liu, D. P. Clark, A. Heine, I. A. Wilson and C. H. Wong, *Bioorg. Med. Chem.*, 2003, 11, 43–52.
70. J. Li, J. Yang, Y. Men, Y. Zeng, Y. Zhu, C. Dong, Y. Sun and Y. Ma, *Appl Microbiol Biotechnol*, **2015**, 99, 7963–7972.
71. X. C. Jiao, J. Pan, G. C. Xu, X. D. Kong, Q. Chen, Z. J. Zhang and J. H. Xu, *Catal. Sci. Technol.*, **2015**, 5, 4048–4054.
72. B. Grabner, Y. Pokhilchuk and H. Gruber-Woelfler, *Catalysts*, **2020**, 10, 137.
73. L. Babich, A. F. Hartog, L. J. C. van Hemert, F. P. J. T. Rutjes and R. Wever, *ChemSusChem*, **2012**, 5, 2348 – 2353.
74. L. H. Andrade, W. Kroutil and T. F. Jamison, *Org. Lett.*, **2014**, 16, 6092 – 6095.
75. G. E. Jeromin, *Biotechnol. Lett.*, **2009**, 31, 1717–1721.

76. A. I. Benítez-Mateos, M. L. Contente, S. Velasco-Lozano, F. Paradisi and F. López-Gallego, *ACS Sustainable Chem. Eng.*, **2018**, 6, 13151–13159.
77. M. Krzek, H. L. van Beek, H. P. Permentier, R. Bischoff, M. W. Fraaije, *Enzyme and Microbial Technology*, **2016**, 82, 138–143.
78. M. P. Thompson, S. R. Derrington, R. S. Heath, J. L. Porter, J. Mangas-Sanchez, P. N. Devine, M. D. Truppo, N. J. Turner, *Tetrahedron*, **2019**, 75, 327-334.
79. T. Keatinge-Clay, *Nat. Prod. Rep.*, **2016**, 33, 141–149.
80. A. Nakamura, H. Minami, I. Urabe and H. Okada, *J. Ferment. Technol.*, **1988**, 66, 267-272.
81. M. Oláh, S. Suba, Z. Boros, P. Kovács, M. Gosselin, C. Gaudreault and G. Hornyánszky, *Periodica Polytechnica Chemical Engineering*, **2018**, 62, 519–532.
82. N. Adebar, J. E. Choi, L. Schober, R. Miyake, T. Iura, H. Kawabata and H. Gröger, *ChemCatChem*, **2019**, 11, 5788–5793.
83. B. Poznansky, L. A. Thompson, S. A. Warren, H. A. Reeve and K. A. Vincent. *Org. Process Res. Dev.*, **2020**, 24, 2281–2287.

3

Probing batch and continuous flow reactions in organic solvents: *Granulicella tundricola* Hydroxynitrile lyase (GtHNL)

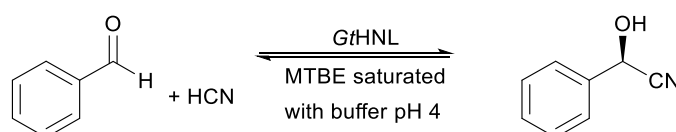
Granulicella tundricola hydroxynitrile lyase (GtHNL) is a manganese dependent cupin which catalyses the enantioselective synthesis of (*R*)-cyanohydrins. The GtHNL triple variant A40H/V42T/Q110H was immobilised on Celite R-633 by adsorption. The synthesis of (*R*)-mandelonitrile in a rotating bed reactor was compared to a continuous flow reactor. A batch reaction was used as reference system. The rotating bed reactor displayed a rate 1.7 times higher than the reference batch model. Moreover, similar conversion (96% after 4 hours) and recyclability were observed as compared to the reference system. The continuous flow reactor displayed rates 2 and 3 times higher than the rotating bed and the reference batch systems, respectively. Good conversions were achieved within minutes. The immobilised enzyme displayed excellent enantioselectivity and high operational stability under all evaluated conditions. Overall, GtHNL triple variant A40H/V42T/Q110H immobilised on Celite R-633 is an excellent catalyst for the synthesis of (*R*)-mandelonitrile with a great potential for continuous flow production of cyanohydrins.

This chapter is based on

José Coloma, Yann Guiavarc'h, Peter-Leon Hagedoorn and Ulf Hanefeld
Catal. Sci. Technol., **2020**, 10, 3613–3621. DOI: 10.1039/d0cy00604a

3.1 Introduction

Enzyme catalysed carbon–carbon bond forming reactions are important in organic chemistry to produce chiral compounds.^{1,2} In plants, hydroxynitrile lyases (HNLs) catalyse the cleavage of cyanohydrins into aldehydes or ketones releasing toxic hydrogen cyanide (HCN). This mechanism is a defense system against the attack of predators (cyanogenesis) and a source of nitrogen for the biosynthesis of L-asparagine (nitrogen fixation).^{3,4} The reverse reaction is of great interest as it enables the synthesis of chiral α -cyanohydrins (Scheme 1).



Scheme 1. GtHNL catalysed hydrocyanation of benzaldehyde yielding (*R*)-mandelonitrile.

The importance of cyanohydrins as platform molecules lies in their two functional groups, the hydroxyl and nitrile moiety, which can be converted into a variety of valuable chiral products such as α -hydroxy acids, primary and secondary β -hydroxy amines, α -hydroxy aldehydes or ketones, etc. All these compounds are known as platform molecules for the production of pharmaceutical and fine chemical products.^{1,5–8} Recently, a new manganese-dependent bacterial HNL was discovered in the soil bacterium *Granulicella tundricola* (GtHNL). The gene was heterologously expressed in *Escherichia coli* and the crystal structure was solved revealing a cupin fold.⁹ The wild type GtHNL (GtHNL-WT) catalysed the synthesis of (*R*)-mandelonitrile with a promising yield and enantioselectivity of 80% and 90% respectively. Site-saturation mutagenesis of active site amino acids produced a triple variant GtHNL-A40H/V42T/Q110H (GtHNL-3V) with a remarkable 490-fold-increase in specific activity in comparison to the wild type enzyme.¹⁰ EPR spectroscopy revealed an unusually high Lewis acidity for the Mn²⁺ as essential metal.¹¹ Moreover Mn²⁺ was bound more tightly in the triple variant than in the wild type enzyme, which resulted in higher stability and activity.

In this study, we describe the immobilisation of GtHNL-3V on Celite R-633, the silicate skeletons of diatoms,¹² for the synthesis of (*R*)-mandelonitrile in batch and continuous flow systems. Enzyme immobilisation plays an important role enhancing the enzyme

stability toward harsh conditions such as extreme pH values, organic solvents, high ionic strengths, etc. Additionally, it allows a straightforward enzyme separation from the reaction mixture as well as the operation in continuous flow processes while minimizing the product contamination with enzymes.^{12–14} Celite was used as a carrier for enzyme immobilisation as it is an environmentally friendly material that has been successfully employed for the immobilisation of several HNLs enabling the production of (*R*)- and (*S*)-cyanohydrins with good yield, enantioselectivity and recyclability.^{5,15–17}

Currently the vast majority of enzyme-catalysed conversions are performed in stirred tank reactors.² To achieve full conversion extended reaction times are often required (affecting the productivity). Rapid stirring is required to avoid diffusion limitations. Especially at industrial scales, this induces shear forces that affect enzyme stability.¹⁸ To overcome these limitations, synthesis in a rotating bed reactor (RBR) and continuous flow reactor (CFR) are gaining attention. RBR enables efficient stirring and percolation of the substrates through the immobilised enzyme bed. This is suggested to result in improved mass transfer without mechanical enzyme attrition.^{19,20} Biosynthesis in continuous flow is also becoming an attractive way to increase productivity, reduce enzyme inhibition and facilitate downstream processing.^{21–26} Additionally reaction volumes are reduced, increasing safety, in particular for toxic compounds such as cyanide.²⁷ Several enzymes have been tested in continuous flow systems such as HNLs,^{21,25} transaminases,^{26,28–30} oxidoreductases,^{31–33} and aldolases.^{34,35}

The aim of this work was to evaluate whether continuous flow reactions facilitate process intensification compared to a rotating bed reactor, reducing shear forces, improving stability and activity of the enzyme. For this purpose, *Gt*HNL-TV was immobilised on Celite R-633 and its catalytic performance and stability were evaluated in RBR and CFR and compared to a batch reaction under the same reaction conditions.

3.2 Results and Discussion

Celite is an environmentally benign siliceous carrier material, produced by diatoms, a type of microalgae.³⁸ Several HNLs were immobilised on this environmentally friendly material and performed better than on other carriers. *Prunus amygdalus* HNL (*Pa*HNL) immobilised on Celite was compared to Avicel,³⁹ controlled pore glass and

Sephadex,¹⁷ in all cases Celite was the best carrier in terms of enzymatic activity. *Hevea brasiliensis* HNL (*HbHNL*) immobilised on Celite gave rise to better enantioselectivity compared to Avicel and EP-700 (hydrophobic polyamide),⁴⁰ and the very acid sensitive *Arabidopsis thaliana* HNL (*AtHNL*) had enhanced stability towards acidic pH values and organic solvents when it was immobilised on Celite R-633.¹⁶ The ability of Celite to bind water, enabling a local environment surrounding the enzyme with organic solvents, might explain these results.^{38,41} Because of these favourable results and to ensure comparability with previous studies Celite R-633 was utilised as a carrier material.

3.2.1 Batch reactions

Both, purified *GtHNL*-WT and *GtHNL*-3V were immobilised on Celite R-633. All batch reactions were performed at 5°C since it was reported earlier⁹ that a significantly higher enantiomeric excess can be obtained under this condition compared to the reaction at 15 °C. After immobilisation, the *GtHNL*-3V showed considerably higher activity and selectivity compared to *GtHNL*-WT (Fig. 1), which is in line with earlier results obtained for the enzyme in solution.¹⁰

The specific activity of *GtHNL*-3V was $56.5 \pm 18 \text{ U mg}^{-1}$ which is 63 times higher compared to the wild type enzyme under the same reaction conditions. This can be ascribed to the additional histidines introduced at positions 40 and 110, improving the deprotonation of the hydrogen cyanide and giving rise to enhanced conversion and enantioselectivity.^{10,11} At the same time these mutations greatly improve the binding of the metal to the active site, indeed metal removal was very difficult.¹¹ Since *GtHNL*-3V proved to be a better catalyst than the wild type enzyme, only the variant enzyme henceforth was tested for the synthesis of (*R*)-mandelonitrile.

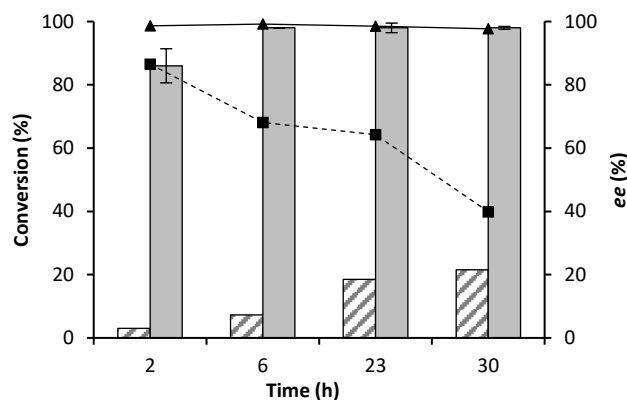


Figure 1. Synthesis of (*R*)-mandelonitrile using *GtHNL*-WT and *GtHNL*-3V. Conditions: ratio benzaldehyde : HCN in acetate buffered MTBE, pH 4, 1 : 4, 100 μ L benzaldehyde (1 mmol), 2 mL HCN solution in acetate buffered MTBE (1.5–2 M) pH 4, 27.5 μ L (0.1 mmol) 1,3,5-tri-isopropylbenzene as internal standard (I.S.), tea bag filled with immobilised enzyme (5 U) on 50 mg (0.1 U mg^{-1}) Celite R-633. The reaction was stirred at 1000 rpm at 5°C. Conversion WT (striped bars), conversion TV (grey bars), ee WT (dashed line), ee 3V (continuous line). Error bars correspond to the standard deviation of duplicate ($n=2$). *GtHNL*-WT conversions are single experiments.

Having established Celite R-633 as suitable carrier on which the enzyme displayed similar activity as in solution, a leaching test was performed (Fig. 2). In earlier studies the structurally unrelated *PaHNL* and *AtHNL* were found not to leach from Celite R-633.^{15,16} As was earlier shown for *AtHNL*¹⁶ the *GtHNL*-3V was found to be active in organic solvents and at low pH without immobilisation (Fig. S2).

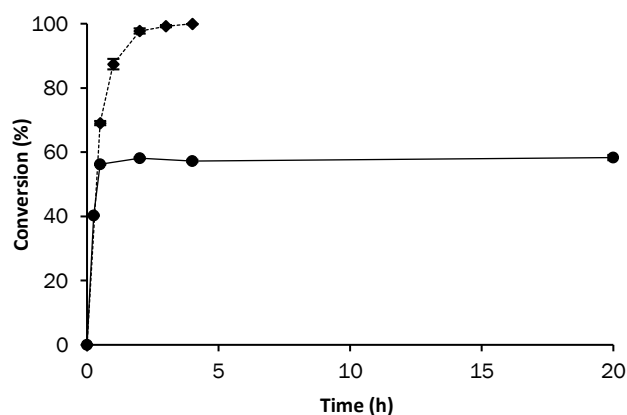


Figure 2. Leaching assay for *GtHNL*-3V immobilised on Celite R-633. Conditions: Ratio benzaldehyde : HCN in acetate buffered MTBE pH 4 ~ 1:4, benzaldehyde (100 μ L, 1 mmol), 2 ml HCN solution in acetate buffered MTBE (1.75 M) pH 4, 27.5 μ L (0.1 mmol) 1,3,5-tri-isopropylbenzene as I.S. and a tea bag filled with *GtHNL*-3V immobilised on 50 mg Celite R-633. The reaction was stirred at 700 rpm at 5°C. Diamonds and the dashed line is the enzyme catalysed reaction (50 U), dots and the solid line is the reaction where the immobilised enzyme (200 U) was removed after 30 min. Error bars correspond to the standard deviation of duplicate ($n=2$) HPLC samples of the single experiment.

However, it precipitated during the reaction making reuse impossible. In the leaching experiment, the immobilised enzyme was removed from the reaction medium after 30

minutes of enzyme catalysed conversion. A high enzyme-support ratio (4 U mg^{-1}) was used intentionally to clearly see any enzyme leaching to the reaction medium. After removal of the enzyme, the reaction did not proceed anymore, demonstrating that no active *GtHNL-3V* leached from the carrier into the reaction medium (Fig. 2). The hydrophilic characteristics of the enzyme-carrier and the insolubility of the enzyme in organic solvents explain this result.¹²

Having firmly established that *GtHNL-3V* was successfully immobilised on Celite R-633, the enzyme loading for the synthesis of (*R*)-mandelonitrile in batch reactions (BR) was studied. As described earlier for *PaHNL* the immobilised enzyme was placed tightly packed inside tea bags¹⁵ (Fig. S7, Table S1). Nearly complete conversion and excellent enantioselectivity ($ee > 99\%$) were achieved after 4 hours of reaction time, regardless of the enzyme loading (Fig. 3).

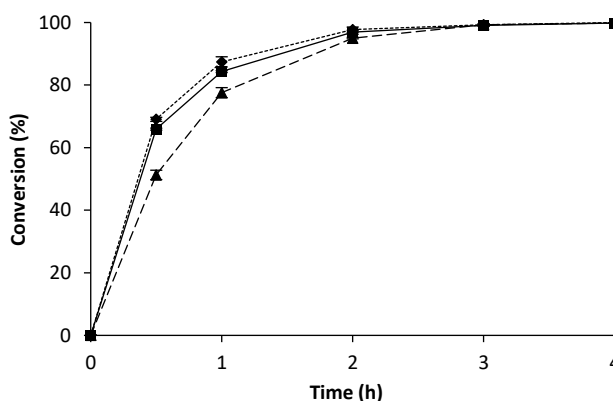


Figure 3. Synthesis of (*R*)-mandelonitrile using different enzyme loadings. Conditions: Ratio benzaldehyde : HCN in acetate buffered MTBE, pH 4, 1:4, benzaldehyde (100 μL , 1 mmol), 2 ml HCN solution in acetate buffered MTBE (1.75 M) pH 4, 27.5 μL (0.1 mmol) 1,3,5-tri-isopropylbenzene as I.S. and a tea bag filled with different amounts of *GtHNL-3V* immobilised on 50 mg Celite R-633. The reaction was stirred at 700 rpm at 5 $^{\circ}\text{C}$. 0.5 U/mg (squares and solid line), 1 U/mg (diamonds and dotted line), 2 U/mg (triangles and dashed line). Final $ee > 99\%$ in all three cases. Error bars correspond to the standard deviation of duplicate ($n=2$) HPLC samples of the single experiments.

Interestingly, higher enzyme loadings did not show faster conversion, indicating that the reaction is mass transfer limited at high enzyme loading. A recycling study was performed utilising 1 U mg^{-1} *GtHNL-3V* immobilised on Celite R-633. With this low catalyst loading any loss of activity will be observed directly while higher catalyst loading might mask an initial activity loss.^{5,15} The biocatalyst exhibited good recyclability, conversions gradually dropped to $> 70\%$ over all cycles but remarkable high enantioselectivity ($>99\%$) was observed during all 8 cycles (Table 1).

Table 1. Recycling of the G#HNL-3V immobilised on Celite R-633 (1 U/mg) in eight successive BR cycles.

Cycle	Conversion (%)	ee (<i>R</i>)-mandelonitrile (%)
1	98.0 ± 0.2	>99
2	90.0 ± 0.3	>99
3	88.0 ± 0.9	98.7
4	88.0 ± 0.1	>99
5	87.0 ± 0.1	>99
6	77.0 ± 0.7	>99
7	74.0 ± 1.0	>99
8	73.0 ± 0.4	>99

Conditions: Ratio benzaldehyde : HCN in buffered MTBE, pH 4, 1:4, 100 μ L benzaldehyde (1 mmol), 2 ml HCN solution in acetate buffered MTBE (1.5-2 M) pH 4, 27.5 μ L 1,3,5-tri-isopropylbenzene (0.1 mmol, internal standard), a tea bag filled with G#HNL-TV immobilised on 50 mg Celite R-633 (1U/mg = 50 U). The reaction was stirred at 700 rpm at 5°C; reaction time: 4h. The enzyme was washed for 1 minute with 100 mM acetate buffer saturated MTBE, pH 4, after each cycle.

With the BR as the reference point, the comparison to the RBR could be performed. The reaction volume was scaled up *circa* 40 times to evaluate the mass transfer influence on the kinetics of the reaction in a RBR. This device has been designed to improve mass transfer, combining the advantages of fixed bed and stirred tank reactors.⁴² At the same time it also displays the typical safety disadvantage of batch reactions; a large scale requires a large amount of a toxic compound in a vessel.²⁷ A first comparison between BR and RBR showed higher reaction rates for the BR (Fig. 4). Surprisingly, when the same immobilised enzyme was placed tightly packed in the above mentioned tea bags into the RBR the conversions and enantioselectivities were enhanced along the reaction times, displaying a similar feature to the batch reaction (Fig. 5). These results are unexpected since the RBR has been designed to boost the efficiency in biocatalytic reactions by reducing diffusion limitations. However, in an earlier study comparing a RBR and a stirred tank reactor, *i.e.* a BR; similar conversions were found in both cases. The transaminase and lipase catalysed kinetic resolution of (*R,S*)-1-phenylethylamine and (*R,S*)-1-phenylethanol respectively were utilised for that comparison.²⁰

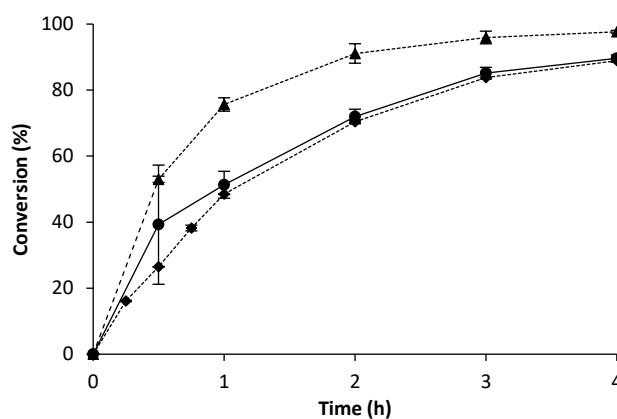


Fig. 4 Synthesis of (*R*)-mandelonitrile using *Gt*HNL-3V immobilised on Celite R-633 in BR and RBR. Reaction conditions RBR: ratio benzaldehyde : HCN in acetate buffered MTBE, pH 4, 1 : 4, 85 mL HCN (1.5–2 M), 4.25 mL (42 mmol) benzaldehyde, 1.16 mL (4.2 mmol) 1,3,5 tri-isopropylbenzene as I.S., immobilised enzyme on 773 mg Celite ($1 \text{ U mg}^{-1} = 773 \text{ U}$) loosely packed or unpacked, 700 rpm, 5 °C. Reaction conditions BR: ratio benzaldehyde : HCN in acetate buffered MTBE, pH 4, 1 : 4, 2 mL HCN (1.5–2 M), 100 μL (1 mmol) benzaldehyde, 27.5 μL (0.1 mmol) I.S., immobilised enzyme on 18 mg Celite R-633 ($1 \text{ U mg}^{-1} = 18 \text{ U}$) tightly packed. Conversion RBR with loosely packed enzyme (diamonds and dotted line, final ee > 99%), conversion RBR with not packed enzyme (circles and solid line, final ee = 85%), conversion BR with tightly packed enzyme (triangles and dashed line, final ee = 98%). Error bars correspond to the standard deviation of duplicates ($n = 2$).

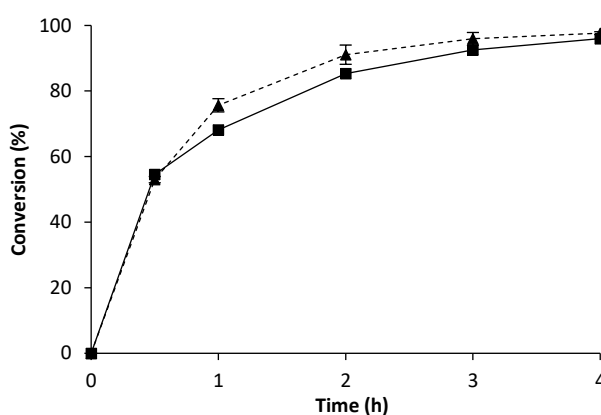


Figure. 5 Comparison between RBR and BR for the synthesis of (*R*)-mandelonitrile using *Gt*HNL-3V immobilised on Celite R-633 always tightly packed. Reaction conditions RBR: ratio benzaldehyde : HCN in acetate buffered MTBE, pH 4, 1 : 4, 85 mL HCN (1.5–2 M), 4.25 mL (42 mmol) benzaldehyde, 1.16 mL (4.2 mmol) 1,3,5 tri-isopropylbenzene as I.S., immobilised enzyme on 773 mg Celite ($1 \text{ U mg}^{-1} = 773 \text{ U}$), 700 rpm, 5°C reaction conditions BR: ratio benzaldehyde : HCN in acetate buffered MTBE, pH 4, 1 : 4, 2 mL HCN (1.5–2 M), 100 μL (1 mmol) benzaldehyde, 27.5 μL (0.1 mmol) I.S., immobilised enzyme on 18 mg Celite ($1 \text{ U mg}^{-1} = 18 \text{ U}$). Conversion BR with tightly packed enzyme (triangles and dashed line, final ee = 98%), conversion RBR with tightly packed enzyme (squares and solid line, final ee = 99%). Error bars correspond to the standard deviation of duplicates ($n = 2$).

Tables 2 and 3 show a clear effect of the packing on the *Gt*HNL-3V recyclability in the RBR. After the first cycle without bag (Table 3), the immobilised enzyme was placed tightly packed into tea bags. Tightly packed enzymes were more stable than loosely

packed enzymes over 4 cycles. A possible explanation might be higher shear forces exerted on the *GtHNL-TV* immobilised on Celite freely placed or loosely packed into the RBR, when compared to tightly packed biocatalyst. Shear forces might result in breaking or stretching molecular bonds. Recovery of the enzyme can occur when the shear force is removed.⁴³ A tightly packed enzyme is better protected against shear forces. The decrease in enantiomeric excess during the first cycle (Table 3, cycle 1), can be explained by a more pronounced chemical background reaction when the immobilised enzyme is placed freely inside the RBR.¹⁵

Table 2. Recycling of *GtHNL-3V* immobilised on Celite R-633 (1 U/mg) in four successive RBR cycles. Loosely packed enzyme in tea bags.

Cycle	Conversion (%)	ee (<i>R</i>)-mandelonitrile (%)
1	88.9 ± 0.2	>99
2	79.0 ± 0.6	>99
3	82.9 ± 0.3	>99
4	60.7 ± 0.2	>99

Conditions: 85 mL HCN (1.5 - 2 M) in 100 mM acetate buffered MTBE, pH 4, 4.25 mL (42 mmol) benzaldehyde, 1.16 mL (4.2 mmol) 1,3,5 tri-isopropylbenzene as internal standard (I.S.), immobilised enzyme on 773 mg Celite (1 U/mg = 773 U), 700 rpm, 5°C. The enzyme was washed for 1 minute with acetate buffer saturated MTBE, pH 4, after each cycle.

Table 3. Recycling of *GtHNL-3V* immobilised on Celite R-633 (1 U/mg) in four successive RBR Cycles. Tightly packed enzyme in tea bags.

Cycle	Conversion (%)	ee (<i>R</i>)-mandelonitrile (%)
1 ^a	90.3 ± 0.3	85.4
2 ^b	96.0 ± 0.2	99.3
3 ^b	93.5 ± 0.3	96.3
4 ^b	84.8 ± 0.2	99.4

Conditions: 85 mL HCN (1.5–2 M) in acetate buffered MTBE, 4.25 mL (42 mmol) benzaldehyde, 1.16 mL (4.2 mmol) 1,3,5 tri-isopropylbenzene as I.S., immobilised enzyme on 773 mg Celite (1 U mg⁻¹ = 773 U), 700 rpm, 5 °C. The enzyme was washed for 1 minute with acetate buffer saturated MTBE, pH 4, after each cycle. ^a Immobilised *GtHNL-3V* was used without tea bags. ^b Immobilised *GtHNL-3V* was placed in tightly packed tea bags

For *Pa*HNL immobilised on Celite this influence of the packing was observed, too.¹⁵ A faster racemic background reaction for loosely packed enzyme was observed in that case as well. Substrate inhibition affecting the RBR reaction by blocking the enzyme active site due to local high concentrations of benzaldehyde or HCN was ruled out by kinetic measurements (Fig. S3). These results (Tables 1–3) show that the recyclability of the enzyme is similar in both batch systems (BR and RBR) when using tightly packed, immobilised enzyme.

3.2.2 Continuous flow reaction

To maximally exploit the potential safety advantage of the flow chemistry, the synthesis of (*R*)-mandelonitrile was evaluated at different flow rates in a CFR of just 1 mL. As expected, a decrease in conversion from 97% to 63% (Fig. 6) was observed by increasing the flow rate from 0.1 mL min⁻¹ to 1.0 mL min⁻¹ (residence time: 240 s to 24 s).^{21,40} More remarkably the enantioselectivity was not influenced although all these experiments were performed at room-temperature, while cooling to 5°C had been necessary to achieve good enantioselectivity in the BR and RBR.

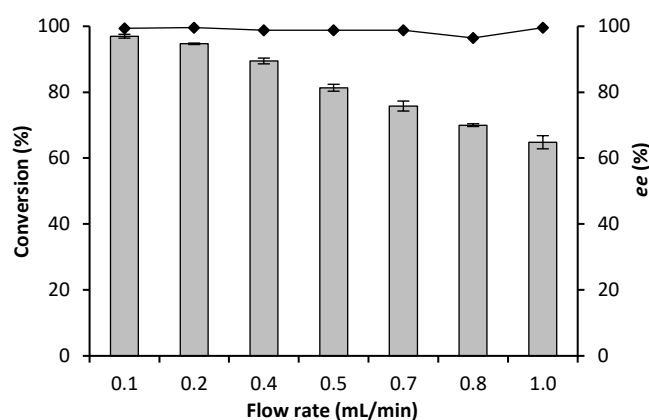


Figure 6. Synthesis of (*R*)-mandelonitrile using *Gt*HNL-3V immobilised on Celite R-633 in CFR. Conditions: ratio benzaldehyde : HCN in buffered MTBE, pH 4, 1 : 4, benzaldehyde (0.5 M), HCN solution in acetate buffered MTBE (1.5–2 M) pH 4, 1,3,5 tri-isopropylbenzene (50 mM, I.S.) with *Gt*HNL-3V immobilised on 150 mg Celite R-633 (1 U mg⁻¹ = 150 U). Reactions were performed at room temperature. Conversion (bars) and enantiomeric excess (solid line). Error bars correspond to the standard deviation of duplicates ($n = 2$)

The stability of *Gt*HNL-3V was evaluated at 0.1 and 0.2 mL min⁻¹, conditions under which complete conversion was (just) observed. Any weaknesses of the system will immediately be revealed at these flow rates. High stability was observed during 13 and 8 hours respectively (Fig. 7 and 8). Remarkably the enantioselectivity remained excellent even when the conversion dropped due to enzyme deactivation. In the case

of *Manihot esculenta* HNL (*MeHNL*) and *Hevea brasiliensis* HNL (*HbHNL*), immobilised on siliceous monoliths, this was not the case, as loss of activity was accompanied by loss of enantioselectivity.²¹

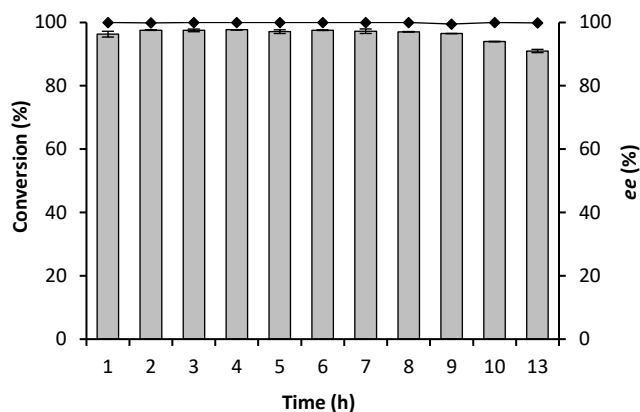


Figure 7. Stability of *GtHNL-3V* for the synthesis of (*R*)-mandelonitrile in CFR at 0.1 mL min⁻¹. Conditions: ratio benzaldehyde : HCN in buffered MTBE, pH 4, 1 : 4, benzaldehyde (0.5 M), HCN solution in acetate buffered MTBE (1.5–2 M) pH 4, 1,3,5 tri-isopropylbenzene (50 mM, I.S.), with *GtHNL-3V* immobilised on 150 mg Celite R-633 (1 U mg⁻¹ = 150 U). Conversion (bars) and enantiomeric excess (solid line). Error bars correspond to the standard deviation of duplicates ($n = 2$)

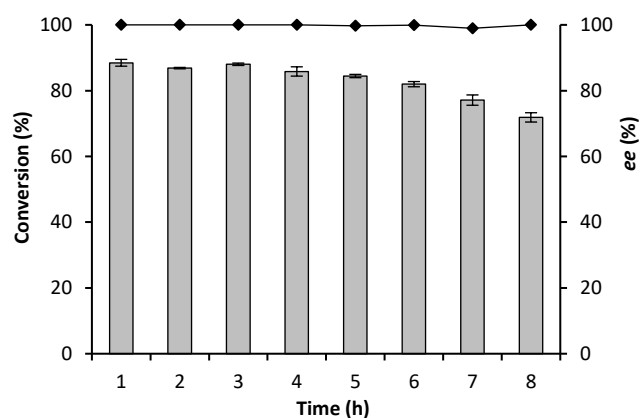


Figure. 8 Stability of *GtHNL-3V* for the synthesis of (*R*)-mandelonitrile in CFR at 0.2 mL min⁻¹. Conditions: ratio benzaldehyde : HCN in buffered MTBE, pH 4, 1 : 4, benzaldehyde (0.5 M), HCN solution in acetate buffered MTBE (1.5–2 M) pH 4, 1,3,5 tri-isopropylbenzene (50 mM, I.S.), with *GtHNL-3V* immobilised on 150 mg Celite R-633 (1 U mg⁻¹ = 150 U). Conversion (bars) and enantiomeric excess (solid line). Error bars correspond to the standard deviation of duplicates ($n = 2$)

The biocatalytic synthesis of (*R*)-mandelonitrile in continuous flow using *AtHNL* immobilised on Celite R-633 has been reported previously.²⁵ With a packed bed reactor (microbore column 3 mm/50 mm), the best conversion (85%) and enantioselectivity (96%) were achieved with 25 mg of pure *AtHNL* on 100 mg of Celite

at a residence time of 35.3 min. Clearly, the conversions reported here (Fig. 6) are a step forward.

3.2.3 Comparison of the reactors

The different reactors can best be compared via specific rates and productivity, expressed as space–time yield (STY). In batch reactions, the RBR showed a specific rate 1.7 times higher compared to the BR, whereas the CFR proved to be 3 and 2 times faster than BR and RBR respectively (Table 4).

Table 4. Specific rates for the different reactor types; data points from Fig. 5 and 6

	Batch reactions		CFR	
	BR	RBR	0.7 mL/min	0.8 mL/min
Specific rates (mmol min ⁻¹ g _{enz} ⁻¹)	3.51 ^a	6.30 ^a	7.93 ^b	8.37 ^c
	2.51 ^b	3.93 ^c		

^a Calculated at ~54% conversion. ^b Calculated at ~76% conversion. ^c Calculated at ~70% conversion.

Importantly, almost full conversion and excellent enantioselectivities were obtained within minutes instead of 4 hours (batch reactions). In addition to this much higher rate, the substantially lower reaction volume in the CFR constitutes a significant improvement of safety.²⁷ The increase in productivity of the CFR can also be explained by the apparent turnover number (k_{app}) observed. BR and RBR displayed k_{app} from 0.77 s⁻¹ and 1.32 s⁻¹ respectively. The CFR exhibited 1.4 s⁻¹ (0.1 mL min⁻¹) to 9.2 s⁻¹ (1 mL min⁻¹) (Fig. 6) without reaching the maximum k_{app} , thus the enzyme is capable of converting even more substrate. In spite of the large macropores of Celite R-633 (6.5 μm average diameter),⁴⁴ which are favourable to internal mass transfer, differences between the reactor types become apparent. In all reactors with heterogeneous processes such as with these mesoporous materials, some boundary layer limiting substrate and product transfer occurs. This contributes to mass transfer limitations and consequently, turnover rate limitations. Increased flow rates improve the k_{app} due to a reduction and almost depletion of this boundary layer, enabling more substrate to be exposed to the enzyme active site, explaining the advantage of CFR over other reactors.^{45–47} The STY, a parameter frequently used to evaluate the

productivity of different systems normalized to a volume of 1 L, shows that the use of the continuous flow system resulted in a prominent increase in (*R*)-mandelonitrile synthesized ($\text{g}_{\text{product}} \text{h}^{-1} \text{L}^{-1}$). In steady state conditions, both batch reactions (BR and RBR) achieved *circa* $12 \text{ g h}^{-1} \text{L}^{-1}$ whereas CFR at 0.1 mL min^{-1} reached $784 \text{ g h}^{-1} \text{L}^{-1}$. This represents 65 times more product in total. Importantly, increasing the flow rate enables higher specific rates and therefore higher STY without significantly affecting the enzyme stability (Fig. 7 and 8). However, it is worthy to point out that higher flow rates lead to unreacted substrate, which may make downstream processing more difficult. Taking into account the amount of enzyme used for the reaction, the STY was $23 \text{ g}_{\text{product}} \text{h}^{-1} \text{L}^{-1} \text{ mg}_{\text{enz}}^{-1}$ at 0.1 mL min^{-1} up to $156 \text{ g}_{\text{product}} \text{h}^{-1} \text{L}^{-1} \text{ mg}_{\text{enz}}^{-1}$ at 1 mL min^{-1} , which shows excellent productivity with a low enzyme loading. Recently, the performance of *MeHNL* and *HbHNL* immobilised on porous, monolithic silica supports has been reported in a continuous flow microreactor. Full conversion and high enantioselectivity were achieved within minutes, but the enzyme stability diminished after 7 and 3 hours operation, respectively. Furthermore, a drastic improvement of the catalytic performance was observed as compared with the batch system, with a 8-fold increase of the specific reaction rate.²¹

3.3 Conclusions

GtHNL-3V showed a better catalytic performance for the production of (*R*)-mandelonitrile compared to the wild type enzyme. Nearly complete conversion and high enantioselectivity were achieved in both BR and RBR systems with tightly packed enzyme on a readily available and environmentally benign carrier, Celite R-633. The RBR did not greatly enhance the reaction rate and showed only a 1.7-fold increase in specific rate at 54% conversion but similar STY ($\text{g}_{\text{product}} \text{h}^{-1} \text{L}^{-1}$). By switching to a CFR, full conversions and excellent enantioselectivity were obtained within minutes. Furthermore, continuous flow enabled to operate at higher k_{app} which resulted in a tremendous increase in STY compared to both batch systems evaluated in this study. Additionally, the much smaller reaction volume improves safety at the same time. The high activity and enantioselectivity of immobilised *GtHNL-3V* together with the enhanced stability in batch and continuous flow systems outperform what has been reported for other HNLs and makes this enzyme a new competitor for the production of chiral cyanohydrins

3.4 Experimental section

3.4.1 Chemicals

All chemicals were bought from Sigma Aldrich (Schnelldorf, Germany) unless reported otherwise. Isopropanol and heptane were of HPLC grade ($\geq 99\%$) and used as HPLC solvents. 1,3,5-tri-isopropylbenzene (97%) was from Fluka Chemie (Buchs, Switzerland). Potassium cyanide (KCN, 97%) from J.T. Baker (Deventer, The Netherlands) was used as cyanide source in the HCN solution. (\pm)-Mandelonitrile from Across Organics (New Jersey, USA) was purified by flash chromatography (PE/MTBE 9:1/3:7).

3.4.2 Heterologous production of wild type GtHNL (GtHNL-WT)

The pET-28a-GtHNL expression plasmid containing the GtHNL gene codon optimized for *E. coli* (SI-A) was obtained from Bio Basic INC (Canada). *E. coli* BL21(DE3) was transformed with the expression plasmid. The production of GtHNL-WT was performed according to literature.¹⁰ A preculture was prepared by inoculating one single colony of *E. coli* BL21(DE3)-pET28aGtHNL in 10 mL of LB medium with kanamycin ($40 \mu\text{g mL}^{-1}$) and incubated overnight (New Brunswick Scientific Incubator Shaker Excella E24 Series) at 37°C , 180 rpm. Then, this preculture was used for the inoculation of 1 L of LB medium containing kanamycin ($40 \mu\text{g mL}^{-1}$) and incubated at 37°C , 120 rpm. When the OD_{600} reached 0.7–0.9 the gene expression was induced by adding 1 mL of 0.1 M isopropyl β -D-thiogalactoside (IPTG) per liter of culture (0.1 mM IPTG final concentration) and cultivation was continued at 25°C , 120 rpm for 22 hours. Moreover, $100 \mu\text{L}$ of 1 M MnCl_2 was added per liter of culture at the induction time (0.1 mM Mn^{2+} final concentration). Cells were harvested at 4°C , 3600 rpm during 20 minutes (Sorvall RC6, Thermo Scientific). The supernatant was discarded and the pellet was washed with 20 mL of 10 mM sodium phosphate buffer, pH 7, and stored at -80°C .

3.4.3 Cloning and expression of triple variant GtHNL-A40H/V42T/Q110H (GtHNL-3V)

The pUC57 shuttle vector containing the gene encoding GtHNL-A40H/V42T/Q110H, codon optimised for *E. coli* (SI-A) was obtained from Bio Basic INC (Canada) and used to transform *E. coli* Top 10. The gene encoding GtHNL-A40H/V42T/Q110H gene was

cloned into pET28a expression vector using NcoI and HindIII restriction enzymes. The resulting pET28a-GtHNL-A40H/V42T/Q110H expression vector was cloned into *E. coli* TOP 10 to obtain a stable host for plasmid DNA. Finally, pET28a-GtHNL-A40H/V42T/Q110H was used to transform the expression host *E. coli* BL21(DE3). The cultivation of the expression strain was performed in TB (terrific broth) medium following the same procedure described before for the GtHNL wild type.

3.4.4 Purification of GtHNL-WT and GtHNL-3V

GtHNL-WT was purified according to the literature¹⁰ with slight modifications. The pellets were resuspended in lysis buffer A (50 mM bis-Tris buffer + 30 mM NaCl + DNase) pH 6.8, respectively, and lysed in a cell disruptor (Constant Systems Ltd., United Kingdom) at 1.5 kBar and 4°C to avoid protein denaturation. The cell free extract (CFE) was collected as the supernatant after centrifugation at 48000 g, 1 h, 4 °C. GtHNL-WT was purified from the CFE by anion exchange chromatography with Q Sepharose Fast Flow columns (HiTrap Q FF, 70 mL; GE Healthcare, Uppsala, Sweden) applying an isocratic step of 10% buffer B and then a gradient from 10% to 100% buffer B (50 mM bis-Tris buffer + 1 M NaCl). GtHNL-WT eluted at 10% buffer B. All the fractions were tested with an activity assay, see below. GtHNL-WT was further purified using ultrafiltration with 100 kDa MWCO Amicon filter (Millipore) in order to remove any large proteins (>100 kDa). GtHNL-TV was purified following the same method with slight modifications. Loading and elution buffers were at pH 7.4 and the ultrafiltration step was omitted because it had a negative effect on the enzyme stability. GtHNL-3V eluted at 10% buffer B.

3.4.5 GtHNL activity assay

GtHNL activity (wild type and variant) was measured spectrophotometrically (Agilent Technologies Cary 60 UV-VIS) using a method previously reported.^{10,36} The cleavage of *rac*-mandelonitrile into benzaldehyde and hydrogen cyanide was followed at 280 nm and 25°C in quartz glass cuvettes. To 1300 µL of reaction buffer (100 mM sodium oxalate buffer, pH 5), 200 µL of enzyme solution (diluted in reaction buffer) and 500 µL of 60 mM *rac*-mandelonitrile solution (dissolved in 3 mM oxalic acid, pH 3) were added. The background reaction was evaluated without enzyme and its slope was subtracted in the final calculation. The activity was calculated based on the following equation:³⁶

$$\text{Activity} = 2.0 \times \Delta A/\text{min} / (\epsilon_{280} \times 1 \times 0.2) \text{ [U ml}^{-1} \text{ diluted sample]}$$

where

$$\Delta A/\text{min} = \Delta A/\text{min}_{\text{sample}} - \Delta A/\text{min}_{\text{blank}}$$

$$\epsilon_{280} = 1.376 \text{ [mM}^{-1} \times \text{cm}^{-1}\text{]}$$

One unit of HNL activity is defined as one micromole of *rac*-mandelonitrile converted per minute in sodium oxalate buffer pH 5 at 25 °C.

3.4.6 Preparation of the hydrogen cyanide (HCN) solution in MTBE

An HCN solution in MTBE was prepared as described previously^{5,15} with slight modifications. 25 mL MTBE and 10 mL MilliQ water were mixed in a 100 mL Erlenmeyer and kept at 0 °C. 0.1 mol potassium cyanide (6.51 g) was dissolved in the mixture and magnetically stirred for 15 minutes. 10 mL of 30% (v/v) HCl solution was added slowly and stirring was continued for 2 minutes. The HCN solution was allowed to reach room temperature (*circa* 20 °C). The organic and aqueous phases were separated using a separation funnel and the organic layer containing HCN was collected. The separation was performed twice more after adding 7 mL of MTBE each time. Finally, 5 mL of 100 mM sodium acetate buffer pH 4 was added to the organic fraction collected and it was stored in a dark bottle at 4 °C. The HCN concentration in solution in MTBE was determined by titration. 1 mL of the HCN solution was added to 5 mL of 2 M NaOH and magnetically stirred for 2 minutes. A small amount of potassium chromate was added as indicator, then the solution was titrated using 0.1 M silver nitrate. The cyanide reacts 1:1 with the silver and precipitates. If there are no cyanide ions left in the mixture it will change colour from light yellow to brown.^{5,37} To determine a concentration between 1.5–2 M is necessary to add 15–20 mL of silver nitrate. The HCN solution was found to be between 1.5 and 2 M.

Caution: Potassium cyanide (KCN) and hydrogen cyanide (HCN) are highly poisonous chemicals. All experiments involving KCN and HCN were performed in a ventilated fume hood with 2 calibrated HCN detectors (inside and outside the fume hood). HCN wastes were neutralized over a large excess of commercial bleach (15% sodium hypochlorite solution) for disposal.

3.4.7 Immobilisation on Celite R-633 for batch and continuous flow reactions

Enzyme immobilisation was performed according to literature.⁵ Celite R-633 was washed with 100 mM sodium acetate buffer pH 4 using a Büchner funnel and dried 24 h under vacuum in a desiccator over silica gel. Given volumes of wild type *GtHNL* or triple variant *GtHNL* were concentrated with Amicon ultrafiltration filters with a 10 kDa MW cut-off, and subsequently added dropwise to Celite R-633 and dried 24 h under vacuum in a desiccator over silica gel. The ratio of enzyme solution to carrier ($\mu\text{L} : \text{mg}$) was 2 : 1. The enzyme concentration in solutions was adjusted in the concentration step to the required amount of enzyme for the immobilisation. By using this ratio of enzyme solution to Celite, the enzyme solution was completely absorbed by the carrier, ensuring that all the enzyme was immobilised into the porous material. The immobilised enzyme was stored in the fridge at 4 °C.

3.4.8 Synthesis reactions of (*R*)-mandelonitrile in batch systems

3.4.8.1 Batch reaction (BR) – tea bag approach.

Several biocatalytic reactions were performed using *GtHNL*-3V immobilised on Celite R-633 and tightly packed into tea bags as described in the literature.¹⁵ (Fig. S6 and S7†) Tea bags can be made from nylon with pore size 0.4 mm or indeed a regular tea bag.¹⁵ All reactions were performed with regular tea bags. The reaction conditions were: benzaldehyde (100 μL , 1 mmol), 27.5 μL 1,3,5-tri-isopropylbenzene (internal standard), 2 mL HCN in 100 mM acetate buffered MTBE pH 4 (1.5–2 M), tea bag filled with 50 mg immobilised enzyme (0.1, 0.5, 1, 2 and 4 U mg^{-1}), 700 rpm and 5 °C. The ratio benzaldehyde to HCN solution was $\sim 1 : 4$.

3.4.8.2 Rotating bed reactor (RBR) reaction.

The reaction was scaled up to a 42 times larger reaction mixture volume, utilising a rotating bed reactor (Spinchem, Sweden). The reaction conditions were: benzaldehyde (4.25 mL, 42 mmol), 1.16 mL 1,3,5-tri-isopropylbenzene (internal standard), 85 mL HCN in 100 mM acetate buffered MTBE pH 4 (1.5–2 M), immobilised *GtHNL*A-40H/V42T/Q110H on 773 mg Celite (1 U mg^{-1} Celite), 700 rpm and 5 °C. The ratio benzaldehyde to HCN solution $\sim 1 : 4$.

3.4.8.3 Enzyme recyclability in batch systems (BR and RBR).

The enzyme recyclability was determined by several cycles of (*R*)-mandelonitrile synthesis as described earlier.¹⁵ Between each cycle the immobilised enzyme in the

tea bag was washed for 1 minute with 100 mM acetate buffered MTBE, pH 4.0, and stored after every second reaction cycle overnight at 4°C in fresh acetate buffered MTBE, pH 4.

3.4.9 Synthesis reactions of (*R*)-mandelonitrile on continuous flow

Immobilised *Gt*HNL-3V on Celite R-633 (1 U mg⁻¹) was placed into a 1 mL stainless steel flow reactor. It was filled with 150 mg of non-porous glass beads and 150 mg of Celite R-633 containing immobilised enzyme. The packed bed reactor had a reaction volume of 0.394 mL (SI-C). 20 cm of polytetrafluoroethylene (PTFE) tubing with 1.5 mm inner diameter connect a high-pressure pump (Knauer, Germany) with the starting materials. Initial conditions were as follow: 0.5 M benzaldehyde, 1.5–2 M HCN in 100 mM acetate buffered MTBE pH 4 and 50 mM 1,3,5 tri-isopropylbenzene as internal standard. The synthesis of (*R*)-mandelonitrile was evaluated at different flow rates (from 0.1 to 1 mL min⁻¹) by chiral HPLC. The flow rate was checked at each sampling time by the difference of weight. Reactions were performed at room temperature.

3.4.9.1 Stability study in continuous flow.

Synthesis reactions with immobilised *Gt*HNL-TV on Celite R-633 (1 U mg⁻¹) were performed for 13 hours (0.1 mL min⁻¹) and 8 hours (0.2 mL min⁻¹) continuously to test the enzyme stability at room temperature. Samples were drawn at regular intervals (Fig. 7 and 8) and analysed by chiral HPLC.

3.4.10. Analysis

Samples (10 µL) were taken at different times during the reaction run and added to 990 µL of heptane : 2-propanol 95 : 5 in 1.5 mL Eppendorf tubes. A small amount of anhydrous magnesium sulphate (MgSO₄) was used to remove the water from the solution. The Eppendorf tubes were centrifuged at 13000 rpm for 1 min. 850 µL of the supernatant was transferred to a 4 mL HPLC vial and 10 µL was injected into the HPLC (Chiralpak AD-H column, column size: 0.46 cm I.D × 25 cm). Heptane and 2-propanol were used as mobile phase with a flow rate of 1 mL min⁻¹ and the UV detector was set at 216 nm. The column temperature was set at 40 °C. The samples in the autosampler were maintained at 4°C.

References

1. J. Holt and U. Hanefeld, *Curr. Org. Synth.*, 2009, 6, 15–37.
2. E. M. M. Abdelraheem, H. Busch, U. Hanefeld and F. Tonin, *React. Chem. Eng.*, 2019, 4, 1878–1894.
3. Nahrstedt, *Plant Syst. Evol.*, **1985**, 150, 35–47.
4. R. Lieberei, D. Selmar and B. Biehl, *Plant Syst. Evol.*, **1985**, 150, 49–63.
5. G. Torrelo, N. van Midden, R. Stloukal and U. Hanefeld, *ChemCatChem*, **2014**, 6, 1096–1102.
6. M. North, *Tetrahedron: Asymmetry*, **2003**, 14, 147–176.
7. M. Dadashipour and Y. Asano, *ACS Catal.*, **2011**, 1, 1121–1149.
8. P. Bracco, H. Busch, J. von Langermann and U. Hanefeld, *Org. Biomol. Chem.*, **2016**, 14, 6375–6389.
9. Hajnal, A. Lyskowski, U. Hanefeld, K. Gruber, H. Schwab and K. Steiner, *FEBS J.*, **2013**, 280, 5815–5828.
10. R. Wiedner, B. Kothbauer, T. Pavkov-Keller, M. Gruber-Khadjawi, K. Gruber, H. Schwab and K. Steiner, *ChemCatChem*, **2015**, 7, 325–332.
11. F. Vertregt, G. Torrelo, S. Trunk, H. Wiltsche, W. R. Hagen, U. Hanefeld and K. Steiner, *ACS Catal.*, **2016**, 6, 5081–5085.
12. U. Hanefeld, *Chem. Soc. Rev.*, **2013**, 42, 6308–6321.
13. M. Hartmann and X. Kostrov, *Chem. Soc. Rev.*, **2013**, 42, 6277–6289.
14. K. Zielinska, K. Szymanska, R. Mazurkiewicz and A. Jarzebski, *Tetrahedron: Asymmetry*, **2017**, 28, 146–152.
15. P. Bracco, G. Torrelo, S. Noordam, G. de Jong and U. Hanefeld, *Catalysts*, **2018**, 8, 287.
16. D. Okrob, M. Paravidino, R. V. A. Orru, W. Wiechert, U. Hanefeld and M. Pohl, *Adv. Synth. Catal.*, **2011**, 353, 2399–2408.
17. E. Wehtje, P. Adlercreutz and B. Mattiasson, *Biotechnol. Bioeng.*, **1990**, 36, 39–46.

18. R. Lindeque and J. Woodley, *Catalysts*, **2019**, 9, 262.
19. H. Larsson, P. A. Schjøtt, E. Byström, K. V. Gernaey and U. Krühne, *Ind. Eng. Chem. Res.*, **2017**, 56, 3853–3865.
20. H. Mallin, J. Muschiol, E. Byström and U. Bornscheuer, *ChemCatChem*, **2013**, 5, 3529–3532.
21. M. P. van der Helm, P. Bracco, H. Busch, K. Szymańska, A. Jarzębski and U. Hanefeld, *Catal. Sci. Technol.*, **2019**, 9, 1189–1200.
22. R. Munirathinam, J. Huskens and W. Verboom, *Adv. Synth. Catal.*, **2015**, 357, 1093–1123.
23. N. N. Rao, S. Lütz, K. Würges and D. Minör, *Org. Process Res. Dev.*, **2009**, 13, 607–616.
24. K. G. Hugentobler, M. Rasparini, L. A. Thompson, K. E. Jolley, A. J. Blacker and N. J. Turner, *Org. Process Res. Dev.*, **2017**, 21, 195–199.
25. Brahma, B. Musio, U. Ismayilova, N. Nikbin, S. Kamptmann, P. Siegert, G. E. Jeromin, S. V. Ley and M. Pohl, *Synlett*, **2016**, 27, 262–266.
26. L. van den Biggelaar, P. Soumillion and D. P. Debecker, *Catalysts*, **2017**, 7, 54.
27. M. Movsisyan, E. I. P. Delbeke, J. K. E. T. Berton, C. Battilocchio, S. V. Ley and C. V. Stevens, *Chem. Soc. Rev.*, **2016**, 45, 4892–4928.
28. L. H. Andrade, W. Kroutil and T. F. Jamison, *Org. Lett.*, **2014**, 16, 6092–6095.
29. M. Bajić, I. Plazl, R. Stloukal and P. Žnidaršič-Plazl, *Process Biochem.*, **2017**, 52, 63–72.
30. M. Planchestainer, M. L. Contente, J. Cassidy, F. Molinari, L. Tamborini and F. Paradisi, *Green Chem.*, **2017**, 19, 372–375.
31. Zor, H. A. Reeve, J. Quinson, L. A. Thompson, T. H. Lonsdale, F. Dillon, N. Grobert and K. A. Vincent, *Chem. Commun.*, **2017**, 53, 9839–9841.
32. F. Dall'Oglio, M. L. Contente, P. Conti, F. Molinari, D. Monfredi, A. Pinto, D. Romano, D. Ubiali, L. Tamborini and I. Serra, *Catal. Commun.*, **2017**, 93, 29–32.

33. V. De Vitis, F. Dall'Oglio, A. Pinto, C. De Micheli, F. Molinari, P. Conti, D. Romano and L. Tamborini, *ChemistryOpen*, **2017**, 6, 668–673.
34. H. Lamble, S. F. Royer, D. W. Hough, M. J. Danson, G. L. Taylor and S. D. Bull, *Adv. Synth. Catal.*, **2007**, 349, 817–821.
35. Grabner, Y. Pokhilchuk and H. Gruber-Woelfler, *Catalysts*, **2020**, 10, 137.
36. U. Hanefeld, A. J. J. Straathof and J. J. Heijnen, *Biochim. Biophys. Acta*, **1999**, 1432, 185–193.
37. L. van Langen, F. van Rantwijk and R. A. Sheldon, *Org. Process Res. Dev.*, **2003**, 7, 828–831.
38. U. Hanefeld, L. Gardossi and E. Magner, *Chem. Soc. Rev.*, **2009**, 38, 453–468.
39. F. Effenberger, J. Eichhorn and J. Roos, *Tetrahedron: Asymmetry*, **1995**, 6, 271–282.
40. Costes, E. Wehtje and P. Adlercreutz, *Enzyme Microb. Technol.*, **1999**, 25, 384–391.
41. Basso, L. De Martin, C. Ebert, L. Gardossi and P. Linda, *J. Mol. Catal. B: Enzym.*, **2000**, 8, 245–253.
42. K. Szymanska, K. Odrozek, A. Zniszczoł, W. Pudło and A. B. Jarzebski, *Chem. Eng. J.*, **2017**, 315, 18–24.
43. S. E. Charma and B. L. Wong, *Enzyme Microb. Technol.*, **1981**, 3, 111–118.
44. H. M. M. El-Sayed, W. M. Mahmoud and R. W. Coughlin, *Biotechnol. Bioeng.*, **1990**, 36, 83–91.
45. N. J. Gleason and J. D. Carbeck, *Langmuir*, **2004**, 20, 6374–6381.
46. T. R. Besanger, R. J. Hodgson, J. R. A. Green and J. D. Brennan, *Anal. Chim. Acta*, **2006**, 564, 106–115.
47. Y. Zhu, Q. Chen, L. Shao, Y. Jiacef and X. Zhang, *React. Chem. Eng.*, **2020**, 5, 9–32.

Supplementary Information

A. Gene and amino-acid sequences

GtHNL wild type – Gene sequence

5'CCATGGAGATTAAACGTGTTGGTTCTCAGGCTTCTGGTAAAGGTCCGGCTGATTGGTTCACTG
GTACTGTTTCGTATCGATCCGCTGTTTCAGGCTCCGGATCCGGCATTAGTAGCTGGTGCTTCTGTT
ACCTTTGAACCGGGTGCTCGTACTGCTTGGCATACTCATCCGTTAGGTCAGACTCTGATTGTAAC
TGCTGGTTGTGGTTGGGCTCAGCGTGAAGGTGGTGCTGTTGAAGAAATTCATCCGGGTGATGTT
GTATGGTTCTCTCCAGGTGAAAAACACTGGCATGGTGCTGCACCAACTACCGCTATGACCCACC
TGGCTATCCAGGAACGTCTGGATGGTAAAGCTGTTGATTGGATGGAACACGTTACTGATGAACA
GTACCGTCGTTAAGCTT -3'

GtHNL wild type – Aminoacid sequence

MEIKRVGSQASGKGPADWFTGTVRIDPLFQAPDPALVAGASVTFEPG
ARTAWHHTHPLGQTLIVTAGCGWAQREGGAVEEIHPGDVVWFSPGEKH
WHGAAPTTAMTHLAIQERLDGKAVDWMEHVTDEQYRRA

GtHNL-A40H/V42T/Q110H

5'CCATGGAGATTAAACGTGTTGGTTCTCAGGCTTCTGGTAAAGGTCCGGCTGATTGGTTCACTG
GTACTGTTTCGTATCGATCCGCTGTTTCAGGCTCCGGATCCGGCATTAGTAGCTGGTCACTCTACT
ACCTTTGAACCGGGTGCTCGTACTGCTTGGCATACTCATCCGTTAGGTCAGACTCTGATTGTAAC
TGCTGGTTGTGGTTGGGCTCAGCGTGAAGGTGGTGCTGTTGAAGAAATTCATCCGGGTGATGTT
GTATGGTTCTCTCCAGGTGAAAAACACTGGCATGGTGCTGCACCAACTACCGCTATGACCCACC
TGGCTATCCACGAACGTCTGGATGGTAAAGCTGTTGATTGGATGGAACACGTTACTGATGAACAG
TACCGTCGTTAAGCTT -3'

GtHNL-A40H/V42T/Q110H – Aminoacid sequence

MEIKRVGSQASGKGPADWFTGTVRIDPLFQAPDPALVAGHSTTFEPG
ARTAWHHTHPLGQTLIVTAGCGWAQREGGAVEEIHPGDVVWFSPGEKH
WHGAAPTTAMTHLAIHERLDGKAVDWMEHVTDEQYRRA

Aminoacids in red show the mutations at positions 40, 42 and 110.

B. SDS-PAGE purified GtHNL-A40H/V42T/Q110H

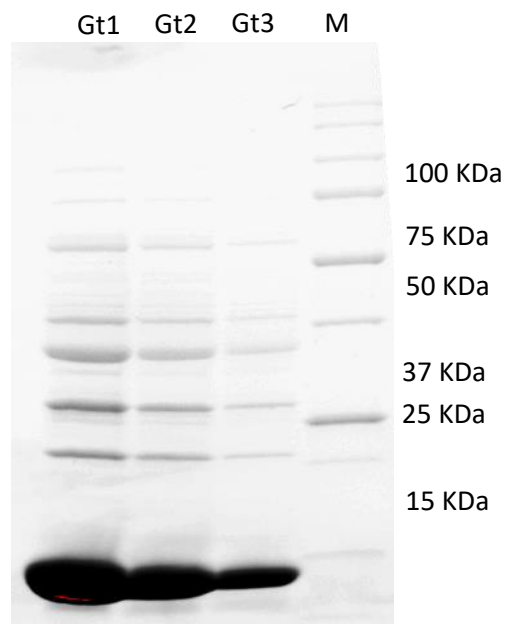


Figure S1. SDS-PAGE of purified GtHNL-A40H/V42T/Q110H. Sample M is the marker and Gt1 to Gt3 are different dilutions of purified GtHNL-A40H/V42T/Q110H

C. Calculation of reaction volume in continuous flow

Interbead volume (Non porous glass beads)

A commonly used inter-beads volume for non-porous beads of similar or close diameters even for well packed columns is between 30% and 40% of the total volume. Since 150 mg of glass beads correspond to 0.5 mL bulk volume, the inter-beads volume is about:

$$0.5 \text{ mL} \times 35\% = 0.175 \text{ mL}$$

Pore volume (Celite R-633)

According to El-Sayed¹, Celite R-633 has a total pore volume of 1.46 mL g⁻¹.

$$0.150 \text{ g Celite R-633} \times 1.46 \text{ mL g}^{-1} = 0.219 \text{ mL}$$

$$\text{Reaction volume} = 0.219 \text{ mL} + 0.175 \text{ mL} = 0.394 \text{ mL}$$

D. Progress of the synthesis of (*R*)-mandelonitrile with non-immobilized GtHNL-3V

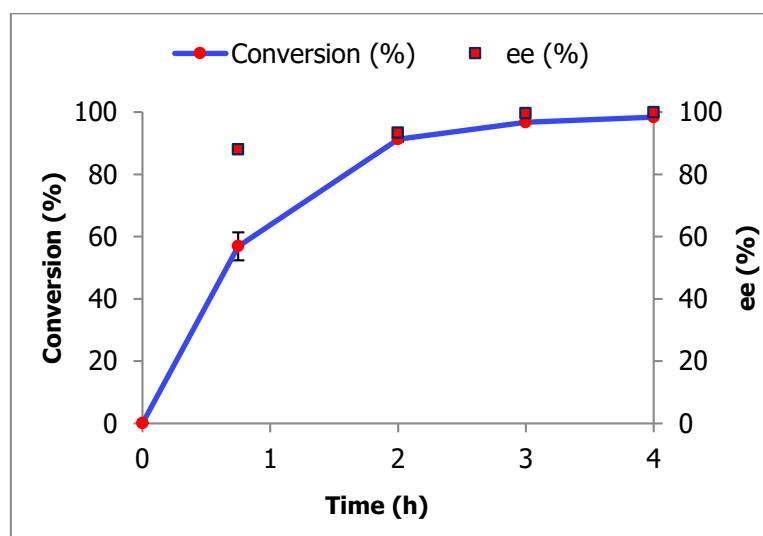


Figure S2: Kinetic trace for the synthesis of (*R*)-mandelonitrile with non-immobilized GtHNL-3V. Conditions: Ratio benzaldehyde : HCN in acetate buffered MTBE pH 4 1:4, GtHNL-3V (11 mg, 50 U). The reaction was stirred at 1000 rpm at 5 °C.

E. Benzaldehyde and HCN kinetics

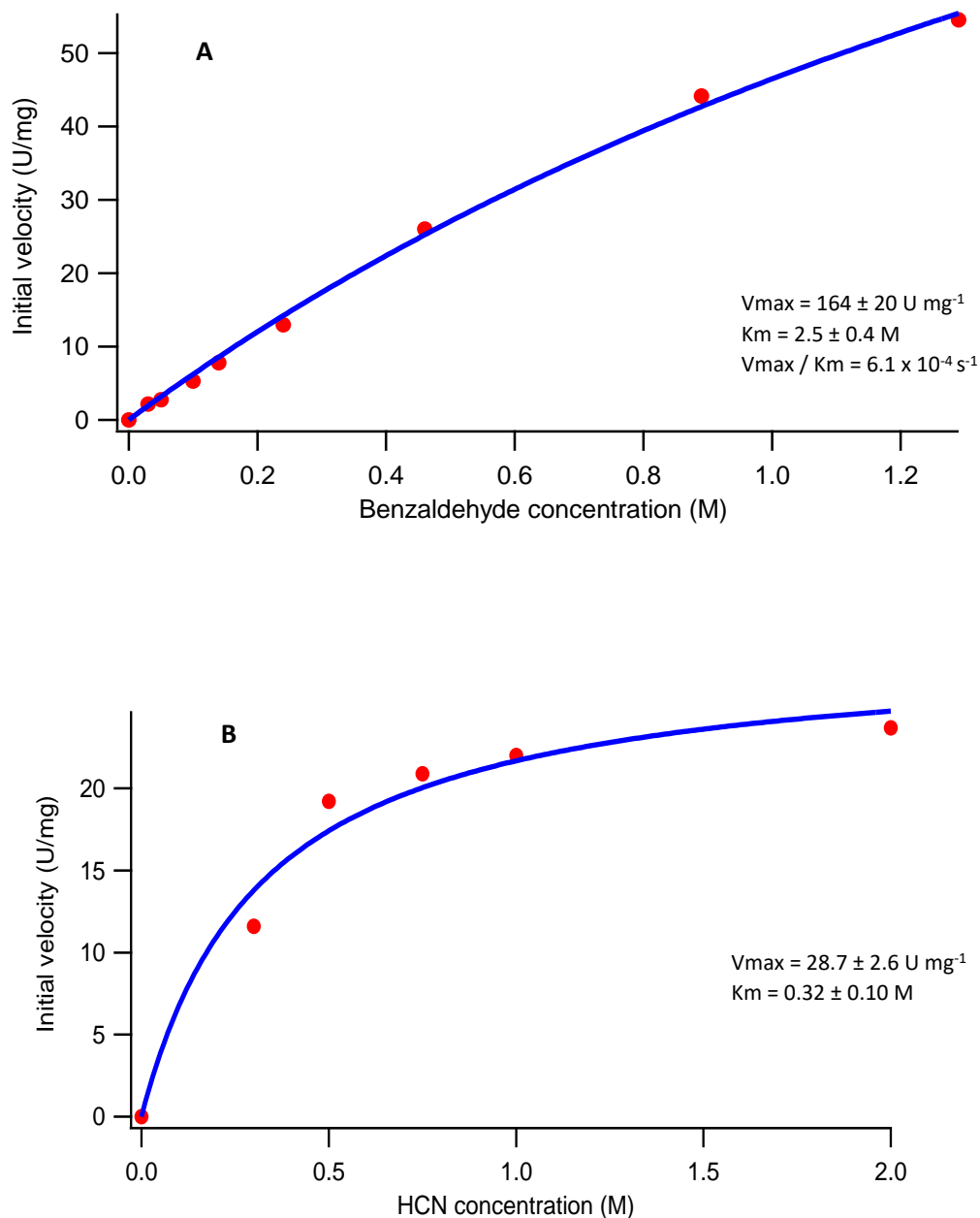


Figure S3. Kinetic traces for the synthesis of (*R*)-mandelonitrile at different benzaldehyde and HCN concentrations. Conditions: Ratio benzaldehyde : HCN in acetate buffered MTBE, pH 4, ~1:4, 2 mL HCN in acetate buffered MTBE (1.5–2 M) pH 4, G β HNL-3V immobilized on 50 mg Celite R-633 (50 U). The reaction was stirred at 700 rpm, 5 °C. Single measurement points were fitted by using Michaelis-Menten equation. Standard deviation was calculated with Igor Pro 5.0.5 software

F. Substrate incubation for evaluation of background reaction during 8 hours

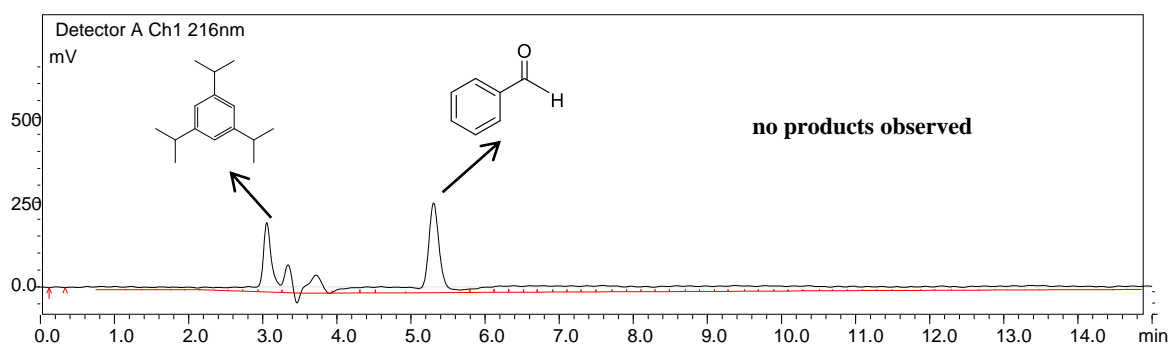


Figure S4. HPLC detection of benzaldehyde and 1,3,5 tri-isopropylbenzene during 8 hours of incubation: Conditions: Ratio benzaldehyde : HCN in buffered MTBE, pH 4, ~1:4, 100 μ L benzaldehyde (1 mmol), 2 mL HCN in acetate buffered MTBE, pH 4 . The reaction was stirred at 1000 rpm at 5 $^{\circ}$ C.

G. Identification of substrates and products during the synthesis of (*R*)-mandelonitrile

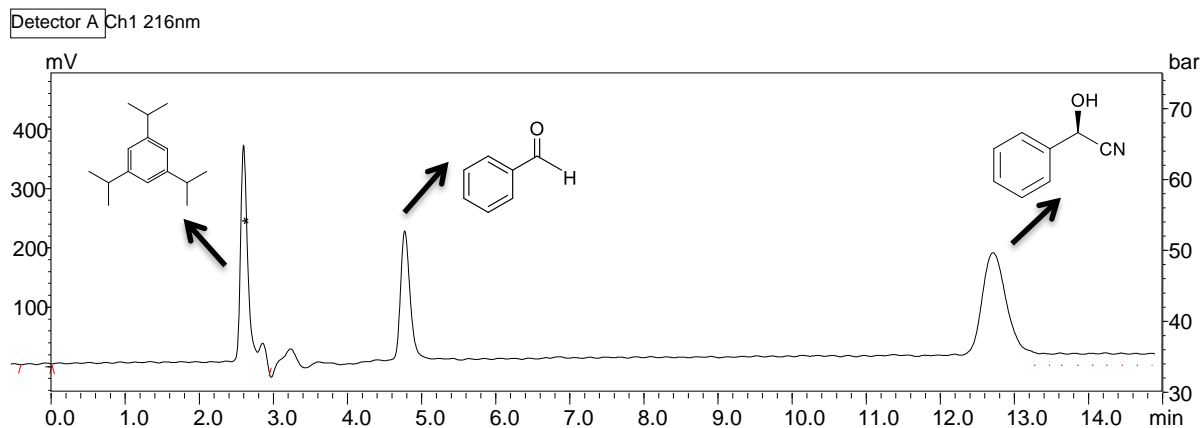


Figure S5. HPLC detection of benzaldehyde, 1,3,5 tri-isopropylbenzene and (*R*)-mandelonitrile. Conditions: Ratio benzaldehyde : HCN in buffered MTBE, pH 4, ~ 1:4, a CFR with G#HNL-3V immobilised on 150 mg Celite R-633 (150 U). Reactions was performed at room temperature.

H. Progress of the synthesis of (*R*)-mandelonitrile with immobilized *Gt*HNL-3V in nylon and regular paper tea bag.

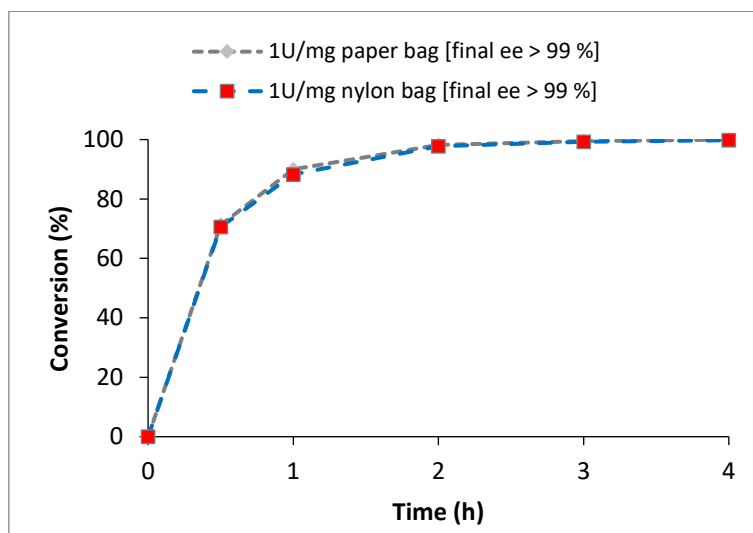


Figure S6: Synthesis of (*R*)-mandelonitrile with immobilized *Gt*HNL-3V in nylon and regular paper tea bags. Paper tea bags are commonly nylon enforced. Conditions: Ratio benzaldehyde : HCN in acetate buffered MTBE, pH 4, ~ 1:4, *Gt*HNL-3V (11 mg, 50 U). The reaction was stirred at 1000 rpm at 5 °C.

Size of tea bags for BR and RBR reactions

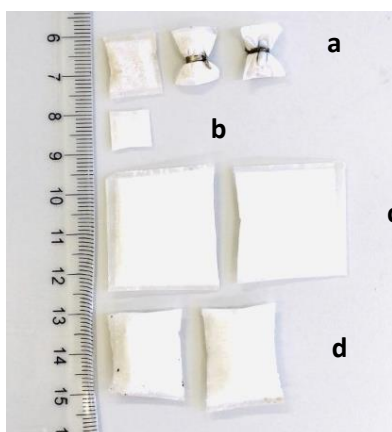


Figure S7: Tea bags with different sizes for tightly or loosely packed *Gt*HNL-3V on Celite R-633. The ruler shows the size in cm. a) tightly packed Celite immobilised *Gt*HNL-3V (50 mg) for BR, b) tightly packed Celite immobilised *Gt*HNL-3V (18 mg) for BR, c) loosely packed Celite immobilised *Gt*HNL-3V (773 mg) for RBR and d) tightly packed Celite immobilised *Gt*HNL-3V (773 mg) for RBR.

Table S1: Size of tea bags for tightly or loosely packed GtHNL-3V on Celite R-633 for BR and RBR reactions.

Reactor	Type of packing	Size	Amount of enzyme -carrier
BR	Tight	1.3 x 1.6 cm	50 mg
BR	Tight	0.7 x 0.8	18 mg
RBR ¹	Loose	2.5 x 2.6 cm	773 mg
RBR ¹	Tight	1.8 x 2.2 cm	773 mg

¹ 2 bags with equal amount of GtHNL-3V on Celite.

SI References

- [1] A.H.M.M. El-Sayed, W.M. Mahmoud and R.W. Coughlin, *Biotechnol. Bioeng.*, **1990**, *36*, 83-91.

4

Immobilization of *Arabidopsis thaliana*

Hydroxynitrile Lyase (AtHNL) on EziG Opal

Arabidopsis thaliana hydroxynitrile lyase (AtHNL) catalyzes the selective synthesis of (*R*)-cyanohydrins. This enzyme is unstable under acidic conditions, therefore its immobilization is necessary for the synthesis of enantiopure cyanohydrins. EziG Opal is a controlled porosity glass material for the immobilization of His-tagged enzymes. AtHNL-EziG Opal achieved 95% of conversion after 30 min of reaction time in batch and it was recycled up to eight times with a final conversion of 80% and excellent enantioselectivity. The continuous flow system achieved 96% of conversion and excellent enantioselectivity at 0.1 mL min⁻¹. Lower conversion and enantioselectivity were observed at higher flow rates. The specific rate of AtHNL-EziG Opal in flow was 0.26 mol h⁻¹ g_{enzyme}⁻¹ at 0.1 mL min⁻¹ and 96% of conversion whereas in batch, the immobilized enzyme displayed a specific rate of 0.51 mol h⁻¹ g_{enzyme}⁻¹ after 30 min of reaction time at a similar level of conversion. However, in terms of productivity the continuous flow system proved to be almost four times more productive than the batch approach, displaying a space-time-yield (STY) of 690 mol_{product} h⁻¹ L⁻¹ g_{enzyme}⁻¹ compared to 187 mol_{product} h⁻¹ L⁻¹ g_{enzyme}⁻¹ achieved with the batch system.

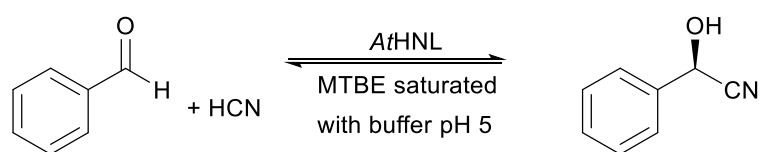
This chapter is based on

José Coloma, Tim Lugtenburg, Muhammad Afendi, Mattia Lazzarotto, Paula Bracco, Peter-Leon Hagedoorn, Lucia Gardossi and Ulf Hanefeld

Catalysts, **2020**, 10, 899. DOI:10.3390/catal10080899

4.1 Introduction

Hydroxynitrile lyases (HNLs) are enzymes that catalyze the synthesis of enantiopure cyanohydrins (Scheme 1), known building blocks for the production of fine chemicals, pharmaceuticals and cosmetics [1–4]. HNL catalyzed reactions are faced with two problems, the chemical formation of racemic cyanohydrins and product racemization due to the reaction equilibrium [5]. These limitations can be overcome by performing the reactions in buffer saturated organic solvent and adjusting the pH to the lower limit accepted for HNLs [5,6]. These conditions are not the natural environment of HNLs, as they have to be stabilized for instance by immobilization on a suitable carrier.



Scheme 1. AtHNL catalyzed hydrocyanation of benzaldehyde yielding (*R*)-mandelonitrile.

Improved stability, activity and selectivity of immobilized enzymes have been reported earlier [7,8]. In addition, immobilization enables the increase of enzyme loading and facilitates recycling and downstream processing. To achieve the beneficial aspects mentioned before, the characteristics of enzyme and carrier must be considered. However, there is not a general method to immobilize an enzyme and its feasibility must be determined experimentally [9,10].

Immobilized metal ion chromatography (IMAC) is a widely used technique for the purification and immobilization of His-tagged enzymes. The enzyme immobilization is based on the affinity of divalent metal ions such as Zn^{2+} , Cu^{2+} , Ni^{2+} or Co^{2+} to the imidazole ring of histidines. Chelated Ni^{2+} on nitrilotriacetic acid (Ni-NTA) has turned out to be the most effective combination for the purification of His-tagged proteins [11]. However, nickel induced genotoxicity, carcinogenicity and immunotoxicity has been reported [12]. Hence, the development of a carrier with a non-toxic metal ion is highly desirable.

A new set of carriers (EziG, provided by EnginZyme AB, Stockholm, Sweden) containing non-toxic Fe^{3+} ($>10 \mu\text{mol g}^{-1}$) on its surface has been developed for the immobilization of His-tagged enzymes. These materials have a core made of controlled porosity glass (CPG) particles facilitating mass transfer from reactants and

products to the material due to its interconnecting pore structure (*circa* 1.8 mL g⁻¹). In addition, its non-compressible non-swelling nature is an advantage compared to NTA agarose. The porous surface can be coated with an organic polymer to tailor carriers with different hydrophobic characteristics such as EziG Opal (hydrophilic), EziG Coral (hydrophobic) and EziG Amber (semi-hydrophobic). Given the hydrophilic surface of His₆-tagged *A β HNL* [13], its immobilization was performed on EziG Opal. Moreover, EziG Opal has been found to be suitable for reactions in organic solvents [14], a crucial property to enable the synthesis of enantiopure cyanohydrins together with low pH required in the reaction medium.

Some successful studies with different immobilized enzymes on EziG carriers have been reported earlier. An ω -transaminase was active in methyl-*tert*-butylether (MTBE) and a Baeyer–Villiger monooxygenase (BVMO) together with two cofactor-regenerating enzymes displayed increased stability [14]. An ω -transaminase from *Arthrobacter* sp. (AsR- ω TA) on EziG Amber was highly stable in batch and continuous flow systems [20]. On the other hand, when an old yellow enzyme (OYE) was immobilized on EziG Opal, poor recyclability was observed, and the initial conversion dropped to 56% after two reaction cycles [21]. The loss of activity of OYE was assumed to be due to enzyme leaching and/or deactivation of the enzyme. Likewise, the enzyme arylmalonate decarboxylase (AMDase) presented a significant loss of activity during recycling studies on all EziG carriers [22]. The loss of activity of AMDase activity on EziG carriers was explained to be due to enzyme leaching because of the lower strength of the coordinate bond and due to local pH changes by the acidic product of the reaction.

Enzyme catalysed reactions in flow are gaining attention due to improved productivity, easier downstream processing and efficiency of scale-up compared to batch systems. Reduced reaction times and enhanced selectivity are reported benefits of performing reactions in flow [23-26]. On top of all these benefits mentioned before, continuous flow reactions allow to optimize resource utilization, reduce reaction volumes and consequently achieve waste reductions and lower energy consumption [27]. Furthermore, they allow handling of toxic and reactive reagents such as cyanide [28] in a safer manner.

The aim of this study is to immobilise *A β HNL* on EziG Opal based on the His-tag/Fe³⁺ affinity and compare its performance for the synthesis of (*R*)-mandelonitrile with the

earlier reported successful immobilisation of *At*HNL on Celite by adsorption [15]. Important parameters such as stability, specific rate and productivity were investigated in batch and flow systems.

4.2 Results and discussion

*At*HNL was recombinantly produced with a His₆-tag to enable its purification and immobilization by metal-ion affinity. It was successfully overexpressed in *E. coli* BL21(DE3) and purified displaying a specific activity of 136.5 ± 3.2 U mg⁻¹. *At*HNL was purified prior to its immobilization to avoid binding of other proteins with affinity to the EziG Opal carrier.

4.2.1 Batch reactions

All batch reactions were performed with *At*HNL-EziG Opal tightly packed into tea bags. Earlier research revealed that while the material of the bags had no influence on the conversion and enantioselectivity, it was essential to pack the bags tightly [16,18,29]. A magnetic stirrer was attached to the tea bag to enable the rotation of the immobilized enzyme and stirrer simultaneously. This set up avoids mechanical attrition of the carrier caused by the stirrer and facilitates the manipulation of the immobilized enzyme for recyclability studies without any loss of enzyme material. A leaching assay showed that *At*HNL did not leach from EziG Opal carrier to the reaction medium (Figure S1). Similarly, no leaching had been reported previously for hydrocyanation reactions catalyzed by immobilized HNLs on siliceous carriers in general and *At*HNL specifically [15,16,18,29].

Once it was established that EziG Opal is a suitable carrier for the immobilization of *At*HNL (Figure S1), preliminary time studies using different enzyme loadings of *At*HNL-EziG Opal for the synthesis of (*R*)-mandelonitrile were performed (Figure 1). The different enzyme loadings showed a huge difference in conversion and enantiopurity during four hours of reaction time. In these preliminary experiments, *At*HNL was immobilized on EziG Opal by incubating an enzyme solution with the carrier in an orbital shaker (see Section 4.4.7 for details). The rotation enabled the enzyme to bind to the carrier but some precipitation was observed and it might explain the results in Figure 1. On the other hand, an earlier report [15] showed that *At*HNL on Celite R-633 displayed near complete conversion and excellent enantioselectivity after 45 min using 5 mg mL⁻¹ (*circa* 400 U) and MTBE saturated with citrate/phosphate buffer pH 5.5. The

enzyme was immobilized by adsorption in that study. In addition, the successful immobilizations of *Prunus amygdalus* HNL (*Pa*HNL) [16], *Manihot esculenta* HNL (*Me*HNL) [18] and *Granulicella tundricola* HNL (*Gt*HNL) [29] on Celite were also performed by adsorbing all the enzyme solution into the carrier until saturation, which means that the enzyme solution is completely adsorbed into the carrier, just like in the case of Celite. All these results suggest that the immobilization of *A*tHNL on EziG Opal had to be optimized.

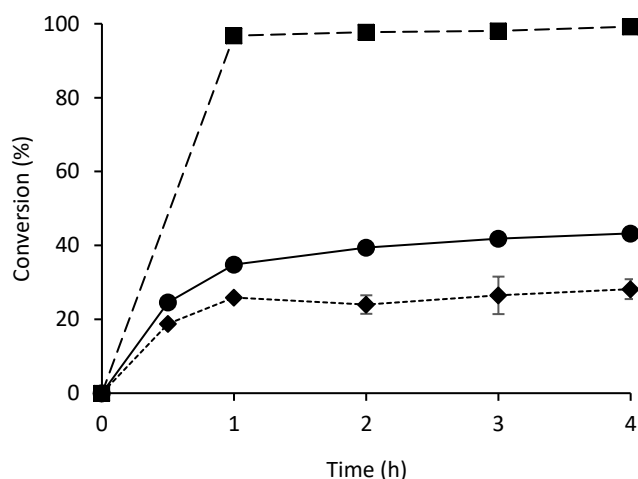


Figure 1. Synthesis of (*R*)-mandelonitrile utilising different enzyme loadings. Immobilization was performed by incubating enzyme and carrier in an orbital shaker and subsequent drying. Dashed line and squares (20 U/mg, final ee = 99 %), solid line and dots (10 U/mg, final ee = 63 %) and dotted line and diamonds (5 U/mg, final ee = 23 %). Conditions: Ratio benzaldehyde : HCN in citrate/phosphate buffered MTBE, pH 5, 1:4, benzaldehyde (100 μ L, 1 mmol), 2 ml HCN solution in citrate/phosphate buffered MTBE (1.5 - 2 M) pH 5, 27.5 μ L (0.1 mmol) 1,3,5-tri-isopropylbenzene as internal standard (I.S) and a teabag filled with *A*tHNL immobilized on 60 mg EziG Opal. The reaction was stirred at 900 rpm at room temperature. Error bars correspond to the standard deviation of duplicates ($n=2$) HPLC samples of the single experiment.

In order to optimize the immobilization of *A*tHNL on EziG Opal, the enzyme was immobilized by either incubating an enzyme solution in an orbital shaker or by adding it dropwise to EziG Opal carrier in such a way that the carrier absorbs the enzyme solution completely, as in the case of Celite [15,16,18,29]. Additionally, the effect of drying *A*tHNL-EziG Opal, which might influence the enzyme performance, was investigated. For this, *A*tHNL-EziG Opal was used either immediately after its immobilization (wet *A*tHNL-EziG Opal) or after 16 h of drying under vacuum in a desiccator over silica gel. Figure 2 shows the effect of drying *A*tHNL-EziG Opal and the immobilization method on the bioconversions. The immobilization of *A*tHNL in an orbital shaker with subsequent drying had a large negative impact on the conversion

and enantioselectivity for the synthesis of (*R*)-mandelonitrile (Figure 2, dotted line and diamonds). The reaction catalyzed by wet *A*tHNL-EziG Opal (Figure 2, dashed line and triangles) proceeded faster and with improved enantioselectivity (92% of conversion and 92% of enantioselectivity) as compared to the dried *A*tHNL-EziG Opal (43% of conversion and 63% of enantioselectivity).

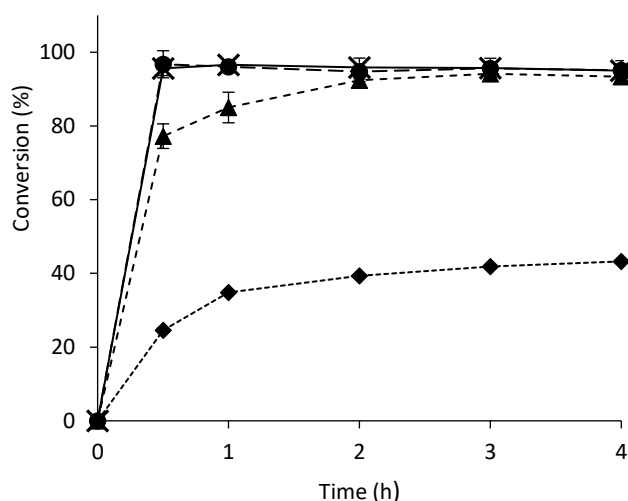


Figure 2. Effect of immobilisation method and drying on the synthesis of (*R*)-mandelonitrile. Continuous line and crosses is the reaction with wet *A*tHNL-EziG Opal (adsorption), final ee = 96.2 %; dashed line and dots is the reaction with dried *A*tHNL-EziG Opal (adsorption) final ee = 93.8 %; dashed line and triangles is the reaction with wet *A*tHNL-EziG Opal (incubation in orbital shaker), final ee = 92.3 % and dotted line and diamonds is the reaction with dried *A*tHNL-EziG Opal (incubation in orbital shaker), final ee = 63.3 %. Conditions: Ratio benzaldehyde : HCN in citrate/phosphate buffered MTBE, pH 5, 1:4, benzaldehyde (100 μ L, 1 mmol), 2 ml HCN solution in citrate/phosphate buffered MTBE (1.5 - 2 M) pH 5, 27.5 μ L (0.1 mmol) 1,3,5-tri-isopropylbenzene as I.S. and a teabag filled with *A*tHNL immobilized on 60 mg EziG Opal. All reactions were performed with enzyme loading of 10 U/mg and the mol ratio of monomeric *A*tHNL:Fe³⁺ was 1:5. The reaction was stirred at 900 rpm at room temperature. Error bars of wet *A*tHNL- EziG Opal (adsorption), wet *A*tHNL-EziG Opal (incubation) and dried *A*tHNL-EziG Opal (incubation) correspond to the standard deviation of duplicate ($n=2$) HPLC samples of the single experiment. Error bars of the reaction with dried *A*tHNL-EziG Opal (adsorption) correspond to the standard deviation of triplicate ($n=3$).

As drying proved to have a negative impact on the enzyme activity and enantioselectivity, two reactions with wet *A*tHNL-EziG Opal immobilized by either incubation in an orbital shaker or adsorption were performed. A faster reaction was observed when the enzyme was immobilized by adsorption (Figure 2, continuous line and crosses), comparable to the results with Celite [15]. Similar conversion (*circa* 95% in both cases) was obtained after 4 h of reaction time, but enantioselectivity was slightly better for the enzyme immobilized by adsorption (96% ee) as compared to the enzyme immobilized by incubation (92% ee). Surprisingly, the effect of drying on the reaction rate was negligible for *A*tHNL immobilised by adsorption on EziG Opal (Figure 2, dashed line and dots). Conversion of *circa* 96% were obtained for both, dried and

non-dried *At*HNL-EziG Opal immobilised by adsorption within 30 minutes and little change was observed in the following 3.5 hours. A possible explanation is that the enzyme is immediately stabilised right after its adsorption into the pores of the carrier, thus it is capable to endure the mechanical stress caused by the orbital shaker as well as the drying.

The lower conversions observed when the enzyme was immobilized by incubation might be explained by the loss of the *At*HNL dimeric structure caused by the rotation in an orbital shaker. In fact, some precipitation was observed after the incubation time. Earlier reports have shown that the enzyme stability is enhanced by higher oligomeric states [30]. Indeed, the ability of *Me*HNL to form tetramers in solution whereas *At*HNL forms dimers, explained the superior stability to higher temperatures and lower pH-values observed for *Me*HNL as compared to *At*HNL [31]. Similarly, *Me*HNL proved to be more stable than dimeric *Hevea brasiliensis* HNL (*Hb*HNL) for the synthesis of (*S*)-mandelonitrile in a monolith microreactor [17]. The formation of *Me*HNL tetrameric structures was attributed as the most likely reason for its higher stability.

Earlier studies [15] demonstrate a significant influence of the water content on enzyme activity of immobilized *At*HNL on Celite R-633, indicating that the minimal water content of *At*HNL-Celite for retaining enzymatic activity is 10% (w/w) of the immobilized enzyme. Additionally, the stability of *Me*HNL as CLEA or immobilized on Celite R-633 is highly dependent on the water entrapped in the carrier [18,32]. This effect can be ruled out here as buffer saturated MTBE was used as solvent.

Silica carriers, such as EziG Opal, are known to catalyze the chemical racemic background reaction [15–19,33,34] (Figures S2 and S3). However, the enantioselectivities achieved here in batch reactions under the optimized immobilization condition demonstrated the efficient suppression of this undesired reaction.

In addition to enzymatic activity and enantioselectivity, the stability of immobilized enzymes is crucial in biocatalytic applications. Indeed, one of the main objectives of enzyme immobilization is the potential for recycling the biocatalyst [4,6,35]. Since the best results for the synthesis of (*R*)-mandelonitrile were obtained with wet *At*HNL-EziG Opal (10 U mg⁻¹) immobilized by adsorption, a recyclability study was performed under these conditions (Figure 3). In order to avoid enzyme overloading on the carrier which might lead to misinterpretations in the recyclability study, the mol ratio of monomeric *At*HNL:Fe³⁺ used was 1:5, thus ensuring any enzyme deactivation is visible during the

reaction cycles. Near complete conversion and excellent enantioselectivity (>99%) were observed during 7 cycles. When 10 U mg⁻¹ of the enzyme were immobilized by incubation in an orbital shaker and subsequent drying, the recycling was unsuccessful (data not shown), whereas an enzyme loading of 20 U mg⁻¹ led to a biocatalyst that could be recycled five cycles (Figure S4).

Figure 3 shows that EziG Opal enables to recycle *A*tHNL over several cycles with good conversion and enantioselectivity under the conditions of this study; accomplishing one of the main objectives of enzyme immobilization.

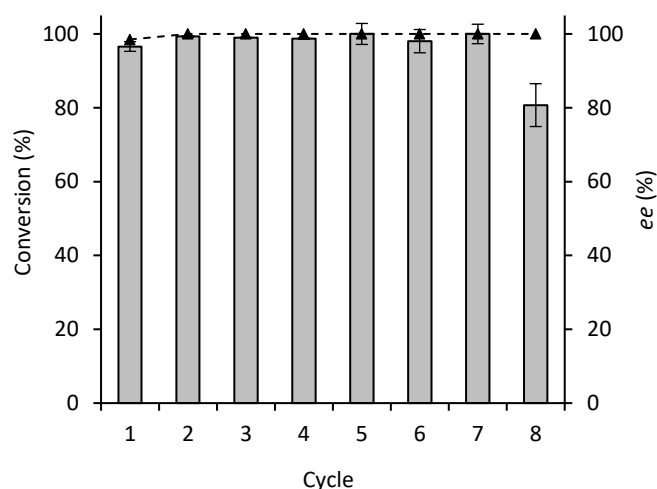


Figure 3. Recycling of wet *A*tHNL-EziG Opal (10 U/mg) in eight successive cycles. Immobilization was performed by adsorption. Conversion (bars), enantiomeric excess (dotted line and triangles). Conditions: Ratio benzaldehyde : HCN in citrate/phosphate buffered MTBE, pH 5, 1:4, benzaldehyde (100 μ L, 1 mmol), 2 ml HCN solution in citrate/phosphate buffered MTBE (1.5 - 2 M) pH 5, 27.5 μ L (0.1 mmol) 1,3,5-tri-isopropylbenzene as I.S. and a teabag filled with *A*tHNL immobilized on 60 mg EziG Opal. Mol ratio of monomeric *A*tHNL:Fe³⁺ was 1:5. The reaction was stirred at 900 rpm at room temperature. The enzyme was washed for 1 minute with 100 mM citrate/phosphate buffer saturated MTBE pH 5 after each cycle. Reaction time: 1 hour. Error bars correspond to the standard deviation of duplicates ($n=2$).

Similarly, *A*tHNL on Celite displayed good conversion (>95%) and excellent enantioselectivity (>98% ee) during five consecutive reaction cycles [15]. Also, the successful recyclability of ω -transaminase from *Arthrobacter* sp. (AsR- ω TA) immobilized on EziG Amber (semi hydrophobic polymer surface) has been reported [20]. The immobilized AsR- ω TA (10 mg, 10% enzyme loading, w w⁻¹) was used for the kinetic resolution of *rac*-methylbenzylamine during 16 consecutive reaction cycles with excellent conversion and enantioselectivity. On the other hand, poor recyclability was recently reported [21] for the bioreduction of α -methyl-trans-cinnamaldehyde with a co-immobilized preparation of old yellow enzyme 3 (OYE3) and glucose dehydrogenase (GDH) on EziG Opal (OYE3/GDH-EziG Opal). The conversion

dropped to 56% after only two reaction cycles. However, it is worthy to mention that after 11 cycles (almost no conversion) the addition of GDH increased the conversion up to 30% suggesting that GDH was gradually deactivated or leached from the carrier over the reaction cycles. Also, the synthesis of enantiopure (*S*)-arylpropionate using arylmalonate decarboxylase (AMDase) immobilized on three EziG carriers with different surface hydrophobicity has been reported [22]. The best activity was obtained with the hydrophilic carrier (EziG Opal). Unfortunately, the enzyme was nearly fully deactivated after the second reaction cycle for the three EziG carriers. This significant loss of enzymatic activity was attributed to enzyme leaching or local pH shifts inside the porous carriers.

4.2.2 Continuous flow reactions

Immobilisation enables the use of enzyme catalysed synthesis reactions in continuous flow. Several advantages have been reported for this approach such as increased productivity, enhanced stability, reduced enzyme inhibition and easier downstream processing [26,36-37]. In addition, the reduced risk of manipulation of hazardous reagents, such as hydrogen cyanide, due to the smaller reaction volume used for the biocatalytic reactions is advantageous [28].

*At*HNL was immobilised on EziG Opal in accordance with the optimised method (adsorption + wet *At*HNL-EziG Opal) developed for batch reactions and tested in a continuous flow reactor (CFR). Figure 4 shows the synthesis of (*R*)-mandelonitrile at different flow rates. Near complete conversion and excellent enantioselectivity were achieved at 0.1 mL min⁻¹. An important decrease in enantioselectivity was observed at flow rates above 0.2 mL min⁻¹ suggesting that *At*HNL on EziG Opal suffers from the competing chemical background reaction catalysed by the carrier. Indeed, the reduced enantioselectivity could be explained as the result of the carrier catalysed chemical reaction (Figure S3). Water content and pH had a major impact on the synthesis of *rac*-mandelonitrile. Pure EziG Opal formed *circa* 5 % of *rac*-mandelonitrile due to the chemical background reaction whereas the addition of 306 μ L of phosphate buffer pH 7 (same volume used for the enzyme immobilisation) increased its formation up to 26 % at 0.1 mL/min (Figure S3).

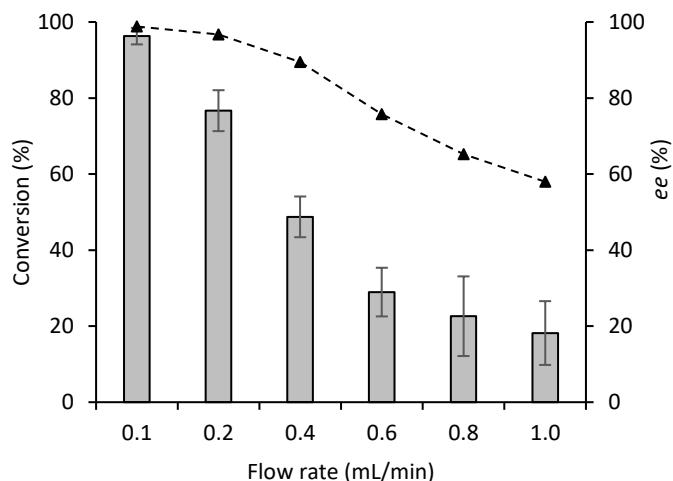


Figure 4. Synthesis of (*R*)-mandelonitrile using wet *A*tHNL-EziG Opal (10 U mg⁻¹) in a CFR. Immobilization was performed by adsorption. Conversion (bars), enantiomeric excess (dotted line and triangles). Conditions: benzaldehyde (0.5 M), HCN solution in citrate/phosphate buffered MTBE (1.5 - 2 M) pH 5, 1,3,5 tri-isopropylbenzene (50 mM, internal standard), a CFR with *A*tHNL immobilised on 150 mg EziG Opal. Mol ratio of monomeric *A*tHNL:Fe³⁺ was 1:4. Reactions were performed at room temperature. Error bars correspond to the standard deviation of triplicates (*n*=3).

The stability of *A*tHNL-EziG Opal was evaluated in the synthesis of (*R*)-mandelonitrile at 0.1 mL/min during 12 hours on continuous operation. At this flow rate near complete conversion was achieved with a mol ratio of monomeric *A*tHNL:Fe³⁺ of 1:4, thus the robustness of the reaction system could be evaluated. Overall, *A*tHNL-EziG Opal displayed good conversion and high enantioselectivity during the stability study (Figure 5). Conversion of 74% and enantioselectivity of 89% respectively were achieved after 12 hours of continuous operation. The decreased conversion and enantioselectivity after 12 hours might be explained by enzyme deactivation due to the low pH 5 and the chemical reaction catalysed by the carrier.

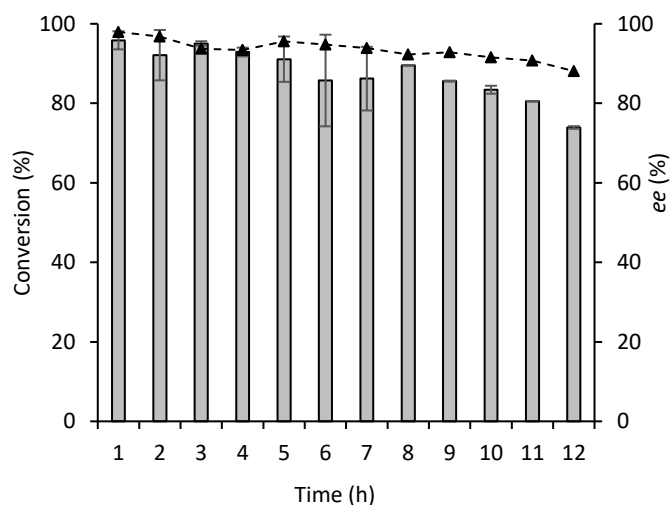


Figure 5. Stability of wet *A*tHNL-EziG Opal (10 U mg⁻¹) in continuous flow at 0.1 mL min⁻¹. Immobilization was performed by adsorption. Conversion (bars), enantiomeric excess (dotted line and triangles).

Conditions: benzaldehyde (0.5 M), HCN solution in citrate/phosphate buffered MTBE (1.5 - 2 M) pH 5, 1,3,5 tri-isopropylbenzene (50 mM, internal standard), a CFR with *At*HNL immobilised on 150 mg EziG Opal. Mol ratio of monomeric *At*HNL:Fe³⁺ was 1:4. Reactions were performed at room temperature. Error bars correspond to the standard deviation of duplicates ($n=2$) during the first 7 hours. From hour 8, error bars correspond to the standard deviation of duplicates ($n=2$) HPLC samples of the single experiment.

4.2.3 Comparison between batch and continuous flow systems

The comparison of the performance of the batch and continuous flow systems cannot be made based on conversions due to the different set ups used. To establish a clear comparison regarding the performance of *At*HNL-EziG Opal in batch and continuous flow, the specific rate and space-time-yield (STY) at a similar level of conversion were calculated.

The specific rate at 0.1 mL/min (96% of conversion) was $0.26 \text{ mol h}^{-1} \text{ g}_{\text{enzyme}}^{-1}$, surprisingly, it is half of the specific rate calculated in batch. At 0.4 mL/min, a similar rate ($0.53 \text{ mol h}^{-1} \text{ g}_{\text{enzyme}}^{-1}$) was observed as compared to the batch system. However, the reduced conversion (49%) might make downstream processing more problematic. Higher flow rates did not further improve the specific rate. *At*HNL-EziG Opal in batch displayed higher specific rate ($0.51 \text{ mol h}^{-1} \text{ g}_{\text{enzyme}}^{-1}$) compared to *At*HNL-Celite [15] ($0.20 \text{ mol h}^{-1} \text{ g}_{\text{enzyme}}^{-1}$) at 96% of conversion. In both cases the reported conversion was achieved after 30 minutes reaction time.

Previously, *At*HNL was immobilised on Celite R-633 [19] and tested for the synthesis of (*R*)-mandelonitrile, the reaction in flow using a packed bed reactor did not enhance the rate of the reaction as compared to the batch system; the best specific rate calculated for the continuous flow system was $0.04 \text{ mol h}^{-1} \text{ g}_{\text{enzyme}}^{-1}$ at 0.04 mL/min (85% of conversion), whereas the batch system showed $0.07 \text{ mol h}^{-1} \text{ g}_{\text{enzyme}}^{-1}$ (*circa* 91% of conversion). These results are *circa* 6 and 7 fold lower as compared to the best specific rate in flow (0.1 mL) and batch respectively reported in this study. In another study [17], the continuous flow synthesis of (*S*)-mandelonitrile with immobilised *Hb*HNL on a siliceous monolith microreactor was 8 times faster as compared to the batch system and displayed a specific rate of $0.50 \text{ mmol min}^{-1} \text{ g}_{\text{enzyme}}^{-1}$ at *circa* 95% conversion and 0.2 mL/min. This result is twice the specific rate observed for *At*HNL-EziG Opal at a similar level of conversion and might be explained by diffusion limitation due to the partial blockage of the pores of EziG Opal during the enzyme immobilisation by adsorption. The irregular structure of the microchannels and mesopores found in monolith microreactors overcome this limitation.

The space-time-yield (STY) is a parameter commonly used to compare the productivity of reactors with different size. Batch systems often require rapid stirring to reduce mass transfer limitations that may shorten the lifetime of the immobilised enzyme. On the other hand, stirring is not required in flow, thus this problem is avoided and better productivities can be achieved [17,25,29]. Indeed, the *AthHNL* on EziG Opal catalyzed synthesis of (*R*)-mandelonitrile in flow displayed a STY of $690 \text{ mol}_{\text{product}} \text{ h}^{-1} \text{ L}^{-1} \text{ g}_{\text{enzyme}}^{-1}$, whereas the batch approach led to only $187 \text{ mol}_{\text{product}} \text{ h}^{-1} \text{ L}^{-1} \text{ g}_{\text{enzyme}}^{-1}$ showing that the flow system greatly enhanced productivity. In batch, a similar productivity has been achieved previously with *AthHNL*-Celite ($150 \text{ mol}_{\text{product}} \text{ h}^{-1} \text{ L}^{-1} \text{ g}_{\text{enzyme}}^{-1}$) [15].

Comparing the results for *AthHNL* of this study with the literature reports again demonstrates the advantages of flow chemistry. The synthesis of (*S*)-mandelonitrile in a siliceous monolith microreactor utilising either *Hevea brasiliensis* HNL (11.3 mg total protein; 1120 U per monolith) or *Manihot esculenta* HNL (17.4 mg total protein; 1310 U per monolith) showed STYs of 555 and 405 $\text{mol}_{\text{product}} \text{ h}^{-1} \text{ L}^{-1} \text{ g}_{\text{enzyme}}^{-1}$ [17]. Recently, a ω -transaminase from *Arthrobacter* sp. (*AsR*- ω TA) was immobilised on EziG Amber (semi-hydrophobic carrier) for the kinetic resolution of *rac*- α -methylbenzylamine (*rac*- α -MBA) [20]. The enzyme was shown to be highly stable on this carrier and was able to perform the kinetic resolution of *rac*- α -MBA during 96 consecutive hours with excellent enantioselectivity (49% conversion and 99% ee). This flow system achieved a space time yield of $184 \text{ mol}_{\text{product}} \text{ h}^{-1} \text{ L}^{-1} \text{ g}_{\text{enzyme}}^{-1}$. The productivities reported in this study are comparable with the productivities reported for immobilised HNLs on siliceous carriers and other enzymes on EziG carriers.

4.3 Conclusion

AthHNL was successfully immobilized on EziG Opal by an optimized methodology. *AthHNL*-EziG Opal was recycled up to seven times in batch with nearly complete conversion and excellent enantioselectivity. The continuous flow system displayed excellent conversion and enantioselectivity at 0.1 mL min^{-1} and allowed to increase four times the productivity for the synthesis of (*R*)-mandelonitrile as compared to the batch system.

4.4 Experimental section

4.4.1 Chemicals

Except when reported otherwise all chemicals were bought from Sigma Aldrich (Schnelldorf, Germany). Isopropanol and heptane were of HPLC grade (>99%) and used as HPLC solvents. 1,3,5-triisopropylbenzene (97%) was from Fluka Chemie (Buchs, Switzerland). Potassium cyanide (KCN, 97%) from J.T. Baker (Deventer, The Netherlands) was used as cyanide source in the HCN solution. (±)-Mandelonitrile from Acros Organics (Geel, Belgium) was purified by flash chromatography (PE/MTBE 9:1/3:7).

4.4.2 Heterologous expression of *Arabidopsis thaliana* HNL (AtHNL)

pET28a-HNL expression plasmid containing the AtHNL gene (GenBank accession number AAN13041, EC:4.1.2.10) codon optimized for *E. coli* and with a polyhistidine tag (His₆-tag) (see Table S1) was obtained from the group of Martina Pohl (Institute of Bio-and Geosciences, Jülich, Germany). *E. coli* BL21(DE3) was transformed with the expression plasmid for the production of the His-tagged AtHNL. A preculture was prepared by inoculating one single colony of *E. coli* BL21(DE3)-pET28aAtHNL in 10 mL of Lysogeny Broth (LB) medium with kanamycin (40 µg mL⁻¹) and incubated overnight

(Eppendorf/New Brunswick Scientific Incubator Shaker Excella E24 Series, Nijmegen, The Netherlands) at 37 °C, 180 rpm. Subsequently, this preculture was used for the inoculation of 1 L of Terrific Broth (TB) medium containing kanamycin (40 µg mL⁻¹) and incubated at 37 °C, 120 rpm. When the OD₆₀₀ reached 0.7–0.9 the protein expression was induced by adding 1 mL of 0.1 M isopropyl β-D-thiogalactoside (IPTG) per liter of culture (0.1 mM IPTG final concentration) and cultivation was continued at 25 °C, 180 rpm for 20 h.

Cells were harvested by centrifugation at 4 °C, 3600 x g rpm during 20 min (Sorvall RC6, Thermo Fisher Scientific, Landsmeer, The Netherlands). The supernatant was discarded and the pellets were washed with 30 mL of 10 mM sodium phosphate buffer pH 7, frozen in liquid nitrogen and stored at - 80 °C.

4.4.3 Enzyme purification

The pellets containing *A*tHNL were resuspended in lysis buffer (10 mM potassium phosphate buffer pH 7.4 + DNase) and lysed in a cell disruptor (Constant Systems Ltd., Daventry, United Kingdom) at 1.5 kBar and 4°C to avoid protein denaturation. The cell free extracts were collected by centrifugation at 48000 x g, 1 h, 4°C (Sorvall RC6, Thermo Fisher Scientific, Landsmeer, The Netherlands). The enzyme was purified by using a NGC Chromatography system (Bio-Rad, Veenendaal, The Netherlands) by immobilized metal ion chromatography (IMAC) with chelating Ni²⁺ Sepharose (HiTrap Chelating HP 5 mL, GE Healthcare) according to the manufacturer [38]. 20 mM sodium phosphate + 0.5 M NaCl + 20 mM imidazole pH 7.4 was used for the enzyme binding and 20 mM sodium phosphate + 0.5 M NaCl + 0.5 M imidazole pH 7.4 was used for the enzyme elution.

The purified *A*tHNL was concentrated with a 10 kDa MWCO Amicon filter (Millipore, Amsterdam-Zuidoost, The Netherlands) and desalted with a PD-10 desalting column (Cytiva, Medemblik, The Netherlands) according to the supplier instructions [39].

4.4.4 Enzymatic activity assay

*A*tHNL activity was determined spectrophotometrically (Agilent Technologies Cary 60 UV-VIS, Amstelveen, The Netherlands) according to the literature [15] with slight modifications. The cleavage of *rac*-mandelonitrile into benzaldehyde and hydrogen cyanide was followed at 280 nm and 25°C in 1 cm quartz glass cuvettes. Briefly, 1400 µL of 50 mM citrate/phosphate buffer pH 5 and 200 µL of enzyme solution (in 5 mM phosphate buffer pH 6.5) were mixed and incubated for 30 s at 25 °C. The reaction was started by adding 400 µL of 60 mM *rac*-mandelonitrile solution (80 µL of *rac*-mandelonitrile in 10 mL 3 mM citrate/phosphate buffer, pH 3.5). The enzymatic activity was calculated with the molar extinction coefficient of benzaldehyde ($\epsilon_{280} = 1.376 \text{ mM}^{-1} \text{ cm}^{-1}$) and the background reaction (performed without enzyme) was subtracted in the final calculation.

One unit of *A*tHNL activity is the amount of micromoles of *rac*-mandelonitrile converted per minute in citrate/phosphate buffer pH 5 at 25 °C.

4.4.5 Synthesis of hydrogen cyanide (HCN) solution in MTBE

A HCN solution in MTBE was made according to earlier studies [15–19,29]. 25 mL MTBE and 10 mL MilliQ water were mixed in a 100 mL Erlenmeyer and kept at 0 °C.

0.1 mol potassium cyanide (6.51 g) was dissolved in the mixture and magnetically stirred for 15 min. 10 mL of 30% (v/v) HCl solution was added slowly and stirring was continued for 2 min. The HCN solution was allowed to reach room temperature (*circa* 20 °C). The organic and aqueous phases were separated using a separation funnel and the organic layer containing HCN was collected. The separation was performed twice more after adding 7 mL of MTBE each time. Finally, 5 mL of 50 mM citrate/phosphate buffer pH 5 was added to the organic fraction collected and it was stored in a dark bottle at 4 °C.

The HCN concentration was determined in accordance to the literature [40]. 1 mL of HCN solution was added to 5 mL of 2 M NaOH in a 25 mL Erlenmeyer. The mixture was stirred for 2 min. Potassium chromate was added as indicator. The solution was titrated with 0.1 M silver nitrate. The cyanide reacts 1:1 with the silver and precipitates.

4.4.6 Immobilization of A β HNL on EziG Opal by adsorption

The immobilization of A β HNL on EziG Opal by adsorption was performed as described previously [16,18,29]. Given volumes of A β HNL solution were concentrated in Amicon filters with a 10 kDa MW cut-off, and subsequently added dropwise to 60 mg of EziG Opal (batch) or 150 mg of EziG Opal (flow). For batch reactions, A β HNL-EziG Opal was tightly packed in a regular paper tea bag [16,29] and either directly used for biocatalytic reactions or dried 16 h under vacuum in a desiccator over silica gel before packing. A magnetic stirrer was attached to the tea bags as reported earlier [16,29] to ensure tight packing and rapid stirring without mechanical attrition of the carrier. Reactions in flow were performed with wet A β HNL-EziG Opal (without drying and packing). The ratio of enzyme solution to carrier (μ L:mg) was 2:1 in all cases to ensure that the enzyme solution was completely absorbed by the carrier. The immobilization of different enzyme units was achieved by determining the enzyme activity and adjusting the amount of enzyme solution before its concentration.

4.4.7 Immobilization of A β HNL on EziG Opal by incubation

The immobilization of A β HNL on EziG Opal by incubation was performed according to the manufacturer (see the instruction manual in the supplementary information). 2 mL of enzyme solution with the required units to be immobilized was incubated with 60 mg of carrier in an orbital shaker (model RM:2M) at 30 rpm during 2 h at room temperature. The binding of the enzyme to the carrier was monitored by determining

the protein concentration of the supernatant after immobilization using the BCA protein determination (Pierce BCA protein assay kit, Thermo Fisher Scientific, Landsmeer, The Netherlands) in accordance with the manufacturer instructions [41].

4.4.8 Synthesis of (*R*)-mandelonitrile in batch

Several (*R*)-mandelonitrile syntheses were performed with 60 mg of immobilized *Ath*HNL-EziG Opal. The reaction conditions were as follows: 100 μ L benzaldehyde (1 mmol), 27.5 μ L 1,3,5-triisopropylbenzene (internal standard (I.S.)), 2 mL HCN in 50 mM citrate/phosphate buffered MTBE pH 5 (1.5–2 M), tea bag filled with 60 mg immobilized enzyme, 900 rpm and room temperature. The ratio benzaldehyde to HCN solution was 1:4. The mole ratio *Ath*HNL:Fe³⁺ was 1:5.

4.4.9 Enzyme Recyclability in Batch

The enzyme recyclability was determined by several cycles of (*R*)-mandelonitrile synthesis according to [15,16,18,29]. The reaction conditions were as follows: benzaldehyde (100 μ L, 1 mmol), 27.5 μ L 1,3,5-triisopropylbenzene (I.S.), 2 mL HCN in 50 mM citrate/phosphate buffered MTBE pH 5 (1.5–2 M), tea bag filled with 60 mg immobilized enzyme, 900 rpm and room temperature. The ratio benzaldehyde to HCN solution was 1:4. The mol ratio *Ath*HNL:Fe³⁺ was 1:5. Between each cycle the immobilized enzyme was washed for 1 min with 50 mM citrate/phosphate buffered MTBE, pH 5, and stored at 4°C in fresh citrate/phosphate buffered MTBE, pH 5.

4.4.10 Synthesis of (*R*)-mandelonitrile in continuous flow

One milliliter stainless steel flow reactor (6.4 cm length, 0.45 cm inner diameter) was used for the continuous synthesis of (*R*)-mandelonitrile with 150 mg of immobilized *Ath*HNL on EziG Opal (10 U mg⁻¹). The reactor was filled with 100 mg of non-porous glass beads (1 mm diameter) and 150 mg of EziG Opal containing immobilized enzyme (final reaction volume = 0.3 mL). 10 cm of polytetrafluoroethylene (PTFE) tubing with 1.5 mm inner diameter was used to connect a syringe pump (Knauer, Germany) with the reactor. Initial conditions were as follows: 0.5 M benzaldehyde, 1.5–2 M HCN in 100 mM citrate/phosphate buffered MTBE, pH 5 and 50 mM 1,3,5-triisopropylbenzene as I.S.. The synthesis of (*R*)-mandelonitrile was evaluated at different flow rates (from 0.1 to 1 mL min⁻¹) by chiral HPLC. The mole ratio *Ath*HNL:Fe³⁺

was 1:4. The flow rate was checked at each sampling time by the difference of weight. Reactions were performed at room temperature. No significant pressure drop or increase was observed within the timeframe of the experiments.

4.4.11 Enzyme stability in continuous flow

The stability of immobilized *At*HNL on EziG Opal (10 U mg⁻¹) was evaluated by performing a synthesis reaction during 12 h at 0.1 mL min⁻¹ on stream at room temperature. The mol ratio *At*HNL:Fe³⁺ was 25%. Samples were drawn at regular intervals and analyzed by chiral HPLC.

4.4.12 Analysis

Samples (10 µL) were taken at different times during the reaction run and added to 990 µL of heptane:2-propanol 95:5 in 1.5 mL Eppendorf tubes. A small amount of anhydrous magnesium sulphate (MgSO₄) was used to remove the water from the solution and the Eppendorf tubes were centrifuged at 13000 x g rpm for 1 min. 850 µL of the supernatant was transferred to a 4 mL HPLC vial and 10 µL was injected into the HPLC (Chiralpak AD-H column, column size: 0.46 cm I.D x 25 cm). Heptane and 2-propanol were used as mobile phase with a flow rate of 1 mL min⁻¹ and the UV detector was set at 216 nm. The column temperature was set at 40 °C. The samples in the autosampler were maintained at 4 °C.

References

- 1 Dadashipour, M.; Asano, Y. Hydroxynitrile lyases: Insights into biochemistry, discovery, and engineering. *ACS Catal.* **2011**, 1, 1121–1149.
- 2 Steiner, K.; Glieder, A.; Gruber-Khadjawi, M. Cyanohydrin formation/Henry reaction. In *Science of Synthesis: Biocatalysis in Organic Synthesis*; Georg Thieme Verlag: Stuttgart, Germany, 2015; Volume 2, pp. 1–30.
- 3 Lanfranchi, E.; Steiner, K.; Glieder, A.; Hajnal, I.; Sheldon, R.A.; van Pelt, S.; Winkler, M. Mini-Review: Recent developments in hydroxynitrile lyases for industrial biotechnology. *Recent Pat. Biotechnol.* **2013**, 7, 197–206.
- 4 Bracco, P.; Busch, H.; von Langermann, J.; Hanefeld, U. Enantioselective synthesis of cyanohydrins catalysed by hydroxynitrile lyases—A review. *Org. Biomol. Chem.* **2016**, 14, 6375–6389.

- 5 Faber, K. *Biotransformations in Organic Chemistry*, 7th ed.; Springer Nature: Basel, Switzerland, 2018; pp. 224–233.
- 6 Hanefeld, U. Immobilisation of hydroxynitrile lyases. *Chem. Soc. Rev.* **2013**, 42, 6308–6321.
- 7 Zhu, Y.; Chen, Q.; Shao, L.; Jia, Y.; Zhang, X. Microfluidic immobilized enzyme reactors for continuous biocatalysis. *React. Chem. Eng.* **2020**, 5, 9–32.
- 8 Cantone, S.; Ferrario, V.; Corici, L.; Ebert, C.; Fattor, D.; Spizzo, P.; Gardossi, L. Efficient immobilisation of industrial biocatalysts: Criteria and constraints for the selection of organic polymeric carriers and immobilisation methods. *Chem. Soc. Rev.* **2013**, 42, 6262–6276.
- 9 Liese, A.; Hilterhaus, L. Evaluation of immobilized enzymes for industrial applications. *Chem. Soc. Rev.* **2013**, 42, 6236–6249.
- 10 Hanefeld, U.; Gardossi, L.; Magner, E. Understanding enzyme immobilisation. *Chem. Soc. Rev.* **2009**, 38, 453–468.
- 11 Block, H.; Maertens, B.; Spriestersbach, A.; Brinker, N.; Kubicek, J.; Fabis, R.; Labahn, J.; Schäfer, F. *Immobilized-Metal Affinity Chromatography (IMAC) in Methods in Enzymology*; Academic Press: Cambridge, MA, USA, 2009; pp. 439–473.
- 12 Das, K.K.; Reddy, R.C.; Bagoji, I.B.; Das, S.; Bagali, S.; Mullur, L.; Khodnapur, J.P.; Biradar, M.S. Primary concept of nickel toxicity—An overview. *J. Basic Clin. Physiol. Pharmacol.* **2018**, 30, 141–152.
- 13 Andexer, J.N.; Staunig, N.; Eggert, T.; Kratky, C.; Pohl, M.; Gruber, K. Hydroxynitrile lyases with α/β -hydrolase fold: Two enzymes with almost identical 3D structures but opposite enantioselectivities and different reaction mechanisms. *ChemBioChem* **2012**, 13, 1932–1939.
- 14 Cassimjee, K.E.; Kadow, M.; Wikmark, Y.; Humble, M.S.; Rothstein, M.L.; Rothstein, D.M.; Bäckvall, J.-E. A general protein purification and immobilization method on controlled porosity glass: Biocatalytic applications. *Chem. Commun.* **2014**, 50, 9134–9137.

- 15 Okrob, D.; Paravidino, M.; Orru, R.V.A.; Wiechert, W.; Hanefeld, U.; Pohl, M. Hydroxynitrile lyase from *Arabidopsis thaliana*: Identification of reaction parameters for enantiopure cyanohydrin synthesis by pure and immobilized catalyst. *Adv. Synth. Catal.* **2011**, 353, 2399–2408.
- 16 Bracco, P.; Torrelo, G.; Noordam, S.; de Jong, G.; Hanefeld, U. Immobilization of *Prunus amygdalus* hydroxynitrile lyase on Celite. *Catalysts* **2018**, 8, 287.
- 17 van der Helm, M.P.; Bracco, P.; Busch, H.; Szymanska, K.; Jarzebski, A.; Hanefeld, U. Hydroxynitrile lyases covalently immobilized in continuous flow microreactors. *Catal. Sci. Technol.* **2019**, 9, 1189–1200.
- 18 Torrelo, G.; van Midden, N.; Stloukal, R.; Hanefeld, U. Immobilized hydroxynitrile lyase: A comparative study of recyclability. *ChemCatChem.*, **2014**, 6, 1096–1102.
- 19 Brahma, A.; Musio, B.; Ismayilova, U.; Nikbin, N.; Kamptmann, S.; Siegert, P.; Jeromin, G.E.; Ley, S.V.; Pohl, M. An orthogonal biocatalytic approach for the safe generation and use of HCN in a multistep continuous preparation of chiral *O*-Acetylcyanohydrins. *Synlett* **2015**, 27, 262–266.
- 20 Böhmer, W.; Knaus, T.; Volkov, A.; Slot, T.K.; Shiju, N.R.; Cassimjee, K.E.; Mutti, F.G. Highly efficient production of chiral amines in batch and continuous flow by immobilized ω -transaminases on controlled porosity glass metal-ion affinity carrier. *J. Biotechnol.* **2019**, 291, 52–60.
- 21 Tentori, F.; Bavaro, T.; Brenna, E.; Colombo, D.; Monti, D.; Semproli, R.; Ubiali, D. Immobilisation of old yellow enzymes via covalent or coordination bonds. *Catalysts* **2020**, 10, 260.
- 22 Aßmann, M.; Mügge, C.; Gaßmeyer, S.K.; Enoki, J.; Hilterhaus, L.; Kourist, R.; Liese, A.; Kara, S. Improvement of the process stability of Arylmalonate decarboxylase by immobilization for biocatalytic profen synthesis. *Front. Microbiol.* **2017**, 8, 448.
- 23 Yu, T.; Ding, Z.; Nie, W.; Jiao, J.; Zhang, H.; Zhang, Q.; Xue, C.; Duan, D.; Yamada, Y.M.A.; Li, P. Recent advances in continuous-flow enantioselective catalysis. *Chem. Eur. J.* **2020**, 26, 5729–5747.

- 24 Yoo, W.J.; Ishitani, H.; Saito, Y.; Laroche, B.; Kobayashi, S. Reworking organic synthesis for the modern age: Synthetic strategies based on continuous-flow addition and condensation reactions with heterogeneous catalysts. *J. Org. Chem.* **2020**, *85*, 5132–5145.
- 25 Thompson, M.P.; Peñafiel, I.; Cosgrove, S.C.; Turner, N.J. Biocatalysis using immobilized enzymes in continuous flow for the synthesis of fine chemicals. *Org. Process Res. Dev.* **2019**, *23*, 9–18.
- 26 Akwi, F.M.; Watts, P. Continuous flow chemistry: Where are we now? Recent applications, challenges and limitations. *Chem. Commun.* **2018**, *54*, 13894–13928.
- 27 Sheldon, R.A.; Woodley, J.M. Role of biocatalysis in sustainable chemistry. *Chem. Rev.* **2018**, *118*, 801–838.
- 28 Movsisyan, M.; Delbeke, E.I.P.; Berton, J.K.E.T.; Battilocchio, C.; Ley, S.V.; Stevens, C.V. Taming hazardous chemistry by continuous flow technology. *Chem. Soc. Rev.* **2016**, *45*, 4892–4928.
- 29 Coloma, J.; Guiavarc'h, Y.; Hagedoorn, P.L.; Hanefeld, U. Probing batch and continuous flow reactions in organic solvents: *Granulicella tundricola* hydroxynitrile lyase (GtHNL). *Catal. Sci. Technol.* **2020**, *10*, 3613–3621.
- 30 Vieille, C.; Zeikus, G.J. Hyperthermophilic enzymes: Sources, uses, and molecular mechanisms for thermostability. *Microbiol. Mol. Biol. Rev.* **2001**, *65*, 1–43.
- 31 Guterl, J.K.; Andexer, J.N.; Sehl, T.; von Langermann, J.; Frindi-Wosch, I.; Rosenkranz, T.; Fitter, J.; Gruber, K.; Kragl, U.; Eggert, T.; et al. Uneven twins: Comparison of two enantiocomplementary hydroxynitrile lyases with α/β -hydrolase fold. *J. Biotechnol.* **2009**, 166–173.
- 32 Paravidino, M.; Sorgedraeger, M.J.; Orru, R.V.; Hanefeld, U. Activity and enantioselectivity of the hydroxynitrile lyase MeHNL in dry organic solvents. *Chem. Eur. J.* **2010**, *16*, 7596–7604.

- 33 Effenberger, F.; Eichhorn, J.; Roos, J. Enzyme catalyzed addition of hydrocyanic acid to substituted pivalaldehydes—A novel synthesis of (*R*)-pantolactone. *Tetrahedron Asymmetry* **1995**, 6, 271–282.
- 34 Costes, D.; Wehtje, E.; Adlercreutz, P. Hydroxynitrile lyase-catalyzed synthesis of cyanohydrins in organic solvents: Parameters influencing activity and enantiospecificity. *Enzym. Microb. Technol.* **1999**, 25, 384–391.
- 35 Abdelraheem, E.M.M.; Busch, H.; Hanefeld, U.; Tonin, F. Biocatalysis explained: From pharmaceutical to bulk chemical production. *React. Chem. Eng.* **2019**, 4, 1878–1894.
- 36 Britton, J.; Majumdar, S.; Weiss, G.A. Continuous flow biocatalysis. *Chem. Soc. Rev.* **2018**, 47, 5891–5918.
- 37 Tamborini, L.; Fernandes, P.; Paradisi, F.; Molinari, F. Flow bioreactors as complementary tools for biocatalytic process intensification. *Trends Biotechnol.* **2018**, 6, 73–88.
- 38 Affinity Chromatography: Principles and Methods. Available online: www.sigmaaldrich.com/content/dam/sigma-aldrich/docs/Sigma-Aldrich/General_Information/1/ge-affinity-chromatography.pdf (accessed on 14 October 2019).
- 39 PD-10 Desalting Columns. Available online: <http://wwwuser.gwdg.de/~jgrossh/protocols/proteinpurification/PD10.pdf> (accessed on 14 October 2019).
- 40 Van Langen, L.M.; van Rantwijk, F.; Sheldon, R.A. Enzymatic hydrocyanation of a sterically hindered aldehyde. Optimization of a chemoenzymatic procedure for (*R*)-2-Chloromandelic Acid. *Org. Process. Res. Dev.* **2003**, 7, 828–831.
- 41 User Guide: Pierce BCA Protein Assay Kit. Available online: [https://www.thermofisher.com/document-connect/document-connect.html?url=https%3A%2F%2Fassets.thermofisher.com%](https://www.thermofisher.com/document-connect/document-connect.html?url=https%3A%2F%2Fassets.thermofisher.com%2Fdocuments/pdf/TFS/Biochemicals/Pierce_BCA_Protein_Assay_Kit.pdf)

Supplementary Information

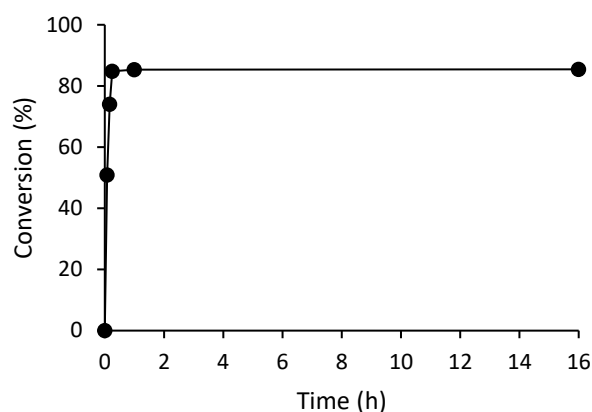


Figure S1. Leaching assay for *A*tHNL on EziG Opal (2 U/mg). Immobilization was performed by adsorption and drying. *A*tHNL on EziG1 was removed after 15 minutes of reaction. Conditions: Ratio benzaldehyde : HCN in citrate/phosphate buffered MTBE, pH 5, 1:4, benzaldehyde (100 μ L, 1 mmol), 2 ml HCN solution in citrate/phosphate buffered MTBE (1.5 - 2 M) pH 5, 27.5 μ L (0.1 mmol) 1,3,5-tri-isopropylbenzene as internal standard (I.S.) and a teabag filled with *A*tHNL immobilized on 50 mg EziG1. The reaction was stirred at 900 rpm at room temperature.

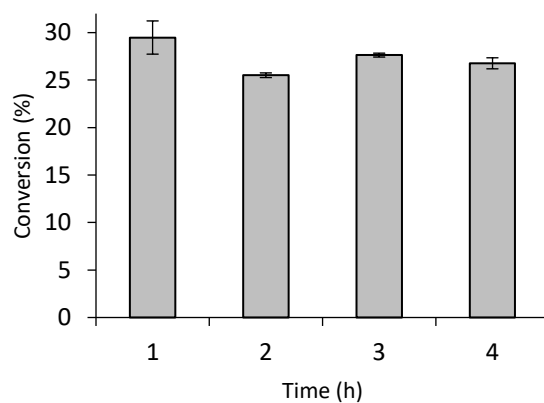


Figure S2. Blank reaction in batch. Conditions: Ratio benzaldehyde : HCN in citrate/phosphate buffered MTBE, pH 5, 1:4, benzaldehyde (100 μ L, 1 mmol), 2 ml HCN solution in citrate/phosphate buffered MTBE (1.5 - 2 M) pH 5, 27.5 μ L (0.1 mmol) 1,3,5-tri-isopropylbenzene as I.S. and 50 mg of dried EziG Opal. The reaction was stirred at 900 rpm at room temperature. Error bars correspond to the standard deviation of duplicates (n=2).

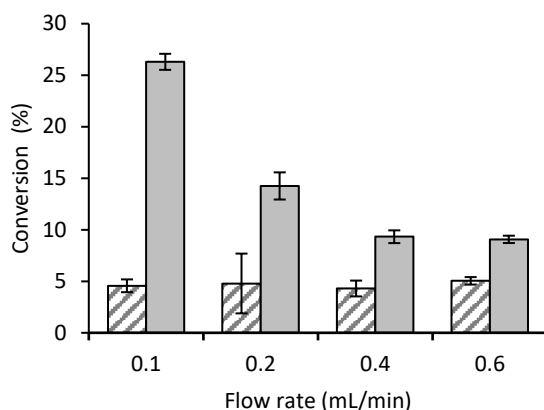


Figure S3. Blank reaction in flow. Grey bars are the reactions performed with wet EziG Opal (carrier + 0.306 mL of citrate/phosphate buffer pH 5). Dashed bars are the reactions performed with dried EziG1. Conditions: Ratio benzaldehyde : HCN in citrate/phosphate buffered MTBE, pH 5, 1:4, benzaldehyde (100 μ L, 1 mmol), 2 ml HCN solution in citrate/phosphate buffered MTBE (1.5 - 2 M) pH 5, 27.5 μ L (0.1 mmol) 1,3,5-tri-isopropylbenzene as I.S. and 150 mg EziG1. The reactions were stirred at 900 rpm at room temperature. Error bars correspond to the standard deviation of duplicates ($n=2$).

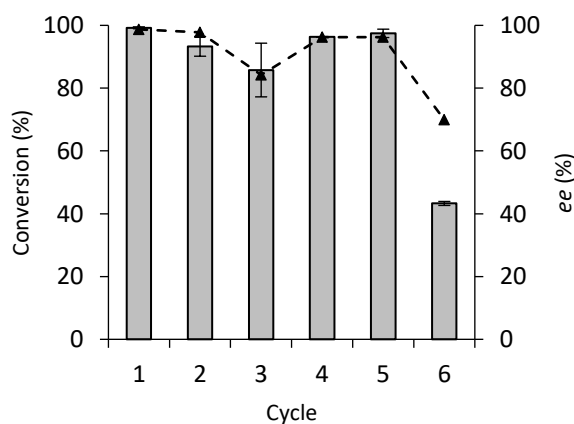


Figure S4. Recycling of A#HNL immobilised on EziG Opal (20 U/mg) in eight successive cycles. Immobilization was performed by incubation and drying. Conversion (bars), enantiomeric excess (dotted line and triangles). Conditions: Ratio benzaldehyde : HCN in citrate/phosphate buffered MTBE, pH 5, 1:4, benzaldehyde (100 μ L, 1 mmol), 2 ml HCN solution in citrate/phosphate buffered MTBE (1.5 - 2 M) pH 5, 27.5 μ L (0.1 mmol) 1,3,5-tri-isopropylbenzene as I.S. and a teabag filled with A#HNL immobilized on 50 mg EziG1. The reaction was stirred at 900 rpm at room temperature. The enzyme was washed for 1 minute with 100 mM citrate/phosphate buffer saturated MTBE pH 5 after each cycle. Error bars correspond to the standard deviation of duplicates ($n=2$).

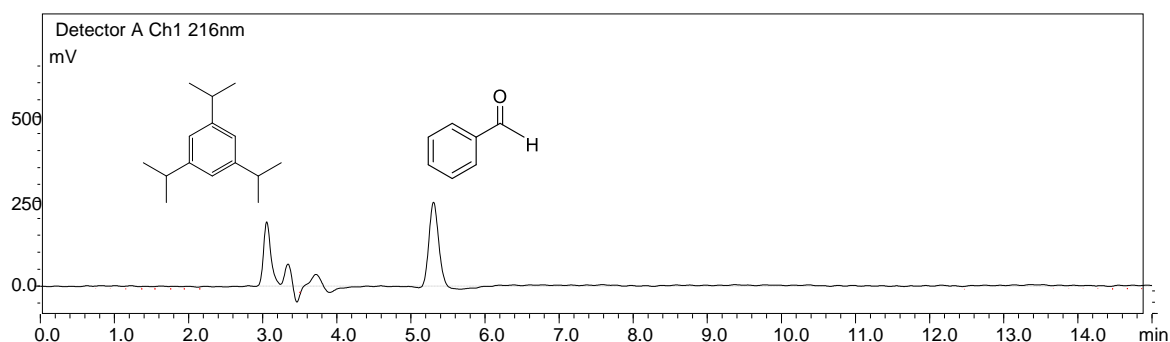


Figure S5. HPLC detection of benzaldehyde and 1,3,5 tri-isopropylbenzene during 8 hours of incubation: Conditions: Ratio benzaldehyde : HCN in buffered MTBE pH 4 ~1:4, 100 μ L benzaldehyde (1 mmol), 2 mL HCN in acetate buffered MTBE pH 4. The reaction was stirred at 1000 rpm at 5 $^{\circ}$ C.

Table S1. *A*#HNL Gene and Aminoacid sequences

<i>A</i> #HNL - Gene sequence	<i>A</i> #HNL - Aminoacid sequence
5'GGRAAATTTACCTCTAGAATAATTTTGTTTACTTTAAGAAG GAGATATACCATGGGCAGCAGCCATCATCATCATCACA GCAGCGCCTGGTGCCGCGCGGCAGCCATATGGAGAGGA AACATCACTTCGTGTTAGTTCACAACGCTTATCATGGAGCCT GGATCTGGTACAAGCTCAAGCCCTCCTTGAATCAGCCGG CCACCGCGTTACTGCTGTGCAACTCGCCGCTCCGGGATC GACCCACGACCAATCCAGGCCGTTGAAACCGTCGACGAAT ACTCCAAACCGTTGATCGAAACCCTCAAATCTCTCCAGAG AACGAAGAGGTAATTCTGGTTGGATTCAGCTTCGGAGGCAT CAACATCGCTCTCGCCGCGACATATTTCCGGCGAAGATTA AGGTTCTTGTTCTCAACGCCTTCTTGCCCGACACAACC CACGTGCCTTCTCACGTTCTGGACAAGTATATGGAGATGCC TGGAGGTTTGGGAGATTGTGAGTTTTTCATCTCATGAAACAA GAAATGGGACGATGAGTTTATTGAAGATGGGACCAAATTC ATGAAGGCACGTCTTTACCAAATTTGTTCCATAGAGGATTA CGAGCTGGCAAAAATGTTGCATAGGCAAGGGTCATTTTTCA CAGAGGATCTATCAAAGAAAGAAAAGTTTAGCGAGGAAGGA TATGGTTCCGGTGAACGAGTTTACGTAATGAGTAGTGAAGA CAAAGCCATCCCCTGCGATTTTCATTGTTGGATGATTGATA ATTTCAACGTCTCGAAAGTCTACGAGATCGATGGCGGAGAT CACATGGTGATGCTCTCCAAACCCCAAAAACCTTTTGACTC TCTCTGCTATTGCCACCGATTATATGTAAGCGGCCGCAC TCGAGCACCACCACCACCACCTGAGATCCGGCTGCTAA CAAGCCCGAAAGGAAGCTGAGTTGGCTGCTGCCACCGCTG AGCAATAACTAGCAWACCCCTTGGGGCCTCTAAACGGTCTT GAGGGTTTTTTGCTGAAGGAGGAACTATATCCGGATTGGCG AATGGGACGCGCCCTGTAGCGGCGCATTAAAGCGCGGCGG G -3'	MGSSHHHHHSSGLVPRGSHMERKHH FVLVHNAYHGAWIWYKLPLESAGHRV TAVELAASGIDPRPIQAVETVDEYSKPLIE TLKSLPENEEVILVGFSGGINIALAADIFP AKIKVLVFLNAFLPDTTHVPSHVLDKYME MPGGLGDCEFSSHETRNGTMSLLKMGF KFMKARLYQNCPIEDYELAKMLHRQGSF FTEDLSKKEKFSEEGYGSVQRVYVMSS EDKAIPCDFIRWMIDNFNVSKVYEIDGGD HVMMLSKPQKLFDSL SAIATDYM

5

Batch and flow nitroaldol synthesis catalysed by *Granulicella tundricola* hydroxynitrile lyase immobilised on Celite R-633

The triple variant GtHNL-A40H/V42T/Q110H (GtHNL-3V) was immobilised on Celite R-633 for the synthesis of (*R*)-2-nitro-1-phenylethanol (NPE) in batch and continuous flow systems. Nitromethane was used as nucleophile. 82% of (*R*)-NPE and excellent enantioselectivity (> 99%) were achieved in batch after 24 hours of reaction time. GtHNL-3V on Celite R-633 was successfully recycled 5 times. The use of a flow system enabled the continuous synthesis of (*R*)-NPE. 15% formation of (*R*)-NPE was reached using a flow rate of 0.1 mL min⁻¹; unfortunately, the enzyme was not stable and the yield decreased to 4% after 4 hours on stream. A similar yield was observed during 15 hours at a rate of 0.01 mL min⁻¹. Surprisingly the use of a continuous flow system did not facilitate process intensification. In fact, the batch system displayed a space-time-yield of 0.10 g L⁻¹ h⁻¹ mg_{enzyme}⁻¹ whereas the flow system displayed 0.02 and 0.003 g L⁻¹ h⁻¹ mg_{enzyme}⁻¹ at 0.1 and 0.01 mL min⁻¹ respectively. In general, the addition of 1 M nitromethane potentially changed the polarity of the reaction mixture affecting the stability of celite-GtHNL-3V. The nature of the batch system maintained the reaction conditions better than the flow system.

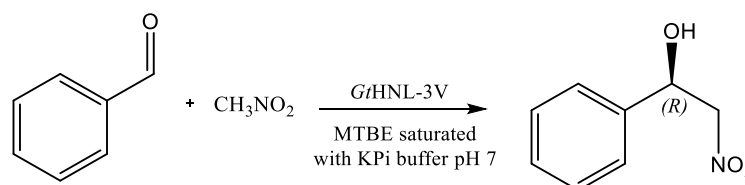
This chapter is based on

José Coloma, Lidwien Teeuwisse, Muhammad Afendi, Peter-Leon Hagedoorn and Ulf Hanefeld

Catalysts, **2022**, 12, 161. DOI:10.3390/catal12020161

5.1 Introduction

Chiral β -nitro alcohols are compounds containing two versatile functional groups, a hydroxyl and a nitro group, attached to adjacent carbon centers of which either one or both are asymmetric. These compounds are precursors of chiral β -amino alcohols, which are important chiral building blocks for the synthesis of bioactive compounds used as pharmaceutical ingredients such as bestatin, ephedrine, norephedrine and sphingosine [1-2]. The synthesis of β -nitro alcohols is base catalysed and many bases have been evaluated. Unfortunately, unwanted side reactions such as aldol reactions, Cannizzaro disproportionation and water elimination catalysed by these strong bases hamper their application [3]. Biocatalysis is an alternative method for producing β -nitro alcohols with high selectivity under mild reaction conditions. Six biocatalytic approaches [4-24] have to date been described as recently reviewed [1]. Of these, the HNL catalysed Henry reaction is particularly attractive as a new carbon-carbon bond and a stereocentre are established simultaneously. This promiscuous HNL activity is based on the similar pK_a value of hydrogen cyanide ($pK_a = 9.21$) and nitromethane ($pK_a = 10.2$) (Scheme 1).



Scheme 1: Synthesis of (*R*)-2-nitro-1-phenylethanol catalysed by GtHNL-3V

The synthesis of (*R*)-2-nitro-1-phenylethanol catalysed by GtHNL-3V, a more active and stable variant compared to the wild type enzyme, was reported using a biphasic system in a batch process [12]. Long reaction times (24 h) were needed to achieve 72.8% of conversion and 94.5% of enantiomeric excess. Flow chemistry is an important tool for process intensification and has been reported to reduce reaction times concomitantly improving enantioselectivities by suppressing undesired side reactions. Additionally, it enhances safety and among others reduces reaction volumes [25-32]. At the same time, it requires the enzymes to be immobilised, which often improves enzyme stability. Celite is an environmentally friendly, food grade carrier that has been used for the immobilisation of several HNLs with good results [33-35]. This cheap hydrophilic carrier has the ability to bind water efficiently. This

enables a local aqueous environment around the enzyme and avoids the use of chemicals during the enzyme immobilisation which might affect the enzyme stability [36]. Indeed, the successful immobilisation of GtHNL-3V on Celite R-633 for the synthesis of (*R*)-mandelonitrile in batch and flow systems has been reported [37]. Good conversion, excellent enantioselectivity and high stability were achieved in both systems. In addition, the continuous flow system enabled an important increase in space-time-yield (65 times) compared to the batch system.

Herein, we aim to evaluate the GtHNL-3V catalysed nitroaldol reaction for the synthesis of (*R*)-2-nitro-1-phenylethanol in batch and flow systems. For this, GtHNL-3V was immobilised on Celite R-633. Monophasic MTBE saturated with 100 mM KPi buffer pH 7 was employed as reaction medium. The activity, stability and productivity of batch and flow systems were investigated.

5.2 Results and discussion

GtHNL-3V was successfully overexpressed in *E. coli* BL21(DE3) and purified by a heat treatment. It displayed a specific activity of 2.2 ± 0.05 U mg⁻¹ for the cleavage of *rac*-mandelonitrile into benzaldehyde and hydrogen cyanide. The enzyme was immobilised on Celite R-633 by adsorption of an enzyme solution in 100 mM potassium phosphate buffer pH 7 as described earlier [37]. The synthesis of (*R*)-NPE (Scheme 1) was performed with MTBE saturated with the same buffer both for batch and flow systems.

5.2.1 Batch reactions

The initial experiments were directed towards rigorously establishing a system that enabled recycling experiments. The immobilisation of GtHNL-3V on Celite R-633 was therefore evaluated by a leaching test under reaction conditions. The immobilised enzyme was removed from the reaction mixture after 2 hours and samples were taken shortly after removing the enzyme and after 4 hours. If the enzyme does not leach from the carrier, no further conversion is expected. Indeed, this was the case. GtHNL-3V did not leach from Celite R-633 into the reaction medium (Figure 1). Different hydroxynitrile lyases (HNLs) such as *Prunus amygdalus* HNL (PaHNL) [35], *Manihot esculenta* HNL [34], *Arabidopsis thaliana* HNL (AtHNL) [33] and GtHNL [37] have been immobilised on Celite for the synthesis of cyanohydrins using buffer saturated organic

solvents as reaction medium. In all cases, the enzyme did not leach from Celite. The insolubility of the enzyme in organic solvents explains these results.

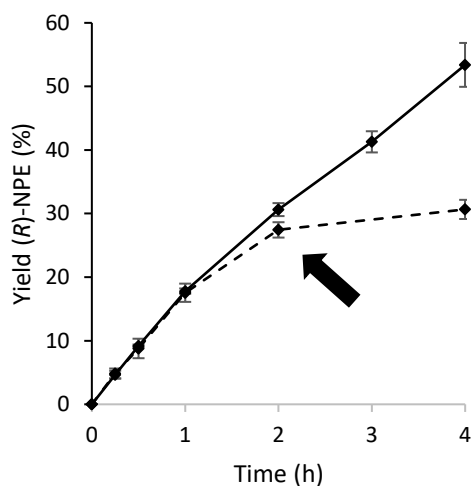


Figure 1. Leaching assay for *GtHNL* on Celite R-633 (10 U/50 mg Celite R-633). Conditions: Ratio benzaldehyde : nitromethane, 1:50, 20 mM benzaldehyde in MTBE saturated with 100 mM KPi pH 7, 1 M nitromethane, 20 mM 1,3,5-tri-isopropylbenzene as internal standard (I.S) in MTBE saturated with 100 mM KPi pH 7 and *GtHNL*-3V immobilised on 50 mg Celite R-633. The immobilised *GtHNL* was freely placed into the glass reaction vial. Reaction volume 1 mL. The reaction was shaken at 1200 rpm at 30 °C. Continuous line and diamonds is the enzyme catalysed reaction (10 U), dashed line and diamonds is the reaction where the immobilised enzyme (10 U) was removed after 2 hours. Error bars correspond to the standard deviation of duplicates ($n=2$). The yield of (*R*)-NPE was calculated by the ratio of (*R*)-NPE concentration to the initial benzaldehyde concentration.

Having established that *GtHNL*-3V does not leach from Celite R-633 under reaction conditions, time studies with different enzyme loadings of immobilised *GtHNL*-3V were performed (Figure 2). 75% formation of (*R*)-NPE and excellent enantioselectivity (> 99%) were achieved with 22 U of *GtHNL*-3V (5.74 mg) on 50 mg Celite R-633 after 4 hours. Commonly a low pH is used for the HNL catalysed synthesis of cyanohydrins to avoid the chemical racemic background reaction. This non-selective product formation is not relevant for the nitroaldol reaction, most probably due to the reduced solubility of nitromethane in the aqueous phase [9, 15]. Therefore, 100 mM potassium phosphate buffer pH 7 was used for the saturation of MTBE. This enables higher *GtHNL*-3V activity as it is in the ideal pH range of the enzyme. Neither Celite R-633 nor 0.25 mM $MnCl_2$ (negative controls) catalysed the non-selective nitroaldol reaction in the absence of *GtHNL*-3V (data not shown). An earlier report [12] showed 30% formation of (*R*)-NPE and enantioselectivity of 95.8% after equal reaction time using 0.5 mg of *GtHNL*-3V, however in a biphasic system.

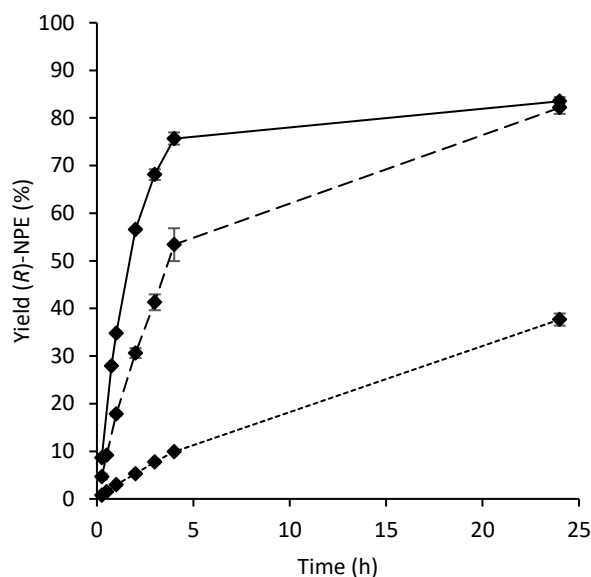


Figure 2: Synthesis of (*R*)-2-nitro-1-phenylethanol using different enzyme loadings on 50 mg of Celite R-633. Solid line (22 U, final ee > 99%), dashed line (10 U, final ee > 99%) and dotted line (1 U, final ee > 99%). Conditions: Ratio benzaldehyde : nitromethane, 1:50, 20 mM benzaldehyde in MTBE saturated with 100 mM KPi buffer pH 7, 1 M nitromethane, 20 mM 1,3,5-tri-isopropylbenzene in MTBE saturated with 100 mM KPi buffer pH 7 as internal standard (I.S) and *Gt*HNL-3V immobilised on 50 mg Celite R-633. The immobilised *Gt*HNL-3V was freely placed into the glass reaction vial. Reaction volume 1 mL. The reaction was shaken at 1200 rpm at 30 °C. Error bars correspond to the standard deviation of duplicates ($n=2$). The yield of (*R*)-NPE was calculated by the ratio of (*R*)-NPE concentration to the initial benzaldehyde concentration.

The *Hevea brasiliensis* HNL (*Hb*HNL) catalysed synthesis of several chiral β -nitroalcohols in a biphasic system [9] gave 63% of (*S*)-NPE with 92% ee. In kinetic resolutions, another approach commonly used to synthesise chiral β -nitroalcohols with HNLs, the (*S*)-selective HNL from *Hevea brasiliensis* (*Hb*HNL) catalysed the decomposition of (*S*)-NPE yielding (*R*)-NPE [13]. The resolution was conducted to almost completion (49%) with excellent enantioselectivity (95%). Product inhibition due to the aldehyde formed during the reaction was overcome by adding hydrogen cyanide to the reaction mixture, this enabled the formation of the less inhibitive mandelonitrile. Likewise, the *At*HNL catalysed kinetic resolution of *racemic* NPE was reported [15]. *At*HNL (27 U) immobilised on Celite R-545 was used in a biphasic system which resulted in 47% of conversion and 97% of enantiomeric excess after six hours of reaction time. Overall, the good yield and excellent enantioselectivity achieved by *Gt*HNL-3V on Celite using buffer saturated MTBE as reaction medium surpass the reduced ee, mass transfer and work-up limitations of the biphasic approach as well as the limited yield (50%) of kinetic resolutions.

In the cyanohydrin synthesis reactions the Celite immobilised HNLs all had to be dried before their application in buffer saturated solvents. Here the opposite was observed. *Gt*HNL-3V on Celite R-633 was not dried after immobilisation. When dried after immobilisation, the synthesis of (*R*)-NPE dropped to 41.12% \pm 0.62 even after prolonged reaction times (24 h). The water content and more accurately the water activity (a_w) of Celite-*Gt*HNL-3V is a crucial parameter in biocatalysis since enzymes, excluding lipases [38], need some water for conformational flexibility. Earlier studies [33] have shown the influence of the water content on the activity of immobilised *At*HNL on Celite R-633, where 10% (w/w) water content inside *At*HNL-Celite was needed for optimal enzymatic activity. Similarly, the stability of *Me*HNL as CLEA or immobilised on Celite R-633 is highly dependent on the water content entrapped in the carrier [34]. In general, the use of buffer saturated organic solvent provides the water that enzymes need for flexibility and facilitate reproducibility. However, in this reaction a high concentration of nitromethane is used. This compound has a low log P of – 0.24 [39] and influences the overall polarity of the reaction mixture. While buffer saturated MTBE would normally represent an a_w of 1, this is no longer the case at high nitromethane concentrations. Thus, the water entrapped in Celite-*Gt*HNL-3V can diffuse into the reaction mixture, as a result, the enzyme was deactivated rapidly. Earlier, the effect of a_w on enzymes in organic media was reported [40]. The activity and enantioselectivity of *Me*HNL-CLEA in organic solvents with different polarity at different a_w were investigated. The release of water from *Me*HNL-CLEA (and subsequent deactivation) depended on changes in polarity of the solvent due to the addition of reagents. The negative effect of dehydration on the catalytic activity of enzymes has been extensively studied [41-43].

Omitting the drying step after the enzyme immobilisation enabled high catalytic activity and excellent enantioselectivity. The stability of *Gt*HNL-3V on Celite R-633 for the synthesis of (*R*)-NPE in batch was evaluated by a recycling study (Figure 3). An enzyme loading of 10 U/50 mg Celite was used to observe any loss of activity due to enzyme deactivation. Higher activity and stability were observed when Celite-*Gt*HNL-3V was rehydrated with 50 μ L of 100 mM potassium phosphate buffer pH 7 after each cycle (Figure 3, blue bars). The increasing yield during the first 3 cycles might be related to the addition of buffer after each cycle and suggests that the a_w was not optimal for the enzymatic activity during the first 2 cycles. After 5 cycles a significant decrease in activity was observed. In contrast, the experiments without buffer addition

between cycles displayed lower yields and lower recyclability (Figure 3, dashed bars). Remarkably, an excellent enantiomeric excess was achieved under all conditions evaluated. The recyclability of *Gt*HNL-3V immobilised on Celite R-633 for the synthesis of (*R*)-mandelonitrile has been reported for the cyanohydrin synthesis [37]. High stability was observed. The biocatalyst was recycled 8 times with excellent enantioselectivity whereas yields gradually dropped to > 70% over all cycles. Recently, the stability of *At*HNL on Celite R-545 for the kinetic resolution of *racemic* NPE was reported [15]. The immobilised enzyme was stable during 4 cycles but a decrease in enantioselectivity (from 97% to 40%) was reported. According to the authors, enzyme leaching might be a possible explanation since the reaction was performed in a biphasic system and the immobilisation of *At*HNL on Celite R-545 involves weak interactions such as hydrogen bonding and van der Waals forces. The use of buffer saturated organic solvent as reaction medium is a straightforward approach to circumvent this limitation.

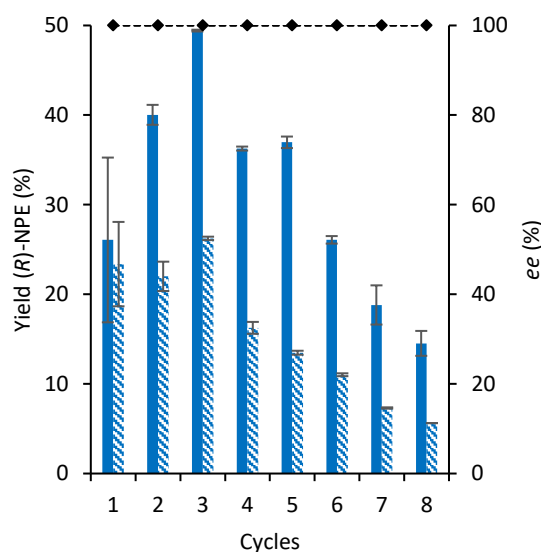


Figure 3. Recycling of *Gt*HNL-3V on Celite R-633 (10 U/50 mg) for the synthesis of (*R*)-2-nitro-1-phenylethanol in eight successive cycles. Blue bars (yields with the addition of 50 μ L of 100 mM potassium phosphate buffer pH 7 after the first cycle), dashed bars (yields without addition of 100 mM potassium phosphate buffer pH 7 between cycles), enantiomeric excess (dotted line and diamonds). Conditions: Ratio benzaldehyde : nitromethane, 1:50, 20 mM benzaldehyde in MTBE saturated with 100 mM KPi buffer pH 7, 1 M nitromethane, 20 mM 1,3,5-tri-isopropylbenzene in MTBE saturated with 100 mM KPi buffer pH 7 as internal standard (I.S) and *Gt*HNL-3V immobilised on 50 mg Celite R-633. The immobilised *Gt*HNL-3V was freely placed into the glass reaction vial. Reaction volume 1 mL. The reaction was shaken at 1200 rpm at 30 $^{\circ}$ C. Error bars correspond to the standard deviation of duplicates ($n=2$). The enzyme was washed for 1 minute (twice) with MTBE saturated with 100 mM KPi buffer pH 7 after each cycle. Reaction time: 2 hours. Error bars correspond to the standard deviation of duplicates ($n=2$). The yield of (*R*)-NPE was calculated by the ratio of (*R*)-NPE concentration to the initial benzaldehyde concentration

5.2.2 Continuous flow reactions

The immobilisation of *GtHNL-3V* allows the continuous synthesis of (*R*)-NPE leading potentially to process intensification. The enzyme was tested in flow either re-hydrated or not dried after immobilisation with a flow rate of 0.1 mL min⁻¹ or 0.01 mL min⁻¹ respectively (Figure 4). Figure 4A shows that the enzyme is not stable at 0.1 mL min⁻¹ and a steady decrease in yield was observed over time during 4 hours on stream. The use of lower flow rate (0.01 mL min⁻¹) (Figure 4B) allowed the continuous synthesis of (*R*)-NPE over a period of 15 hours. The potentially enhanced stability at lower flow rate might be explained by the improved ability of Celite to keep the water entrapped whereas higher flow rate removes the water inside Celite-*GtHNL-3V* more rapidly. This suggest that higher yield might be possible at longer residence times. Indeed, when *GtHNL-3V* on Celite R-633 and substrates were allowed to react during 2 h or even 20 h in the flow reactor the yield increased to 47.5% and 80.3% respectively (Table 1). This pulsed flow approach can solve the problem of water removal.

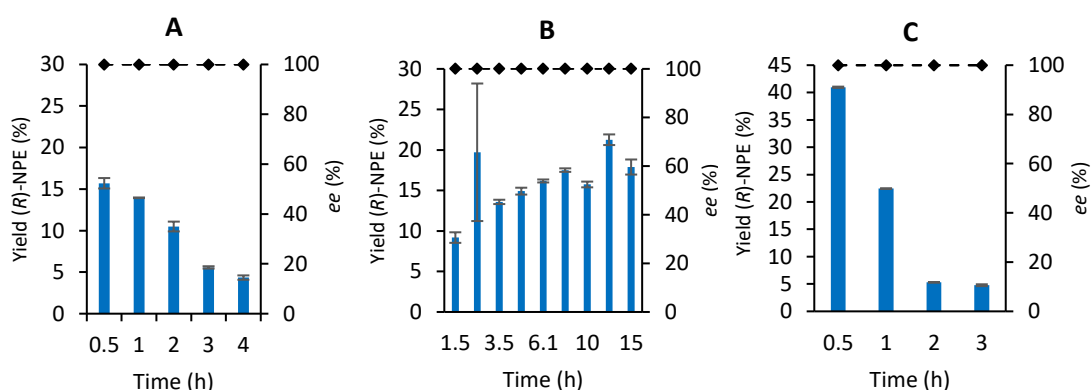


Figure 4. Stability of *GtHNL-3V* on Celite R-633 for the continuous synthesis of (*R*)-2-nitro-1-phenylethanol in a packed bed reactor. A: Conditions: Ratio benzaldehyde : nitromethane, 1:50, 20 mM benzaldehyde, 1 M nitromethane, 20 mM 1,3,5-tri-isopropylbenzene as internal standard (I.S) in MTBE saturated with 100 mM KPi buffer pH 7 with *GtHNL-3V* (400 U) immobilised on 300 mg Celite R-633. The flow rate was 0.1 mL min⁻¹. The enzyme was dried 24 h under vacuum in a desiccator over silica gel and re-hydrated with 1 mL 100 mM potassium phosphate buffer pH 7 prior to the reaction. B: Conditions: Ratio benzaldehyde : nitromethane, 1:50, 20 mM benzaldehyde, 1 M nitromethane, 20 mM 1,3,5-tri-isopropylbenzene as internal standard (I.S) in MTBE saturated with 100 mM KPi buffer pH 7 with *GtHNL-3V* (450 U) immobilised on 500 mg Celite R-633. The flow rate was 0.01 mL min⁻¹. The enzyme was not dried after its immobilisation. C: Conditions: Ratio benzaldehyde : nitromethane, 1:50, 40 mM benzaldehyde, 2 M nitromethane, 40 mM 1,3,5-tri-isopropylbenzene as internal standard (I.S) in MTBE saturated with 100 mM KPi buffer pH 7, 100 mM KPi buffer pH 7 with *GtHNL-3V* (450 U) immobilised on 500 mg Celite R-633. The reaction was performed in a biphasic 50/50% system. The flow rate was 0.1 mL min⁻¹. The enzyme was not dried after its immobilisation. Yield (bars) and enantiomeric excess (dashed lines). Error bars correspond to the standard deviation of duplicates (n=2).

The yield of (*R*)-NPE was calculated by the ratio of (*R*)-NPE concentration to the initial benzaldehyde concentration

Likewise, the development of a biphasic system is another approach to maintain Celite-GtHNL-3V constantly hydrated over time. Figure 4C shows a higher yield of (*R*)-NPE (44%) during the first 30 minutes of reaction time. Unfortunately, the biphasic system (50/50%) was not stable and a significant decrease in yield was observed after 1 hour. This can be explained by the leaching of the enzyme to the reaction medium due to the weak interactions between Celite-GtHNL-3V and the solubility of the enzyme in the reaction medium as observed earlier for a similar system [15]. The immobilization of GtHNL-3V by covalent attachment might be a viable alternative to overcome the leaching limitation observed in this biphasic system. Remarkably, the enantiomeric excess is excellent in all conditions evaluated.

Table 3: Influence of residence time on the continuous synthesis of (*R*)-NPE catalysed by GtHNL-3V on Celite R-633 in potassium phosphate buffer (100 mM, pH 7) saturated MTBE as reaction medium

Flow rate (mL min ⁻¹)	Residence time ^a (min)	Enzyme loading (U)	Yield (<i>R</i>)-NPE ^b (%)	ee (%)
0.1	7.3	400	15.7 ^c	>99
0.01	43.8	450	16.2 ^d	>99
0.01	120 ^e	450	47.5	>99
0.01	1200 ^e	450	80.3	>99

^a Calculated as the ratio of reaction volume to flow rate. The reaction volume was calculated based on the pore volume of Celite R-633 (1.46 mL g⁻¹ [38]) and the amount (g) of carrier used. ^b Calculated by the ratio of (*R*)-NPE concentration to the initial benzaldehyde concentration. ^c Calculated after 30 min reaction time. ^d Average of 15 hours of reaction time. ^e The pump was turned off to allowed the desired retention time.

5.2.3 Comparison between batch and continuous flow systems

A fair comparison between batch and continuous flow systems can be made based on their space-time-yields (STY). The product formation over time is not a linear function in batch and flow systems; thus, the comparison must be made at the same level of conversion [25]. Table 2 shows the STYs of the batch and continuous flow systems using MTBE saturated with 100 mM KPi buffer pH 7 as reaction medium.

Table 2: Comparison of batch and flow systems based on their productivity

	Batch	Flow
STY ^a (g L ⁻¹ h ⁻¹)	0.60	4.31 ^b 0.69 ^c
STY ^a (g L ⁻¹ h ⁻¹ mg _{enzyme} ⁻¹)	0.10	0.02 ^b 0.003 ^c

^a Calculated at similar yield levels (*circa* 16%) ^b Calculated at 0.1 mL min⁻¹. ^c Calculated at 0.01 mL min⁻¹.

The batch and flow systems displayed similar productivity at 0.01 mL min⁻¹. The use of a higher flow rate (0.1 mL min⁻¹) improved the STY (g L⁻¹ h⁻¹) 7 times. However, the enzyme is not stable at this flow rate (Figure 4A). When the amount of enzyme used for the reactions is taken into account, the productivity of the batch system is 5 and 37 times higher compared to both flow rates (0.1 mL min⁻¹ and 0.01 mL min⁻¹) respectively. The reaction conditions for the Celite-GtHNL-3V catalysed synthesis of (*R*)-NPE evaluated in this study are more stable and controlled in batch. This explains its higher productivity. This result is unexpected since flow systems commonly allowed process intensification [25-26, 37, 45-46]. However, the high concentration (1 M) and low polarity (log P = -0.24) of nitromethane might not allow to keep a constant *a_w* on Celite-GtHNL-3V. While significant fluctuations in enzyme activity and therefore yield were observed, remarkably the enantioselectivity of the reaction was unaffected and always excellent.

5.3 Experimental section

5.3.1 Chemicals

Except when reported otherwise all chemicals were bought from Sigma Aldrich (Schnelldorf, Germany). Isopropanol and heptane were of HPLC grade (≥99%) and used as HPLC solvents. 1,3,5-triisopropylbenzene (97%) was from Fluka Chemie (Buchs, Switzerland). (±)-Mandelonitrile from Across Organics (New Jersey, USA) was purified by flash chromatography (PE/MTBE 9:1/3:7). (±)-2-nitro-1-phenylethanol was prepared according to the literature [47].

5.3.2 Cloning and heterologous expression of *Granulicella tundricola* HNL (GtHNL)

The pUC57 shuttle vector containing the gene encoding G θ HNL-A40H/V42T/Q110H, codon optimised for *E. coli* was obtained from Bio Basic INC (Canada) and used to transform *E. coli* Top 10. The gene encoding G θ HNL-A40H/V42T/Q110H gene was cloned into pET28a expression vector using NcoI and HindIII restriction enzymes. The resulting pET28a-G θ HNL-A40H/V42T/Q110H expression vector was cloned into *E. coli* TOP 10 to obtain a stable host for plasmid DNA and sequenced to ensure the successful introduction of the H96A mutation (Table 3). Finally, pET28a-G θ HNL-A40H/V42T/Q110H was used to transform the expression host *E. coli* BL21(DE3). The enzyme cultivation was performed in accordance to the literature [37]. A preculture was prepared by inoculating one single colony of *E. coli* BL21(DE3)-pET28aG θ HNL in 10 mL of LB medium with kanamycin (40 μ g/mL) and incubated overnight (New Brunswick Scientific Incubator Shaker Excella E24 Series) at 37°C, 180 rpm. Then, this preculture was used for the inoculation of 1 L of LB medium containing kanamycin (40 μ g/mL) and incubated at 37°C, 120 rpm. When the OD600 reached 0.7 – 0.9 the gene expression was induced by adding 1 mL of 0.1 M isopropyl β -D-thiogalactoside (IPTG) per liter of culture (0.1 mM IPTG final concentration) and cultivation was continued overnight at 25°C, 120 rpm. Moreover, 100 μ L of 1 M MnCl₂ was added per liter of culture at the induction time (0.1 mM Mn²⁺ final concentration). Cells were harvested at 4°C, 5000 rpm during 20 minutes (Sorvall RC6, Thermo Scientific). The supernatant was discarded and the pellet was washed with 20 mL of 10 mM sodium phosphate buffer, pH 7, and stored at -80 °C.

Table 3: G θ HNL- A40H/V42T/Q110H gene sequence

G θ HNL-A40H/V42T/Q110H	G θ HNL-A40H/V42T/Q110H – Aminoacid sequence
5'CCATGGAGATTAACGTGTTGGTTCTCAGGCTT CTGGTAAAGGTCCGGCTGATTGGTTCAGTGGTAC TGTTTCGATCGATCCGCTGTTTCAGGCTCCGGAT CCGGCATTAGTAGCTGGTCACTCTACTACCTTTG AACCGGGTCTCGTACTGCTTGGCATACTCATCC GTTAGGTCAGACTCTGATTGTAAGTCTGGTTGT GGTTGGGCTCAGCGTGAAGGTGGTCTGTTGAA GAAATTCATCCGGGTGATGTTGTATGGTTCTCTC CAGGTGAAAAACACTGGCATGGTCTGCACCAAC TACCGCTATGACCCACCTGGCTATCCACGAACGT CTGGATGGTAAAGCTGTTGATTGGATGGAACACG TACTGATGAACAGTACCGTCGTTAAGCTT -3'	MEIKRVGSQASGKGPADWFTG TVRIDPLFQAPDPALVAGHSTT FEPGAR ^T AWHTHPLGQTLIVTA GCGWAQREGGAVEEIHPGDVV WFSPGEEKHWHGAAPTTAMTHL AI ^H ERLDGKAVDWMEHVTDEQ YRRA

Aminoacids in red show the mutations at positions 40, 42 and 110.

5.3.3 Enzyme purification

The pellets of GtHNL-3V were resuspended in lysis buffer (50 mM potassium phosphate buffer + DNase) pH 7 and lysed in a cell disruptor (Constant Systems Ltd., United Kingdom) at 20 kPSI and 4°C to avoid protein denaturation. The cell free extract (CFE) was collected as the supernatant after centrifugation at 4500 g, 1 h, 4°C, heated during 30 min at 65°C, and centrifuged during 15 min at 4500 g. The purified enzyme is found as the supernatant.

5.3.4 Enzymatic activity assay

GtHNL-3V activity was measured spectrophotometrically (Agilent Technologies Cary 60 UV-VIS) using a method previously reported [48]. The cleavage of *rac*-mandelonitrile into benzaldehyde and hydrogen cyanide was followed at 280 nm and 25°C in quartz glass cuvettes. To 1300 µL of reaction buffer (100 mM sodium oxalate buffer, pH 5), 200 µL of enzyme solution (diluted in reaction buffer) and 500 µL of 60 mM *rac*-mandelonitrile solution (dissolved in 3 mM oxalic acid, pH 3) were added. The background reaction was evaluated without enzyme and its slope was subtracted in the final calculation. The activity was calculated based on the following equation:

$$\text{Activity} = (2.0 \times \Delta A/\text{min}) / (\epsilon_{280} \times 1 \times 0.2) \text{ [U/ml diluted sample]}$$

Where

$$\Delta A/\text{min} = \Delta A/\text{min}_{\text{sample}} - \Delta A/\text{min}_{\text{blank}}$$

$$\epsilon_{280} = 1.376 \text{ [mM}^{-1} \times \text{cm}^{-1}\text{]}$$

One unit of HNL activity is defined as one micromole of *rac*-mandelonitrile converted per minute in 100 mM sodium oxalate buffer pH 5 at 25°C.

5.3.5 Immobilisation of GtHNL-3V on Celite R-633 by adsorption

Enzyme immobilisation on Celite R-633 was performed according to literature [34, 37] with slight modifications. Celite R-633 has a pore diameter of 6.5 µm, a pore volume of 1.47 mL g⁻¹ and a water absorption capability of 240%. It was washed with 100 mM potassium phosphate buffer pH 7 using a Büchner funnel and dried 24 h under vacuum in a desiccator over silica gel or used directly. Given volumes of GtHNL-3V were concentrated with Amicon ultrafiltration filters with a 10 kDa MW cut-off, and

subsequently added dropwise to Celite R-633 and dried 24 h under vacuum in a desiccator over silica gel. The ratio of enzyme solution to carrier ($\mu\text{L}:\text{mg}$) was 2:1. The enzyme concentration in solutions was adjusted to the required amount of enzyme for the immobilisation. By using this ratio of enzyme solution to Celite, the enzyme solution was completely absorbed by the carrier, ensuring that all the enzyme was immobilised into the porous material. The immobilised enzyme was stored in the fridge at 4°C when needed.

5.3.6 Synthesis of (*R*)-2-nitro-1-phenylethanol in batch

Several (*R*)-2-nitro-1-phenylethanol synthesis were performed with 50 mg of immobilised GtHNL-3V on Celite R-633. The reaction conditions were as follow: 20 mM benzaldehyde, 20 mM 1,3,5-tri-isopropylbenzene (internal standard), 1 M nitromethane and MTBE saturated with 100 mM KPi buffer pH 7, 50 mg immobilised enzyme, 1200 rpm and 30°C . Shaking and temperature were controlled by using an Eppendorf thermomixer (Germany). Saturated MTBE was prepared by adding 5 mL of 100 mM KPi buffer pH 7 to 25 mL of dry MTBE. Reaction volume: 1 mL. The ratio benzaldehyde to nitromethane was 1:50. The immobilised GtHNL-3V was freely placed into the glass reaction vial.

5.3.7 Enzyme recyclability in batch

The enzyme recyclability was determined by several cycles of (*R*)-2-nitro-1-phenylethanol synthesis according to the literature [34, 37]. Between each cycle the immobilised enzyme was washed twice for 1 minute with MTBE saturated with 100 mM KPi buffer pH 7. When required, 50 μL of 100 mM KPi buffer were added to the immobilised enzyme. At the end of the working day the immobilised enzyme was stored at 4°C in fresh MTBE saturated with 100 mM KPi buffer pH 7. The immobilised GtHNL-3V was freely placed into the glass reaction vial. Saturated MTBE was prepared by adding 5 mL of 100 mM KPi buffer pH 7 to 25 mL of dry MTBE.

5.3.8 Enzyme stability in continuous flow in a monophasic KPi saturated MTBE system

1 mL stainless steel flow reactor was used for the continuous synthesis of (*R*)-2-nitro-1-phenylethanol. 10 cm of polytetrafluoroethylene (PTFE) tubing with 1.5 mm inner

diameter connect a syringe pump (Knauer, Germany) with the reactor. The stability of 400 U of immobilised GtHNL-3V on 300 mg Celite R-633 was evaluated by performing a synthesis reaction during 4 hours at 0.1 mL min⁻¹ (reaction volume = 0.73 mL). Likewise, the stability of 450 U of immobilised GtHNL-3V on 500 mg Celite R-633 was evaluated during 15 hours at 0.01 mL min⁻¹ (reaction volume = 0.44 mL). Ratio benzaldehyde : nitromethane, 1:50, 20 mM benzaldehyde, 1 M nitromethane, 20 mM 1,3,5-tri-isopropylbenzene as internal standard (I.S) in MTBE saturated with 100 mM KPi buffer pH 7. Reactions were performed at room temperature. Saturated MTBE was prepared by adding 5 mL of 100 mM KPi buffer pH 7 to 25 mL of dry MTBE. Samples were drawn at regular intervals and analysed by chiral HPLC. The flow rate was checked at each sampling time by the difference of weight.

5.3.9 Enzyme stability in continuous flow in a biphasic system

A similar set up as described in 3.8 was used. In this case, two syringes were connected to a mixing unit (T-piece assembly) to ensure a mixture of substrates and buffer. Syringe 1 was used for 40 mM benzaldehyde, 2 M nitromethane and 40 mM in 1,3,5-tri-isopropylbenzene in MTBE saturated with 100 mM KPi pH 7. Syringe 2 was used for 100 mM KPi pH 7. The stability of 450 U of immobilised GtHNL-3V on 500 mg Celite R-633 was evaluated by performing a synthesis reaction during 3 hours at 0.1 mL min⁻¹ (reaction volume = 0.73 mL). The reaction was performed in a biphasic 50/50% system. The enzyme was not dried after its immobilisation. Reactions were performed at room temperature. Saturated MTBE was prepared by adding 5 mL of 100 mM KPi buffer pH 7 to 25 mL of dry MTBE. Samples were drawn at regular intervals and analysed by chiral HPLC. The flow rate was checked at each sampling time by the difference of weight.

5.3.10 Analysis

Samples (50 µL) were taken at different times during the reaction run and added to 450 µL of heptane:2-propanol 90:10 in 1.5 mL Eppendorf tubes. A small amount of anhydrous magnesium sulphate (MgSO₄) was used to remove the water from the solution and the Eppendorf tubes were centrifuged at 13000 rpm for 1 min. The supernatant was transferred to a 1.5 mL HPLC vial and 10 µL was injected into the HPLC (Chiralcel OD column, column size: 0.46 cm I.D x 25 cm). Heptane and 2-

propanol were used as mobile phase with a flow rate of 1 mL/min and the UV detector was set at 210 nm. The column temperature was set at 40°C. The samples in the autosampler were maintained at 4°C.

References

1. Rao, D.H.S.; Chatterjee, A.; Padhi, S.K. Biocatalytic approaches for enantio and diastereoselective synthesis of chiral β -nitroalcohols. *Org. Biomol. Chem.*, **2021**, 19, 322–337. DOI: 10.1039/d0ob02019b.
2. Ono, N. *The Nitro Group in Organic Synthesis*, Wiley, New York, 2001.
3. Milner, S. E.; Moody, T. S.; and Maguire, A. R. Biocatalytic approaches to the Henry (Nitroaldol) reaction. *Eur. J. Org. Chem.*, **2012**, 3059–3067. DOI: 10.1002/ejoc.201101840
4. Lahssen, E. B.; Ahbala, M.; Bolte J.; and Lemaire, M. Straightforward chemo-enzymatic synthesis of new aminocyclitols, analogues of valiolamine and their evaluation as glycosidase inhibitors. *Tetrahedron Asymmetry*, **2006**, 17, 2684–2688.
5. Kühbeck, D.; Mayr, J.; Häring, M.; Hofmann, M.; Quignard F.; and Díaz Díaz D. Evaluation of the nitroaldol reaction in the presence of metal ion-crosslinked alginates. *New J. Chem.*, **2015**, 39, 2306–2315. DOI: 10.1039/c4nj02178a
6. Vongvilai, P.; Angelin, M.; Larsson R.; and Ramström, O. Dynamic combinatorial resolution: Direct asymmetric lipase mediated screening of a dynamic nitroaldol library. *Angew. Chem., Int. Ed.*, **2007**, 46, 948–950.
7. Vongvilai, P.; Larsson, R.; and Ramström, O. Direct asymmetric dynamic kinetic resolution by combined lipase catalysis and nitroaldol (Henry) reaction. *Adv. Synth. Catal.*, **2008**, 350, 448–452. DOI: 10.1002/adsc.200700432
8. Zhang, Y.; Hu, L.; and Ramström, O. Double parallel dynamic resolution through lipase-catalyzed asymmetric transformation. *Chem. Commun.*, **2013**, 49, 1805–1807. DOI: 10.1039/c3cc38203f
9. Purkarthofer, T.; Gruber, K.; Gruber-Khadjawi, M.; Waich, K.; Skranc, W.; Mink, D.; and Griengl, H. A Biocatalytic Henry Reaction—The hydroxynitrile lyase from *Hevea brasiliensis* also catalyzes nitroaldol reactions. *Angew. Chem. Int. Ed.*, **2006**, 45, 3454–3456. DOI: 10.1002/anie.200504230

10. Gruber-Khadjawi, M.; Purkarthofer, T.; Skranc, W.; and Griengl, H. Hydroxynitrile lyase-catalyzed enzymatic nitroaldol (Henry) reaction. *Adv. Synth. Catal.*, **2007**, 349, 1445 – 1450. DOI: 10.1002/adsc.200700064.
11. Fuhshuku, K.; Asano, Y. Synthesis of (*R*)- β -nitro alcohols catalyzed by *R*-selective hydroxynitrile lyase from *Arabidopsis thaliana* in the aqueous–organic biphasic system. *J. Biotechnol.*, **2011**, 153, 153–159. DOI: 10.1016/j.jbiotec.2011.03.011
12. Bekerle-Bogner, M.; Gruber-Khadjawi, M.; Wiltsche, H.; Wiedner, R.; Schwab, H.; Steiner, K. (*R*)-selective nitroaldol reaction catalyzed by metal-dependent bacterial hydroxynitrile lyases. *ChemCatChem.*, **2016**, 8, 2214–2216, doi:10.1002/cctc.201600150.
13. Yuryev, R.; Briechle, S.; Gruber-Khadjawi, M.; Griengl, H.; and Liese, A. Asymmetric retro-Henry reaction catalyzed by hydroxynitrile lyase from *Hevea brasiliensis*. *ChemCatChem.*, **2010**, 2, 981 – 986. DOI: 10.1002/cctc.201000147
14. Rao, D. H. S.; and Padhi, S. K. Production of (*S*)- β -Nitro alcohols by enantioselective C-C bond cleavage with an *R*-selective hydroxynitrile lyase. *ChemBioChem.*, **2019**, 20, 371 – 378. DOI: 10.1002/cbic.201800416
15. Rao, D.H.S.; Shivani, K.; Padhi, S.K. Immobilized *Arabidopsis thaliana* hydroxynitrile lyase-catalyzed retro-henry reaction in the synthesis of (*S*)- β -Nitroalcohols. *Appl. Biochem. Biotechnol.*, **2021**, 193, 560-576. DOI: 10.1007/s12010-020-03442-3.
16. Von Langermann, J.; Nedrud D. M.; and Kazlauskas, R. J. Increasing the reaction rate of hydroxynitrile lyase from *Hevea brasiliensis* towards mandelonitrile by copying active site residues from an esterase that accepts aromatic esters. *ChemBioChem.*, **2014**, 15, 1931–1938. DOI: 10.1002/cbic.201402081.
17. Devamani, T.; Rauwerdink, A. M.; Lunzer, M.; Jones, B.J.; Mooney, J. L.; Tan, M. A.O.; Zhang, Z. J.; Xu, J. H.; Dean, A. M.; and Kazlauskas, R. J. Catalytic promiscuity of ancestral esterases and hydroxynitrile lyases. *J. Am. Chem. Soc.*, **2016**, 138, 1046–1056. DOI: 10.1021/jacs.5b12209
18. Tentori, F.; Brenna, E.; Colombo, D.; Crotti, M.; Gatti, F.G.; Ghezzi, M.C.; Pedrocchi-Fantoni, G. Biocatalytic approach to chiral β -nitroalcohols by

- enantioselective alcohol dehydrogenase-mediated reduction of α -nitroketones. *Catalysts*, **2018**, 8, 308. DOI: 10.3390/catal8080308
19. Wang, Z.; Wu, X.; Li, Z.; Huang, Z.; and Chen, F. Ketoreductase catalyzed stereoselective bioreduction of α -nitro ketones. *Org. Biomol. Chem.*, **2019**, 17, 3575–3580. DOI: 10.1039/C9OB00051H
 20. Venkataraman, S.; and Chadha, A. Enantio- δ chemo-selective preparation of enantiomerically enriched aliphatic nitro alcohols using *Candida parapsilosis* ATCC 7330. *RSC Adv.*, **2015**, 5, 73807–73813. DOI: 10.1039/c5ra13593a
 21. Chadha, A.; Venkataraman, S.; Preetha, R.; and Padhi, S. K. *Candida parapsilosis*: A versatile biocatalyst for organic oxidation-reduction reactions. *Bioorg. Chem.*, **2016**, 68, 187–213. DOI: 10.1016/j.bioorg.2016.08.007 0045-2068
 22. Wallner, S. R.; Lavandera, I.; Mayer, S. F.; Öhrlein, R.; Hafner, A.; Edegger, K.; Faber, K.; and Kroutil, W. Stereoselective anti-Prelog reduction of ketones by whole cells of *Comamonas testosteroni* in a ‘substrate-coupled’ approach. *J. Mol. Catal. B: Enzym.*, **2008**, 55, 126–129. DOI: 10.1016/j.molcatb.2008.02.009
 23. Hasnaoui, G.; Lutje Spelberg J. H.; De Vries, E.; Tang, L.; Hauer, B.; and Janssen, D. B. Nitrite-mediated hydrolysis of epoxides catalyzed by halohydrin dehalogenase from *Agrobacterium radiobacter* AD1: a new tool for the kinetic resolution of epoxides. *Tetrahedron: Asymmetry*, **2005**, 16, 1685–1692. DOI: 10.1016/j.tetasy.2005.03.021
 24. Hasnaoui-Dijoux, G.; Elenkov, M. M.; Lutje Spelberg, J. H.; Hauer, B.; and Janssen, D. B. Catalytic promiscuity of halohydrin dehalogenase and its application in enantioselective epoxide ring opening. *ChemBioChem.*, **2008**, 9, 1048–1051. DOI: 10.1002/cbic.200700734
 25. Coloma, J.; Guiavarc’h, Y.; Hagedoorn, P. L.; and Hanefeld, U. Immobilisation and flow chemistry: tools for implementing biocatalysis. *Chem. Commun.*, **2021**, 57, 11416. DOI: 10.1039/d1cc04315c
 26. Brahma, A.; Musio, B.; Ismayilova, U.; Nikbin, N.; Kamptmann, S.; Siegert, P.; Jeromin, G.E.; Ley S.V. and Pohl, M. An orthogonal biocatalytic approach for the safe generation and use of HCN in a multistep continuous preparation of chiral *O*-Acetylcyanohydrins. *Synlett*, **2016**, 27, 262–266. DOI: 10.1055/s-0035-1560644.

27. Bouchaut, B.; Asveld, L.; Hanefeld, U.; Vlierboom, A. Value Conflicts in Designing for Safety: Distinguishing Applications of Safe-by-Design and the Inherent Safety Principles. *Int. J. Environ. Res. Public Health*, **2021**, *18*, 1963. DOI: 10.3390/ijerph18041963
28. Naramittanakul, S.; Buttranon, A.; Petchsuk, P.; Chaiyen, N.; Weeranoppanant, N. Development of a continuous-flow system with immobilised biocatalysts towards sustainable bioprocessing. *React. Chem. Eng.* **2021**, *6*, 1771-1790. DOI: 10.1039/D1RE00189B.
29. Benitez-Mateos, I.; Contente, M.L.; Roura Padrosa, D.; Paradisi, F. Flow biocatalysis 101: design, development and applications. *React. Chem. Eng.* **2021**, *6*, 599. DOI: 10.1039/D0RE00483A
30. Boodhoo, K. V. K.; Flickinger, M. C.; Woodley, J. M.; Emanuelsson, E. A. C. Bioprocess intensification: A route to efficient and sustainable biocatalytic transformations for the future. *Chem. Eng. Process. -Process Intensif.* **2022**, 108793. DOI:10.1016/j.cep.2022.108793.
31. De Santis, P.; Meyer, L. -E.; Kara, S. The rise of continuous flow biocatalysis - fundamentals, very recent developments and future perspectives. *React. Chem. Eng.* **2020**, *5*, 2155-2184. DOI: 10.1039/ D0RE00335B
32. Cosgrove, C.; Matthey, A.P. Reaching new biocatalytic reactivity using continuous flow reactors. *Chem. Eur. J.* **2021**, e202103607. DOI: 10.1012/chem.202103607
33. Okrob, D.; Paravidino, M.; Orru, R.V.A.; Wiechert, W.; Hanefeld, U. and Pohl, M. Hydroxynitrile lyase from *Arabidopsis thaliana*: Identification of reaction parameters for enantiopure cyanohydrin synthesis by pure and immobilized catalyst. *Adv. Synth. Catal.*, **2011**, *353*, 2399–2408. DOI: 10.1002/adsc.201100199.
34. Torrelo, G.; van Midden, N.; Stloukal, R.; Hanefeld, U. Immobilized hydroxynitrile lyase: A comparative study of recyclability. *ChemCatChem.*, **2014**, *6*, 1096–1102. DOI: 10.1002/cctc.201300892.
35. Bracco, P.; Torrelo, G.; Noordam, S.; de Jong, G. and Hanefeld, U. Immobilization of *Prunus amygdalus* hydroxynitrile lyase on Celite. *Catalysts*, **2018**, *8*, 287. DOI: 10.3390/catal8070287.
36. Hanefeld, U.; Gardossi, L. and Magner, E. Understanding enzyme immobilisation. *Chem. Soc. Rev.*, **2009**, *38*, 453–468. DOI: 10.1039/b711564b.

37. Coloma, J.; Guiavarc'h, Y.; Hagedoorn, P.L.; Hanefeld, U. Probing batch and continuous flow reactions in organic solvents: *Granulicella tundricola* hydroxynitrile lyase (GtHNL). *Catal. Sci. Technol.*, **2020**, *10*, 3613–3621, doi:10.1039/d0cy00604a.
38. Bracco, P.; van Midden, N.; Arango, E.; Torrelo, G.; Ferrario, V.; Gardossi L.; and Hanefeld, U. *Bacillus subtilis* Lipase A-Lipase or esterase? *Catalysts*, **2020**, *10*, 308. DOI: 10.3390/catal10030308
39. Valivety, R. H.; Johnston, G. A.; Suckling, C. J.; and Halling, P. J. Solvent effects on biocatalysis in organic systems: equilibrium position and rates of lipase catalyzed esterification. *Biotechnol. Bioeng.*, **1991**, *38*, 1137-1143.
40. Paravidino, M.; Sorgedrager, M.J.; Orru, R.V. and Hanefeld, U. Activity and enantioselectivity of the hydroxynitrile lyase MeHNL in dry organic solvents. *Chemistry*, **2010**, *16*, 7596 – 7604.
41. Klibanov, A. M. Why are enzymes less active in organic solvents than in water? *Trends Biotechnol.*, **1997**, *15*, 97 –101.
42. Griebenow, K.; Klibanov, A. M. Lyophilization-induced reversible changes in the secondary structure of proteins *Proc. Natl. Acad. Sci. USA*, **1995**, *92*, 10969 – 10976.
43. Griebenow, K.; Klibanov, A. M. Can Conformational Changes Be Responsible for Solvent and Excipient Effects on the Catalytic Behavior of *Subtilisin Carlsberg* in Organic Solvents? *Biotechnol. Bioeng.*, **1997**, *53*, 351 –362.
44. El-Sayed, A. H. M. M.; Mahmoud, W. M.; and Coughlin, R. W. Comparative study of production of dextransucrase and dextran by cells of *Leuconostoc mesenteroides* immobilized on Celite and in calcium alginate beads *Biotechnol. Bioeng.*, **1990**, *36*, 83-91.
45. Coloma, J.; Lugtenburg, T.; Afendi, M.; Lazzarotto, M.; Bracco, P.; Hagedoorn, P.L.; Gardossi, L.; and Hanefeld, U. Immobilization of *Arabidopsis thaliana* hydroxynitrile lyase (AtHNL) on EziG Opal. *Catalysts*, **2020**, *10*, 899. DOI: 10.3390/catal10080899.
46. van der Helm, M.P.; Bracco, P.; Busch, H.; Szymańska, K.; Jarzębski, A. and Hanefeld, U. Hydroxynitrile lyases covalently immobilized in continuous flow microreactors. *Catal. Sci. Technol.*, **2019**, *9*, 1189–1200. DOI: 10.1039/c8cy02192.

47. Lu, G.; Zheng, F.; Wang, L.; Guo, Y.; Li, X.; Cao, X.; Wang, C.; Chi, H.; Dong, Y.; Zhang, Z. Asymmetric Henry reaction catalyzed by Cu(II)-based chiral amino alcohol complexes with C₂-symmetry. *Tetrahedron Asymmetry*, **2016**, 27, 732–739. DOI: 10.1016/j.tetasy.2016.06.018.
48. Wiedner, R.; Kothbauer, B.; Pavkov-Keller, T.; Gruber-Khadjawi, M.; Gruber, K.; Schwab, H.; and Steiner, K. Improving the properties of bacterial *R*-selective hydroxynitrile lyases for industrial applications. *ChemCatChem.*, **2015**, 7, 325 – 332. DOI: 10.1002/cctc.201402742.

Supplementary information

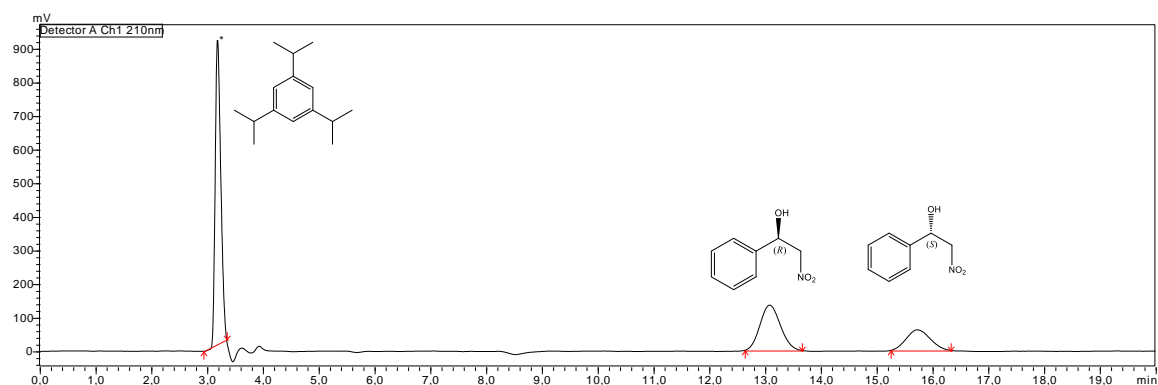


Figure S1. HPLC detection of 1,3,5 tri-isopropylbenzene (internal standard), (*R*)-NPE and (*S*)-NPE

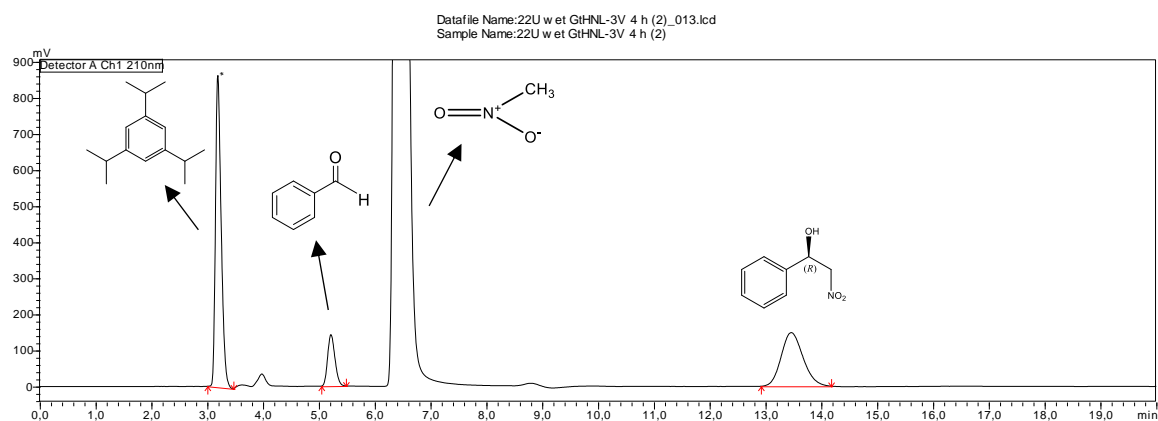


Figure S2. HPLC detection of benzaldehyde, 1,3,5 tri-isopropylbenzene, nitromethane and (*R*)-NPE
Conditions: Ratio benzaldehyde : nitromethane, 1:50, 20 mM benzaldehyde, 1 M nitromethane, 20 mM 1,3,5-tri-isopropylbenzene as internal standard (I.S) in MTBE saturated with 100 mM KPi buffer pH 7 with GtHNL-3V (22 U) immobilised on 500 mg Celite R-633. Reaction volume: 1 mL.

6

Oxidative cleavage of styrenes: Expanding the potential of *Granulicella tundricola* hydroxynitrile lyase (GtHNL)

Granulicella tundricola hydroxynitrile lyase (GtHNL) is a manganese dependent cupin that catalyses the enantioselective synthesis of cyanohydrins. The analysis of its active site showed high similarity with the active site of cupin *Thermotoga maritima* 1459, an enzyme that catalyses the oxidative cleavage of styrene derivatives. Based on the molecular analysis of the active site the variants GtHNL-H96A, GtHNL-H96F and GtHNL-A40H/V42T/H96A/Q110H were evaluated. This mutation provides an additional manganese coordination site and a larger active site. Remarkably, all variants were able to catalyse the oxidative cleavage of α -methyl styrene. However, the best results were observed using GtHNL-H96A as catalyst. GtHNL-H96A displayed higher yield of acetophenone (42%) as compared to GtHNL-A40H/V42T/H96A/Q110H (12%) and GtHNL-H96F (11%) after 20 hours of reaction time. Control reactions using 0.1 and 0.5 mM of MnCl₂ were performed. The precise reaction mechanism remains unknown. Electron paramagnetic resonance (EPR) studies did not confirm the oxidation of Mn(II) to Mn(III), while evidence for a radical mechanism is presented.

Manuscript in preparation

José Coloma, Peter-Leon Hagedoorn and Ulf Hanefeld

6.1 Introduction

Oxidative alkene cleavage is an important reaction in organic chemistry for the synthesis of aldehydes and ketones, important volatile compounds that are extensively employed in fragrances as flavours for the food and cosmetic industry. The reactivity of the carbonyl functionality allows its transformation to valuable precursors for the pharmaceutical and chemical industry [1-3]. Ozonolysis and metal-based oxidant catalysis are methods commonly used to obtain aldehydes and ketones. However, the explosive characteristic of ozonides, over-oxidation of aldehydes and poor regioselectivity are disadvantages commonly reported for both approaches [4-6]. Biocatalysis offers an alternative method to synthesize aldehydes or ketones. Peroxidases such as the one from *Caldariomyces fumago* (CPO) [7] or mammalian myeloperoxidase (MPO) [8] catalyse the oxidation of alkenes. Unfortunately, the oxidative cleavage reaction is commonly a secondary activity of these enzymes characterized by a low catalytic efficiency [1]. For this reason, the development of new biocatalytic approaches is highly desirable. Recently, the ability of *Granulicella tundricola* hydroxynitrile lyase (GtHNL) for the synthesis of enantiopure (*R*)-cyanohydrins was reported [9-11]. GtHNL is a Mn(II) dependent cupin superfamily enzyme [12] with an excellent activity towards (*R*)-cyanohydrin synthesis (Figure 1A). Likewise, the discovery [13] and improvement [14] of a Mn(II) dependent cupin superfamily enzyme from *Thermotoga maritima* (TM1459) with oxidative cleavage activity towards styrene derivatives has been reported. It was speculated that a Mn(III) active site species is responsible for this catalytic activity by a yet unknown reaction mechanism. Interestingly, GtHNL and TM1459 have similar active sites. The metal in GtHNL is penta-coordinated by four histidine nitrogens and one glutamine oxygen whereas in TM1459 the metal is tetra-coordinated by four histidine nitrogens in equivalent positions to the three histidines and the glutamine in GtHNL (Figure 1B). Based on the fact that enzymes often have promiscuous capabilities by nature and that one single amino acid substitution may be enough (and more likely) to introduce a new functionality to a former enzyme [15], we hypothesised that providing an additional coordination site to the Mn(II) in GtHNL for substrate binding might enable it to catalyse the oxidative cleavage of styrene derivatives (Scheme 1). Herein, we examined a new, non-natural reaction catalysed by GtHNL. Electron paramagnetic resonance (EPR) studies were performed to explore the mechanism of this reaction.

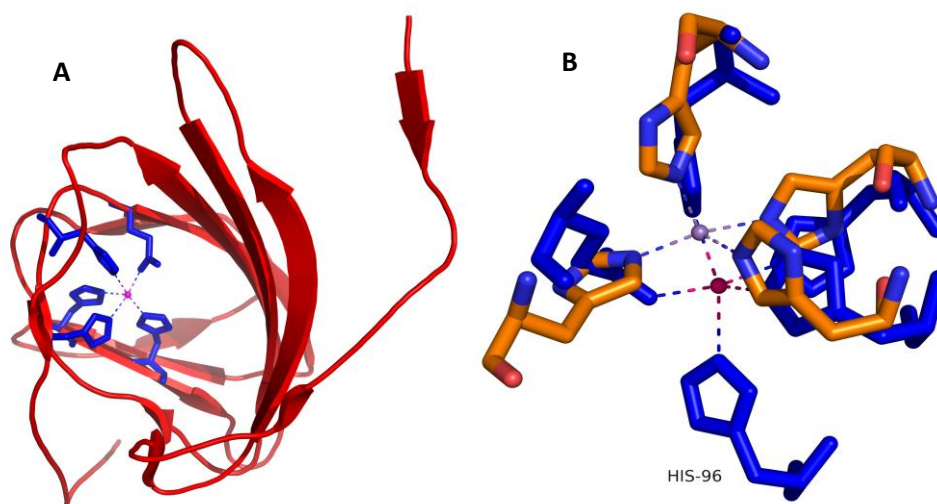
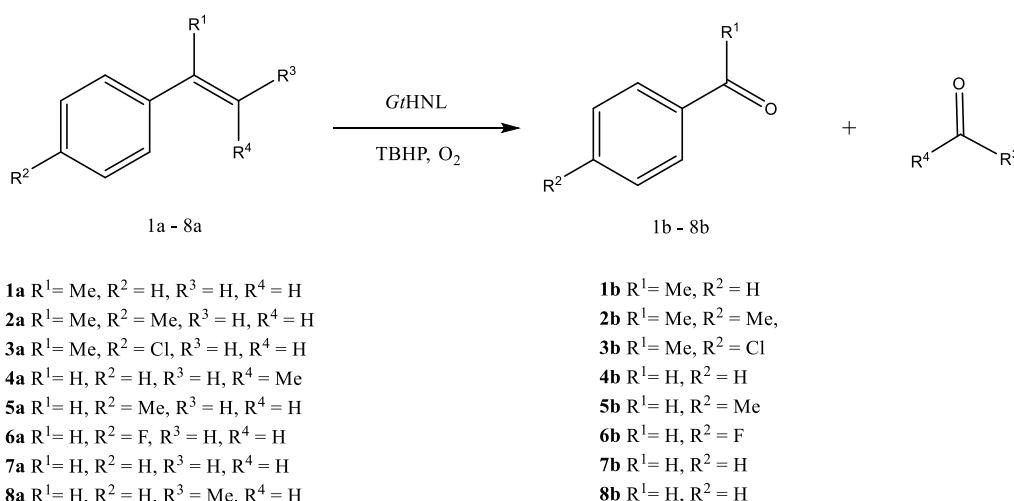


Figure 1: A: *GtHNL* active site (PDB code: 4UXA). The manganese ion (pink sphere) is coordinated by four histidines and one glutamine. B: Superimposition of *GtHNL* (PDB code: 4UXA) and *Thermotoga maritima* 1459 (PDB code: 1VJ2) active sites. The manganese ion (pink sphere) is pentacoordinated by four histidines and one glutamine in *GtHNL* whereas the manganese ion (purple sphere) is tetracoordinated in *TM1459*. The images were created using PyMOL molecular graphic system.



Scheme 1: *GtHNL*-catalysed oxidative cleavage of styrene derivatives 1a – 9a

6.2 Results and Discussion

6.2.1 Time course reactions

The incorporation of rational design in biocatalysis is a powerful strategy to improve enzyme stability, substrate scope, stereospecificity and to introduce novel functionalities in enzymes [16]. The rational design performed in this study was based on the analysis of the molecular structures of *GtHNL* and *TM1459*. The mutation H96A was introduced to *GtHNL* wild type (*GtHNL*-WT) and *GtHNL*-A40H/V42T/Q110H

(GtHNL-3V), a more active and stable variant for the synthesis of (*R*)-cyanohydrins compared to the wild type enzyme [10-11]. GtHNL has a pentacoordinated Mn(II) ion within its active site. Thus, this mutation (H96A) enables a wider active site and provides an additional coordination site for substrate binding, without affecting the incorporation of manganese during the enzyme overexpression [9]. Also, the mutation H96F was introduced into GtHNL-WT since a phenylalanine is located in close proximity to Mn(II) in TM1459 enzyme active site. α -methyl styrene was used as model substrate. To our delight, initial experiments showed that GtHNL-H96A and GtHNL-A40H/V42T/H96A/Q110H (GtHNL-4V) were able to catalyse the oxidative cleavage of α -methyl styrene with yields of 18.8% and 9.3% respectively after 20 hours of reaction time. A small amount of sodium bisulfite (*circa* 50 – 70 mg) was used to stop the reactions. Conversely, higher yields were observed when the reactions were not quenched with sodium bisulfite and instead were analysed rapidly without chemical quenching. GtHNL-H96A reached 31% yield of acetophenone after 20 hours of reaction time, similar to the 30% conversion that has been reported for TM1459 under similar reaction conditions [14]. The lower conversion of the reactions that were chemically quenched might be explained by the potential formation of bisulfate adducts. GtHNL-4V and GtHNL-H96F reached only 12% and 11% yield of acetophenone respectively; therefore the variant GtHNL-H96A was chosen for further analysis. The improved catalytic activity of GtHNL-H96A compared to GtHNL-H96F might be explained by its more open active site. The bulky phenylalanine potentially blocks the active site entrance. Larger active sites have been reported as one of the mechanisms of catalytic promiscuity because the substrates can adopt different orientations within the active site [17]. Control reactions using either 0.1 mM MnCl₂ or without MnCl₂ displayed 4.1 ± 0.65 % and 1.43 ± 0.01 % yield of acetophenone respectively after 20 hours reaction time.

The enzymatic reactions are clearly distinguishable compared to the control reaction (Figure 2). ICP-OES analysis revealed a Mn(II) loading of 9.3% and 25% for GtHNL-H96A and GtHNL-4V overexpressed with 0.1 mM MnCl₂ respectively.

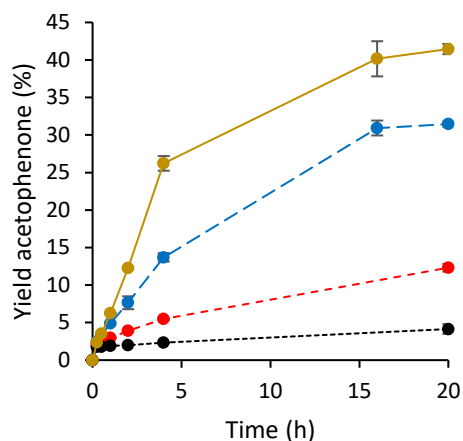


Figure 2: Oxidative cleavage of α -methyl styrene catalysed by *GtHNL*. Continuous yellow line (*GtHNL*-H96A overexpressed in the presence of 0.5 mM MnCl_2), dashed blue line (*GtHNL*-H96A overexpressed in the presence of 0.1 mM MnCl_2), dashed red line (*GtHNL*-A40H/V42T/H96A/Q110H) overexpressed in the presence of 0.1 mM MnCl_2) and dotted line (control reaction – 0.1 mM MnCl_2). Reaction conditions: 50 mM α -methyl styrene, 150 mM *tert*-butyl hydroperoxide (TBHP), 2 mg *GtHNL*-H96A or *GtHNL*-A40H/V42T/H96A/Q110H, 50 mM sodium phosphate buffer pH 7, 30°C, 1000 rpm. Reaction volume: 1 mL

Since manganese is essential for the catalytic activity of *GtHNL* for the synthesis of cyanohydrins [9], different MnCl_2 loadings were investigated during *GtHNL*-H96A overexpression (from 0.1 to 1 mM) to potentially improve the catalytic activity of *GtHNL*-H96A. Higher yields of acetophenone were achieved when *GtHNL*-H96A was obtained from cells in which the enzyme was overexpressed in the presence of 0.5 mM MnCl_2 (Figure 2 and Figure 3). In addition, the in-vitro incubation of *GtHNL*-H96A (obtained from cells in which the enzyme was overexpressed in the presence of 0.1 mM MnCl_2) with 10 molar equivalents of MnCl_2 during five hours allowed higher manganese loadings (ICP-OES 30%) and the product yield increased from 31.5% to 35% (Figure 3, yellow bar). Similarly, *GtHNL*-4V was incubated with 10 molar equivalents of MnCl_2 without significant improvement on the acetophenone yield (15%) after 20 hours of reaction time. In this case, the final Mn(II) concentration in the enzyme was not determined. Overall, *GtHNL*-H96A proved to be a better variant for the oxidative cleavage of α -methyl styrene although the manganese loading was lower than the observed in *GtHNL*-4V. Remarkably, this is the first time any HNL catalysed the oxidative cleavage of styrene derivatives, a completely different and, to the best of our knowledge, not previously reported activity for HNLs.

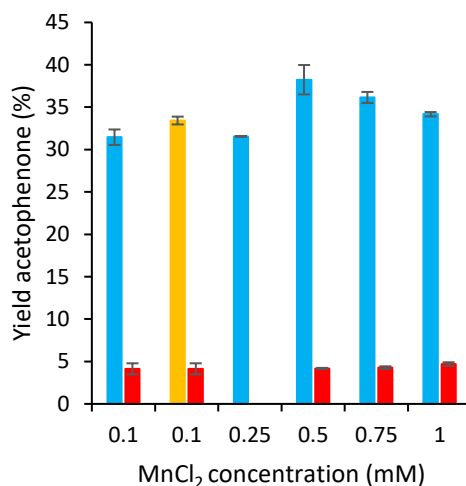


Figure 3: Influence of different MnCl₂ concentrations on the GtHNL-H96A catalysed oxidative cleavage of α -methyl styrene. Solid light blue bars are the yield of acetophenone with different MnCl₂ during overexpression. Yellow bar is the yield of acetophenone with GtHNL-H96A overexpressed with 0.1 MnCl₂ plus incubation with 10 molar equivalents of MnCl₂ during 5 hours. Red bars are control reactions with different MnCl₂ concentrations. A control reaction with 0.25 MnCl₂ was not performed. Reaction conditions: 50 mM substrate, 150 mM TBHP, 2 mg GtHNL-H96A, 50 mM sodium phosphate buffer pH 7, 30°C, 1000 rpm. Reaction volume: 1 mL

6.2.2 Reaction optimisation

The reaction was optimised by evaluating different parameters such as *tert*-butyl hydroperoxide (TBHP) concentration, pH, temperature, co-solvents and buffers (Figure 4). Significantly higher yields of acetophenone were reached at concentrations of TBHP higher than 50 mM, i.e. with an excess of TBHP. Additionally, the chemical reaction was slightly accelerated (Figure 4A). GtHNL-H96A did not catalyse the oxidative cleavage of styrenes in absence of TBHP (data not shown). When the reaction was performed in the absence of oxygen the yield of acetophenone decreased to 6.75%. The known decomposition of TBHP into alkoxy radicals and molecular oxygen during the Mn catalytic cycle [18-19] suggests a low oxygen concentration environment while not being strictly anaerobic. This proposes that both TBHP and oxygen are important for the GtHNL-H96A catalysed oxidative cleavage of styrene derivatives.

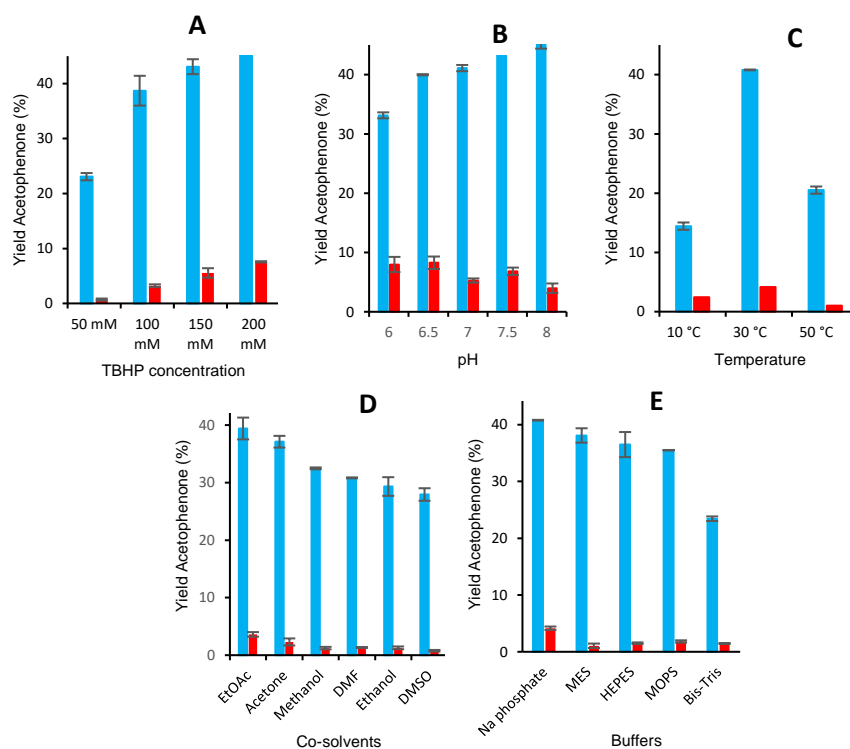


Figure 4. Reaction optimization for the oxidative cleavage of α -methyl styrene catalysed by *GtHNL-H96A*. Solid light blue bars are the enzymatic reactions and red bars are control reactions. A: Influence of different TBHP concentrations. Reaction conditions: 50 mM substrate in ethyl acetate, 50-200 mM TBHP, 2 mg *GtHNL-H96A*, 50 mM sodium phosphate buffer pH 7, 30°C. B: Influence of different pH. Reaction conditions: 50 mM substrate in ethyl acetate, 150 mM TBHP, 2 mg *GtHNL-H96A*, 50 mM sodium phosphate buffer pH 6-8, 30 C. C: Influence of temperatures. Reaction conditions: 50 mM substrate in ethyl acetate, 150 mM TBHP, 2 mg *GtHNL-H96A*, 50 mM sodium phosphate buffer pH 7, 10-50 °C. D: Influence of different co-solvents. Reaction conditions: 50 mM substrate in different co-solvents, 150 mM TBHP, 2 mg *GtHNL-H96A*, 50 mM sodium phosphate buffer pH 7, 30 °C. E: Influence of different buffers. Reaction conditions: 50 mM substrate in ethyl acetate, 150 mM TBHP, 2 mg *GtHNL-H96A*, 50 mM sodium phosphate, MES, HEPES, MOPS or Bis-Tris buffers pH 7, 30 °C. Control reactions were performed with 0.5 mM $MnCl_2$. All reactions were performed in 1 mL reaction volume and shaken at 1000 rpm.

The influence of different pH was evaluated for the synthesis of acetophenone. *GtHNL-H96A* displayed higher yield at slightly basic pH (7-8) (Figure 4B). An earlier report showed that *GtHNL* is active and more stereoselective at low temperatures for the synthesis of (*R*)-mandelonitrile [10-11]. On the other hand, during preliminary experiments *GtHNL-3V* displayed a high thermostability. For this reason, the effect of different temperatures (10, 30 and 50°C) was evaluated. Higher yield of acetophenone was observed at 30°C (Figure 4C). The decrease in conversion observed at 50°C could be explained either by the degradation or evaporation of the substrates or product at this temperature. Indeed, the flash point of TBHP is 38°C. The mass

balance analysis of the reactions showed that it was accomplished only for the reactions performed at 10°C suggesting that higher temperatures induces loss or degradation of substrates or product.

50 mM of α -methyl styrene was dissolved in 5 different co-solvents to evaluate their influence on the synthesis of acetophenone. The reactions were performed with 5% (v/v) of co-solvent. Ethyl acetate and acetone with log P of 0.71 and -0.24 respectively displayed the highest yields of acetophenone (Figure 4D). No clear relation between log P and yield was observed. Special attention must be taken when TBHP is mixed with acetone to avoid explosions. Organic peroxides are known as highly flammable, extremely reactive and toxic. When TBHP is mixed with organic solvents under acidic conditions, a violent decomposition will occur. In addition, the temperature must not exceed 55.6°C to assure safety [20]. Different buffers at 50 mM in the same pK_a range (~7) were used to evaluate their influence on the catalytic activity of GtHNL-H96A (Figure 4E). The highest yield was reached with sodium phosphate buffer pH 7 and an important decrease in yield was observed with Bis-Tris buffer as reaction medium.

6.2.3 Substrate scope

Having established the best reaction conditions for the GtHNL-H96A catalysed oxidative cleavage of α -methyl styrene, the substrate scope was evaluated. GtHNL-H96A was active and chemoselective for the oxidative cleavage of a range of styrene derivatives. Control reactions with 0.5 mM of MnCl₂ showed lower conversions compared to the enzymatic reactions (Table 1). The presence of a methyl group at the α position (1a, 2a and 3a) favoured the oxidative cleavage. The corresponding ketones were formed in yields of 37.7%, 31.8% and 37.1% respectively and identified by Gas Chromatography Mass Spectrum (GC-MS) (Figure 5). The absence of a methyl group at the α -position (5a, 6a, 7a) or location of at β -position (4a) resulted in a drastic decrease in conversion. Electron donating (5a) or withdrawing groups (6a) on the phenyl ring did not further improve the yields. Overall the presence of a methyl group at the alpha position exerted the highest influence on the yields achieved. This suggest that an electron donor on the double bond at the alpha position might stabilise a radical potentially formed during the catalytic cycle. Further details are shown in the reaction mechanism studies. Table 1 shows that aldehydes and ketones are accessible. GtHNL-H96A did not catalyse the oxidative cleavage of aliphatic alkenes.

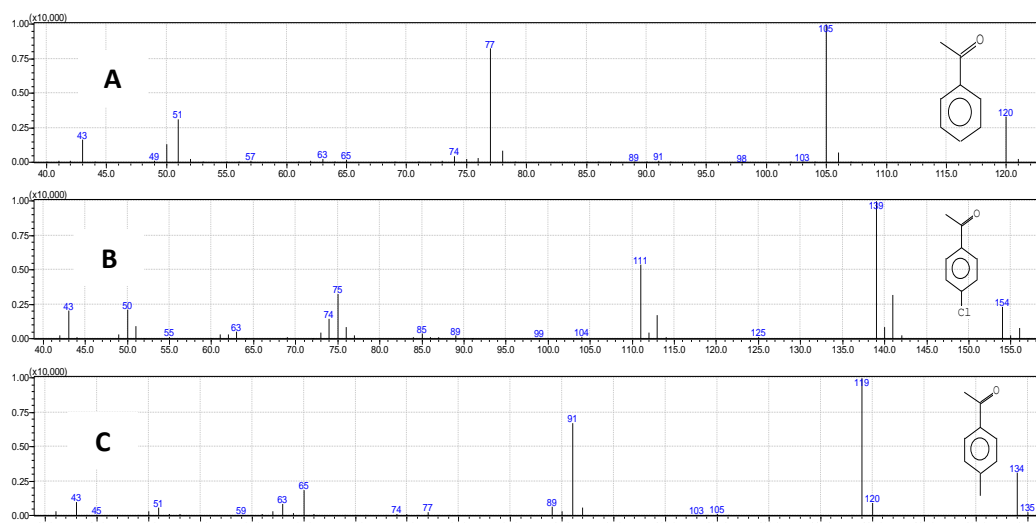
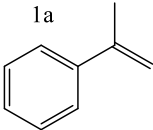
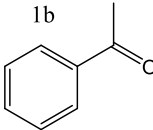
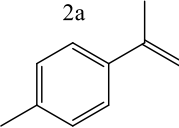
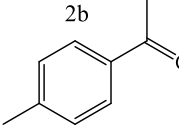
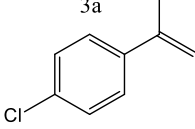
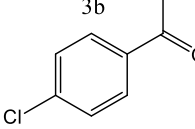
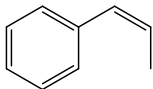
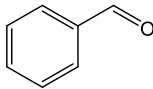
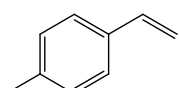
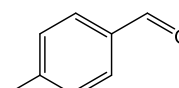
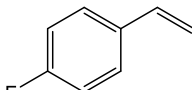
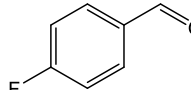
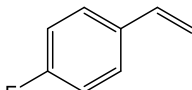
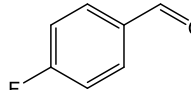
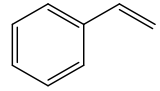
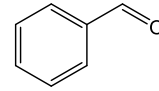
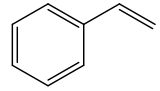
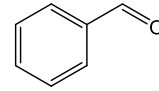
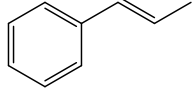
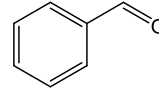
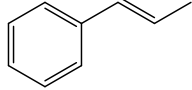
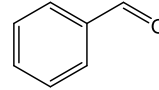


Figure 5: GC-MS chromatograms of acetophenone, 4-Cl-acetophenone and 4-methyl acetophenone of *GtHNL-H96A* catalysed oxidative cleavage of styrene derivatives. A: identification of acetophenone. B: identification of 4-Cl-acetophenone. C: identification of 4-methyl acetophenone.

The data in table 1 shows that the oxidative cleavage product is around 50% of the reacted substrate for most of the styrenes evaluated. Minor products identified by GC-MS during the oxidative cleavage of 1a, 2a and 3a are shown in table 2.

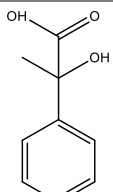
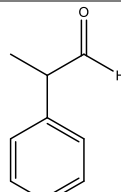
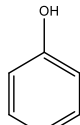
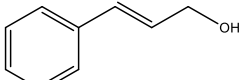
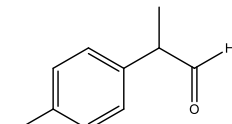
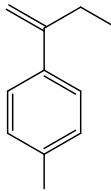
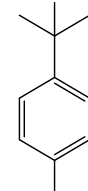
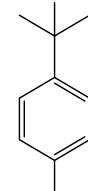
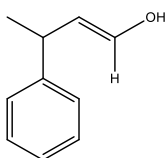
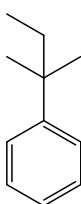
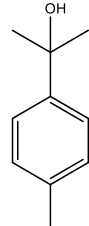
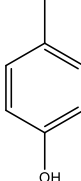
Table 1: Oxidative cleavage of styrene derivatives catalysed by *GtHNL-H96A*

Reaction	Substrate	Product	Substrate Conversion (%) ^a	Product Yield (%) ^b
<i>GtHNL-H96A</i>	1a 	1b 	70.66 ± 3.36	37.7 ± 0.85
Control			32.80 ± 0.53	3.91 ± 0.13
<i>GtHNL-H96A</i>	2a 	2b 	74.32 ± 0.38	31.8 ± 0.7
Control			23.63 ± 1.71	1.3 ± 0.07
<i>GtHNL-H96A</i>	3a 	3b 	64.94 ± 1.86	37.1 ± 0.3
Control			21.27 ± 0.17	8.6 ± 0.2
<i>GtHNL-H96A</i>	4a 	4b 	53.77 ± 7.00	12.3 ± 2
Control			38.17 ± 0.76	0
<i>GtHNL-H96A</i>	5a 	5b 	59.26 ± 3.60	24.4 ± 1.3
Control			30.73 ± 2.80	3.1 ± 0.1

GfHNL-H96A	6a 	6b 	65.58 ± 7.32	25.6 ± 2.47
Control			38.48 ± 7.88	2.3 ± 0.1
GfHNL-H96A	7a 	7b 	61.37 ± 5.19	26.7 ± 1.07
Control			40.44 ± 4.97	1.1 ± 0.09
GfHNL-H96A	8a 	8b 	61.44 ± 3.50	25.9 ± 0.6
Control			27.42 ± 0.43	0

Reaction conditions: 50 mM substrate, 150 mM TBHP, 2 mg GfHNL-H96A, 50 mM sodium phosphate buffer pH 7, 30 °C, 1000 rpm. Control reactions were performed with 0.5 mM MnCl₂. ^aBased on reacted substrate, ^bBased on the product concentration relative to the initial substrate concentration. Reaction time: 16 h. Reaction volume: 1 mL

Table 2: Minor products identified by GC-MS during the oxidative cleavage of 1a, 2a and 3a catalysed by GfHNL-H96A

Substrate	Minor products identified by GC-MS			
1a				
2a				
3a				

6.2.4 Reaction mechanism

Earlier reports have presented that Mn(III) is the active species for the oxidative cleavage of alkenes catalysed by the enzyme *TM1459* [13] or a cell free preparation of *Trametes hirsuta* [21]. Previous electron paramagnetic resonance (EPR) studies have shown that Mn(II) (spin state $S = 5/2$) is the active species in GfHNL and plays a crucial role for the synthesis of chiral cyanohydrins [12]. Therefore, the nature of the

manganese under the influence of TBHP as oxidant during the oxidative cleavage of α -methyl styrene was explored by EPR studies. Figure 6A shows the spectrums of GtHNL-H96A before and after the addition of TBHP and α -methyl styrene in perpendicular mode. Additional low field signals appear after addition of the oxidant which we putatively attribute to Mn(IV) ($S = 3/2$) (Figure 6B). However, the Mn(IV) and Mn(II) signals overlap and are difficult to distinguish.

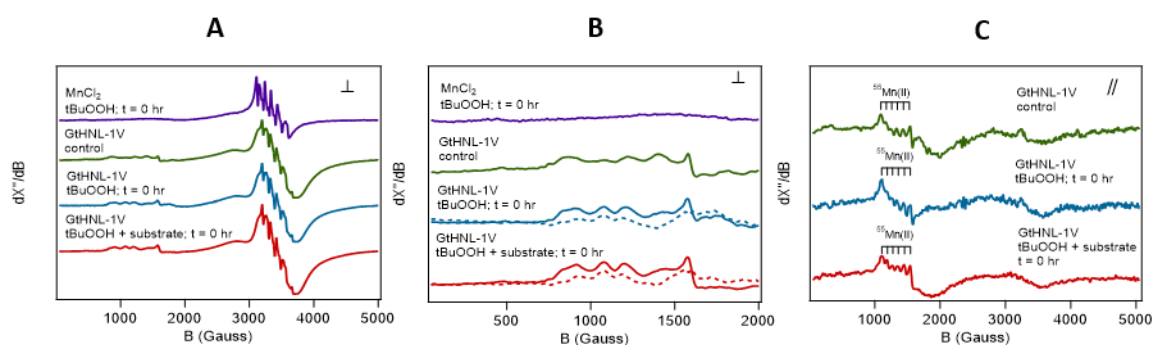


Figure 6: EPR spectrums of GtHNL-H96A. A: Perpendicular mode, B: Perpendicular mode with amplification between 0 and 2000 B (Gauss). Dotted lines give the difference spectrum with the control sample (without tBuOOH) and thereby the putative Mn(IV) and C: parallel mode. EPR conditions: microwave frequency 9.624 GHz (perpendicular mode), 9.295 (parallel mode); microwave power 20 mW; modulation frequency 100 kHz; modulation amplitude 10 G; temperature 12.5 K. Each spectrum was averaged four times (perp mode) or nine times (para mode).

A control reaction using $MnCl_2$ and TBHP as oxidant did not show the low field signals observed with GtHNL-H96A (Figure 6A and 6B). Performing EPR spectroscopy in parallel mode enables the identification of integer spin values such as Mn(III) species (Figure 6C). A spectrum of GtHNL-H96A + TBHP showed the characteristic 6 line pattern for Mn(III) at around 1200 Gauss ($g = 5$). However, the control reaction using GtHNL-H96A without any oxidant showed the same pattern. We therefore attribute this signal to the spin forbidden $m_s = \pm 2$ transition of Mn(II) and not due to Mn(III) (Figure 6C). The EPR studies did not demonstrate the expected oxidation of manganese from Mn(II) to Mn(III) but suggest the possibility of Mn(IV). Organic radicals were not observed in any of the EPR spectra which indicates that these may be too short lived and do not sufficiently accumulate in the samples. However, the best substrates for the oxidative cleavage bear a methyl group at the alpha position which might stabilize the more stable benzyl radical potentially formed after the addition of *tert*-butylperoxy radical. If the reasoning of a radical mechanism is correct, then the addition of a radical scavenger should suppress the reaction. Indeed, this was the

case. One equivalent of a radical scavenger such as butylated hydroxytoluene (BHT) suppressed the reaction and resulted in only 2% yield of acetophenone (Figure 7).

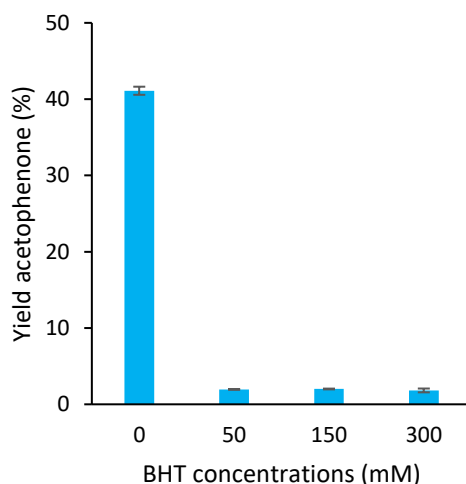


Figure 7: Influence of butylated hydroxytoluene (BHT) as radical scavenger on the synthesis of acetophenone catalysed by *GtHNL-H96A*. Reaction conditions: 50 mM α -methyl styrene, 150 mM TBHP, 2 mg *GtHNL-H96A* (overexpressed with 0.5 mM $MnCl_2$), 50, 150 or 300 mM BHT, 50 mM sodium phosphate buffer pH 7, 30°C, 1000 rpm. Reaction time: 20 h. Reaction volume: 1 mL

Thus, the formation of *tert*-butylperoxy radical is crucial for the enzymatic oxidative cleavage of styrene derivatives catalysed by *GtHNL-H96A*. This supports the radical mechanism of this reaction. The formation of radicals during the catalytic cycle of oxidative enzymatic alkene cleavage is not surprising. Earlier, the formation of alkoxy radicals with the incorporation of two different oxygen atoms from two different oxygen molecules has been reported for the alkene cleavage catalysed by an enzyme preparation of *Trametes hirsuta* [22]. Moreover, radical formation has been reported for the oxidative cleavage of alkenes catalysed by a chloroperoxidase (CPO) from *Caldariomyces fumago* [23] and horseradish peroxidase [23]. Manganese-(II) complexes can activate oxygen, hydrogen peroxide (H_2O_2) or TBHP and have been reported to catalyse the oxidation of cyclohexene. It was observed that the Mn(II) complex is initially oxidised by either H_2O_2 or TBHP to produce a Mn(III) complex which is reduced back to Mn(II) by cyclohexene. The formation of Mn(III) and Mn(IV) complexes was confirmed [25]. The ability of Mn(II) complexes to catalyse the superoxide (O_2^-) disproportionation with the subsequent oxidation of Mn(II) to Mn(III) has been reported [26]. Similarly, many years ago [27] it was demonstrated that O_2^- does oxidise Mn(II) to Mn(III) and also reduce Mn(III) complexes with the consequent cycling of the metal between the divalent and trivalent states. The latter observation

suggests that the alkoxy radical potentially formed during the oxidative cleavage of styrene derivatives allows the oxidation/reduction of Mn(II)/Mn(III).

Synthesis reactions of (*R*)-mandelonitrile were performed to evaluate if GtHNL-H96A, GtHNL-H96F and GtHNL-4V switch their natural cyanogenesis activity to a peroxidase-like enzyme or the oxidative cleavage activity was added to its natural activity. The three variants maintained their natural activity. GtHNL-H96A displayed a conversion of 47% \pm 0.008 (*ee* = 19%). GtHNL-4V and GtHNL-H96F showed almost full conversion (98%) but their enantioselectivities were 98% and 2.6% respectively. The excellent enantioselectivity observed for GtHNL-4V is not surprising since the former GtHNL-3V is an excellent enzyme for the synthesis of chiral cyanohydrins [10-11]. The improved deprotonation of hydrogen cyanide facilitated by additional histidines, a narrower active site and tightly bound manganese can explain this result.

This indicates that the introduction of the mutation H96A enables a new activity to GtHNL. Another remarkable example where one single amino acid substitution allowed promiscuous activity was reported earlier [28]. An esterase from *Burkholderia gladiolis* with significant homology to HNLs from *Hevea brasiliensis* and *Manihot esculenta* was converted to an HNL-like enzyme by introducing the single mutation S276L. The introduced positively charged amino acid is necessary for the stabilization of the negatively charged cyanide ion. 70% conversion was achieved for the synthesis of mandelonitrile with poor enantioselectivity (value not reported). Recently, the promiscuous esterase activity of an ancestral hydroxynitrile lyase (HNL1) from the α/β -hydrolase-fold has been reported [17]. In this case, three amino acid substitutions (Thr11Gly, Lys236Gly, Glu79His) were introduced to HNL1. The analysis of the X-ray crystal structure of this ancestral enzyme variant revealed a larger and more flexible active site compared to the modern *Hevea brasiliensis* HNL.

6.3 Conclusions

The oxidative cleavage of styrenes, a new non-natural activity for hydroxynitrile lyases was introduced in GtHNL. 41% of acetophenone was reached after 20 hours of reaction time by using GtHNL-H96A. The enzyme catalysed the oxidative cleavage of several styrenes derivatives with yields ranging from 12% to 37% after 16 hours of reaction time. EPR studies did not show the oxidation of Mn(II) to Mn(III). The reaction

mechanism remains unknown. However, a radical mechanism involving at least a Mn(IV) as the active species is probable.

The development of new biocatalysts by changing or adding new activities in former enzymes is a fascinating idea. Using this approach, new and better biocatalysts will be developed and used for inefficient or challenging reactions contributing to the further development of biocatalysis.

6.4 Experimental section

6.4.1 Chemicals

All chemicals were bought from Sigma Aldrich (Schnelldorf, Germany) unless reported otherwise.

6.4.2 Cloning and heterologous production of GtHNL-H96A and GtHNL-H96F

pET28a(+)-GtHNL expression plasmids containing GtHNL-H96A genes codon optimized for *E. coli* were ordered to Bio Basic (Canada). Then, *E. coli* BL21(DE3) was transformed with the expression plasmids for the overexpression of GtHNL-H96A and sequenced (Table 3).

Table 3: Sequencing results of GtHNL- H96A

>template – GtHNL-WT	GtHNL-H96A
MEIKRVGSQASGKGPADWFTGTVRIDP	MEIKRVGSQASGKGPADWFTGTVRIDP
LFQAPDPALVAGASVTFEPGARTAWHT	LFQAPDPALVAGASVTFEPGARTAWHT
HPLGQTLIVTAGCGWAQREGGAVEEIH	HPLGQTLIVTAGCGWAQREGGAVEEIH
PGDVVWFSPGEKHW H GAAPTTAMTHLA	PGDVVWFSPGEKHW A GAAPTTAMTHLA
IQERLDGKAVDWMEHVTDEQYRRA	IQERLDGKAVDWMEHVTDEQYRR

For the heterologous production of both enzymes, a preculture was prepared by inoculating one single colony of *E. coli* BL21(DE3)-pET28aGtHNL-H96A in 10 mL of Lysogeny Broth (LB) medium with kanamycin (50 µg/mL) and incubated overnight (New Brunswick Scientific Incubator Shaker Excella E24 Series) at 37°C, 120 rpm. Subsequently, this precultures were used for the inoculation of 1 L of TB medium containing kanamycin (50 µg/mL) and incubated at 37°C, 120 rpm. When the OD₆₀₀ reached 0.6 – 0.8 the gene expression was induced by adding 1 mL of 0.1 M isopropyl β-D-thiogalactoside (IPTG) per liter of culture (0.1 mM IPTG final concentration). Moreover, 100-1000 µL of 1 M MnCl₂ was added per liter of culture at the induction

time (0.1 - 1 mM Mn(II) final concentration) and cultivation was continued at 25°C, 120 rpm for 20 hours. Cells were harvested at 4°C, 5000 rpm during 20 minutes (Sorvall RC6, Thermo Scientific). The supernatant was discarded and the pellets were washed with 30 mL of 50 mM sodium phosphate buffer pH 7, frozen in liquid nitrogen and stored at -80°C. Identical methodology was followed for the cloning and production of GtHNL-H96F.

6.4.3 Cloning and heterologous production of GtHNL-A40H/V42T/Q110H/H96A (GtHNL-4V)

pET28a(+)-GtHNL-A40H/V42T/Q110H was used as template for the cloning of GtHNL-4V. The mutation H96A was introduced by overlap-extension PCR. GtHNL-4V gene was cloned into pET28a expression vector using NcoI and HindIII restriction enzymes. The resulting pET28a-GtHNL-4V expression vector was cloned into *E. coli* TOP 10 and sequenced to ensure the successful introduction of the H96A mutation (Table 4). Finally, the expression host *E. coli* BL21(DE3) was transformed with pET28a(+)-GtHNL-4V for the overexpression of the GtHNL-4V enzyme. The heterologous production and harvesting of GtHNL-4V followed the same methodology described for GtHNL-H96A.

Table 4: Sequencing results of GtHNL- 4V

>template – GtHNL- A40H/V42T/Q110H	>sample_ GtHNL-4V
MEIKRVGSQASGKGPADWFTGTVRIDPLFQ APDPALVAGHS ^T TFEPGARTAWHTHPLGQT LIVTAGCGWAQREGGAVEEIH ^P GDVVWFSP GEKHW ^H GAAPTTAMTHLAI ^H ERLDGKAVDW MEHVTDEQYRR	MEIKRVGSQASGKGPADWFTGTVRIDPLFQ APDPALVAGHS ^T TFEPGARTAWHTHPLGQT LIVTAGCGWAQREGGAVEEIH ^P GDVVWFSP GEKHW ^A GAAPTTAMTHLAI ^H ERLDGKAVDW MEHVTDEQYRR

6.4.4 Purification of GtHNL-H96A, GtHNL-H96F and GtHNL-4V

The pellets of GtHNL-H96A, GtHNL-H96F and GtHNL-4V were resuspended in lysis buffer (50 mM sodium phosphate buffer + DNase) pH 7 and lysed in a cell disruptor (Constant Systems Ltd., United Kingdom) at 20 kPSI and 4°C to avoid protein denaturation. The cell free extract (CFE) was collected as the supernatant after centrifugation at 4500 g, 30 min, 4°C, heated during 30 min at 65°C, and centrifuged during 15 min at 4500 g. The purified enzyme was obtained as the supernatant. For the EPR studies, GtHNL-H96A was further purified by anion exchange

chromatography with Q Sepharose Fast Flow columns (HiTrap Q FF, 70 mL; GE Healthcare, Uppsala, Sweden) [11]. 50 mM Bis-Tris buffer + 30 mM NaCl, pH 7.2 (buffer A) and 50 mM Bis-Tris buffer + 1 M NaCl, pH 7.2 (buffer B) were used as binding and elution buffers respectively. An isocratic step of 10% buffer B allowed the elution of pure GtHNL-H96A.

6.4.5 Alkene cleavage reactions

The reactions were performed in a biphasic system in 2 mL plastic reaction tubes in accordance with an earlier report [13] with slight modifications. 50 μ L of 1 M substrate in ethyl acetate or other (50 mM final concentration) and 50 μ L of 3 M TBHP in n-Decane (150 mM final concentration) were supplemented with 2 mg of GtHNL-H96A, GtHNL-H96F or GtHNL-4V enzyme and 50 mM sodium phosphate buffer pH 7. As result, the final reaction volume was 1 mL. A thermomixer was used to shake the reaction tubes at 1000 rpm and to maintain 30°C. A small amount of sodium bisulfite (*circa* 50 – 70 mg) was used to quench the reactions. Later on, it was noticed a negative impact of quenching on the product yield. Therefore, this step was omitted. The product was extracted twice with ethyl acetate spiked with 10 mM n-Dodecane as internal standard (1x350 μ L and 1x500 μ L). The combined organic phases were dried using anhydrous MgSO₄ and injected for gas chromatography (GC) analysis.

6.4.6 Concentration of tert-butyl hydroperoxide (TBHP)

The concentration of TBHP was determined by iodometric titration with thiosulfate in accordance with the literature [29]. Briefly, 100 μ L of TBHP were dissolved in 10 mL acetic acid:chloroform (3:2) and nitrogen was sparged through the solution for 2 minutes to remove oxygen. 500 μ L of saturated potassium iodide solution were added and the head space was flushed with nitrogen for 1 minute. Then, 15 mL of distilled water (sparged with nitrogen) and 4 drops of 1% starch (indicator) were added to produce a noticeable purple color. The sample was titrated with 0.01 N sodium thiosulfate until the purple color disappeared.

6.4.7 Inductively Couple Plasma Optical Emission Spectrometry (ICP-OES)

0.5 mg of sample were destructed in 4.5 ml milliQ water +1.5 ml 65% HNO₃ using a microwave PRO during 60 minutes at maximum power. Then, the samples were analysed with ICP-OES (Perkin Elmer Optima 5300 DV).

6.4.8 Electron paramagnetic resonance (EPR) studies

EPR spectra were recorded on a Bruker EMXplus spectrometer using a dual-mode resonator (Bruker ER 4116DM) with a helium-flow cryostat [30–31] using the following EPR parameters: microwave frequency 9.624 GHz (perpendicular mode), 9.295 GHz (parallel mode); microwave power 20 mW; modulation frequency 100 kHz; modulation amplitude 10 Gauss; temperature 12.5 K. Perpendicular mode spectra were 4 times averaged, parallel mode spectra were 9 times averaged.

6.4.9 Analysis

Gas chromatography (GC) analysis were performed on a GC-2014 (Shimadzu) equipped with a AOC-20i auto injector by using a N₂ as carrier gas, a cp wax 52 CB column (length: 50 m, I.D: 0.53 mm, film thickness: 2 μm, max temp: 250 °C) and a FID detector. Table 5 shows the temperature profile used:

Table 5: Temperature profile

Rate (°C/min)	Temperature °C	Time (min)
---	100	3
20	From 100 to 245	7.25
---	245	1

References

1. Rajagopalan, A.; Lara, M.; Kroutil, W. Oxidative Alkene Cleavage by Chemical and Enzymatic Methods. *Adv. Synth. Catal.* **2013**, 355, 3321 – 3335. DOI: 10.1002/adsc.201300882
2. Lara, M.; Mutti, F. G.; Glueck, S. M.; Kroutil, Biocatalytic Cleavage of Alkenes with O₂ and *Trametes hirsuta* G FCC 047. *Eur. J. Org. Chem.*, **2008**, 3668–3672. DOI: 10.1002/ejoc.200800261
3. Wu, S.; Zhou, Yi.; Li, Zhi. Biocatalytic selective functionalisation of alkenes via single-step and one-pot multi-step reactions. *Chem. Commun.*, **2019**, 55, 883—896. DOI: 10.1039/c8cc07828a
4. Mutti, F. G. Alkene Cleavage Catalysed by Heme and Nonheme Enzymes: Reaction Mechanisms and Biocatalytic Applications. *Bioinorg Chem Appl.* **2012**, 2012:626909. DOI:10.1155/2012/626909

5. Mang, H.; Gross, J.; Lara, M.; Goessler, C.; Schoemaker, H. E.; Guebitz G. M.; Kroutil, W. Optimization of a biocatalytic single-step alkene cleavage of aryl alkenes. *Tetrahedron*, **2007**, 63, 3350–3354. DOI: 10.1016/j.tet.2007.02.034
6. Paul, C. E.; Rajagopalan, A.; Lavandera, I.; Gotor-Fernández, V.; Kroutil, W.; Gotor, V. Expanding the regioselective enzymatic repertoire: oxidative mono-cleavage of dialkenes catalyzed by *Trametes hirsuta*. *Chem. Commun.*, **2012**, 48, 3303–3305. DOI: 10.1039/c2cc17572j
7. Bougioukou, D. J.; Smonou, I. Chloroperoxidase-catalyzed oxidation of conjugated dienoic esters. *Tetrahedron Letters*, **2002**, 43, 339–342.
8. Tuynman, A.; Spelberg, J. L.; Kooter I. M.; Schoemaker H. E.; Wever, R. Enantioselective Epoxidation and Carbon–Carbon Bond Cleavage Catalyzed by *Coprinus cinereus* Peroxidase and Myeloperoxidase. *The journal of biological chemistry*, **2000**, 275 (5), 3025–3030.
9. Hajnal, I.; Lyskowski, A.; Hanefeld, U.; Gruber, K.; Schwab, H.; Steiner, K. *FEBS Journal*, **2013**, 280, 5815–5828. DOI:10.1111/febs.12501.
10. Wiedner, R.; Kothbauer, B.; Pavkov-Keller, T.; Gruber-Khadjawi, M.; Gruber, K.; Schwab, H.; Steiner K. *ChemCatChem*, **2015**, 7, 325 – 332. DOI: 10.1002/cctc.201402742.
11. Coloma, J.; Guiavarc'h, Y.; Hagedoorn, P.L.; Hanefeld, U. Probing batch and continuous flow reactions in organic solvents: *Granulicella tundricola* hydroxynitrile lyase (GtHNL). *Catalysis Science & Technology*, **2020**, 10, 3613–3621. DOI: 10.1039/d0cy00604a.
12. Vertregt, F.; Torrelo, G.; Trunk, S.; Wiltsche, W.; Hagen, W.R.; Hanefeld U.; K. Steiner. *ACS Catal.*, **2016**, 6, 5081–5085. DOI: 10.1021/acscatal.6b01204.
13. Hajnal, I.; Faber, K.; Schwab, H.; Hall, M.; Steiner, K. Oxidative Alkene Cleavage Catalysed by Manganese-Dependent Cupin TM1459 from *Thermotoga maritima*. *Adv. Synth. Catal.* **2015**, 357, 3309 –3316. DOI: 10.1002/adsc.201500608.

14. Fink, M.; Trunk, S.; Hall, M.; Schwab, H.; Steiner, K. Engineering of TM1459 from *Thermotoga maritima* for Increased Oxidative Alkene Cleavage Activity. *Front. Microbiol.*, **2016**, 7:1511. DOI: 10.3389/fmicb.2016.01511.
15. Smith, J. M. Natural Selection and the Concept of a Protein Space. *Nature*, 1970, 225, 563-564.
16. Otten, L. G.; Hollmann, F.; Arends, I. W. C. E. Enzyme engineering for enantioselectivity: from trial-and-error to rational design. *Trends Biotechnol.*, 2010, 28(1), 46-54. DOI:10.1016/j.tibtech.2009.10.001.
17. Jones, B. J.; Evans, R. L.; Mylrea, N. J.; Chaudhury, D.; Luo, C.; Guan, B.; Pierce, C. T.; Gordon, W. R.; Wilmot, C. M.; Kazlauskas, R. J. Larger active site in an ancestral hydroxynitrile lyases increases catalytically promiscuous esterase activity. *PLoS ONE*, 2020, 15(6): e0235341. DOI: 10.1371/journal.pone.0235341
18. Hiatt, R.; Clipsham, J.; Visser, T. The induced decomposition of *tert*-butyl hydroperoxide. *Can. J. Chem.*, **1964**, 42, 2754-2757.
19. Qi, L.; Qi, X.; Wang, L.; Feng, L.; Lu, S. Decomposition of *tert*-butyl hydroperoxide into *tert*-butyl alcohol and O₂ catalyzed by birnessite-type manganese oxides: Kinetics and activity. *Catalysis Communications*, **2014**, 49, 6–9. DOI: 10.1016/j.catcom.2014.01.028
20. Huiping, L.; Lanyun, G.; Peng, Z.; Zhangrui, L.; Bo, Z.. Evaluation on thermal hazard of *ter*-butyl hydroperoxide by using accelerating rate calorimeter. *Procedia Engineering*, **2012**, 45, 574 – 579. DOI: 10.1016/j.proeng.2012.08.206
21. Rajagopalan, A.; Schober, M.; Emmerstorfer, A.; Hammerer, L.; Migglautsch, A.; Seisser, B.; Glueck, S. M.; Niehaus, F.; Eck, J.; Pichler, H.; Gruber, K.; Kroutil, W. Enzymatic aerobic alkene cleavage catalyzed by a Mn³⁺-dependent Proteinase A homologue. *ChemBioChem*, **2013**, 14, 2427 – 2430. DOI: 10.1002/cbic.201300601

22. Lara, M.; Mutti, F. G.; Glueck, S. M.; Kroutil, W. Oxidative Enzymatic Alkene Cleavage: Indications for a Nonclassical Enzyme Mechanism. *J. Am. Chem. Soc.*, **2009**, 131, 5368–5369. DOI: 10.1021/ja8097096 CCC
23. Charnulitrat, W.; Takahashi, N.; Mason, R. P. Peroxyl, Alkoxy, and Carbon-centered Radical Formation from Organic Hydroperoxides by Chloroperoxidase. *The Journal of Biological Chemistry*, **1989**, 264, 14, 7889-7899.
24. Ortiz de Montellano, P. R.; Grab, L. A. Cooxidation of Styrene by Horseradish Peroxidase and Phenols: A Biochemical Model for Protein-Mediated Cooxidation. *Biochemistry*, **1987**, 26, 5310-5314.
25. Rydel-Ciszek, K. Charczuk, M.; Paczes´niak, T.; Chmielarz, P. Manganese(II) complexes with Bn-tpen as powerful catalysts of cyclohexene oxidation. *Chem. Pap.*, **2017**, 71, 2085–2093. DOI 10.1007/s11696-017-0201-0
26. Barnese, K.; Gralla, E. B.; Valentine, J. S.; and Cabelli, D. E. Biologically relevant mechanism for catalytic superoxide removal by simple manganese compounds. *PNAS*, 2012, 109 (18).
27. Archibald, F. S.; Fridovich, I. The scavenging of superoxide radical by manganous complexes: *In Vitro*. *Archives of Biochemistry and Biophysics*. **1982**, 214 (2), 452-463
28. Steiner, K.; Glieder, A.; Gruber-Khadjawi, M. In *Biocatalysis in Organic Synthesis 2* (Eds.: K. Faber, W.-D. Fessner, N. J. Turner), Thieme, Stuttgart, 2015, Chapter 2.1.1.
29. AOAC official method 41.1.16. Peroxide value of oils and fats. Official method of Analysis of AOAC International, 16th edn., AOAC International, Gaithersburg, 1997.
30. Salmeen, I.; Palmer, G. Electron Paramagnetic Resonance of Beef-Heart Ferricytochrome. *C. J. Chem. Phys.* **1968**, 48 (5), 2049-52.
31. Lundin, A.; Aasa, R. A Simple Device to Maintain Temperatures in the Range 4.2–100 K for EPR Measurements. *J. Magn. Reson.* **1972**, 8 (1), 70-73.

Supplementary information

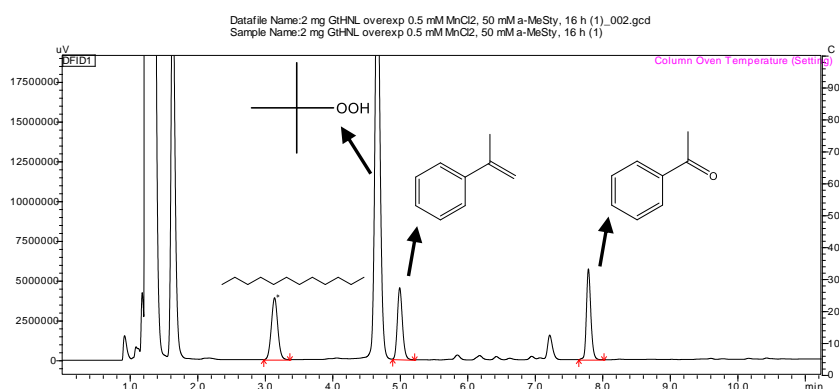


Figure S1. GC detection of dodecane (internal standard), *tert*-butyl hydroperoxide, α -methyl styrene and acetophenone. 50 mM α -methyl styrene, 150 mM *tert*-butyl hydroperoxide (TBHP), 2 mg GtHNL-H96A, 50 mM sodium phosphate buffer pH 7, 30°C, 1000 rpm. Reaction volume: 1 mL

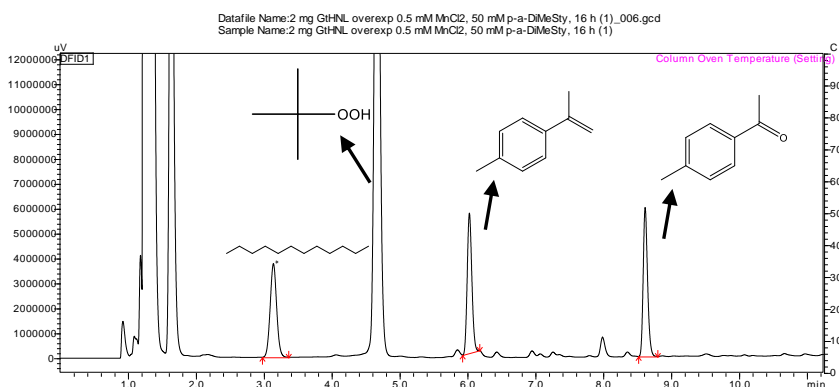


Figure S2. GC detection of dodecane (internal standard), *tert*-butyl hydroperoxide, p- α -dimethyl styrene and p-acetophenone. 50 mM p- α -dimethyl styrene, 150 mM *tert*-butyl hydroperoxide (TBHP), 2 mg GtHNL-H96A, 50 mM sodium phosphate buffer pH 7, 30°C, 1000 rpm. Reaction volume: 1 mL

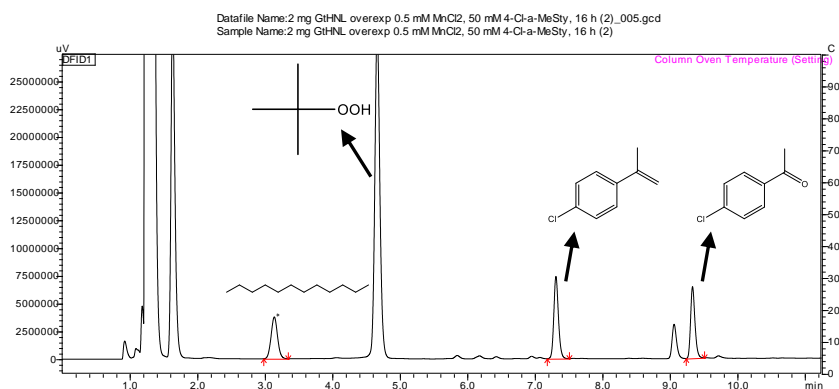


Figure S3. GC detection of dodecane (internal standard), *tert*-butyl hydroperoxide, 4-Cl- α -methyl styrene and 4-Cl-acetophenone. 50 mM 4-Cl- α -methyl styrene, 150 mM *tert*-butyl hydroperoxide (TBHP), 2 mg GtHNL-H96A, 50 mM sodium phosphate buffer pH 7, 30°C, 1000 rpm. Reaction volume: 1 mL

7

Conclusion and Outlook

This thesis was aimed to explore the use of flow biocatalysis and enzyme immobilisation as valuable tools for high productivity and stability in biocatalysis. The improved hydroxynitrile lyase (HNL) from *Granulicella tundricola* (GtHNL-A40H/V42T/Q110H) was immobilised on Celite R-633 by adsorption. It was active, stable and enantioselective for the synthesis of (*R*)-mandelonitrile in batch and continuous flow systems. Moreover, significant process intensification, reduced volume and safer process conditions were achieved in flow. The use of buffer saturated organic solvent as reaction medium allowed high substrate loading (500 mM) and suppressed the racemic background reaction efficiently. In a similar fashion, the acid-sensitive HNL from *Arabidopsis thaliana* (AtHNL) was immobilised on EziG Opal, a controlled porosity glass material with non-toxic Fe³⁺ on the carrier surface. High activity, enantioselectivity and stability were observed in batch and flow systems. Likewise, the continuous flow system achieved higher productivity compared to the batch system. These two examples highlight the potential of flow biocatalysis and immobilisation for the synthesis of chiral cyanohydrins. Moreover, immobilised enzymes in buffer saturated organic solvents as reaction medium are able to perform as well as in an aqueous system, at least these systems.

The promiscuous catalytic activity of GtHNL allows the synthesis of chiral β -nitro alcohols using nitromethane as nucleophile. This is possible due to the similar pKa values of hydrogen cyanide and nitromethane. GtHNL-3V was immobilised on Celite R-633 and evaluated for the synthesis of (*R*)-2-nitro-1-phenylethanol (NPE) in batch and flow systems. Surprisingly, if the enzyme was dried after immobilisation (as for the cyanohydrin synthesis), the synthesis of (*R*)-NPE dropped from 80% to 42% after 24 hours of reaction time. Unexpectedly, the flow system did not allow process intensification even using low flow rates (0.01 mL min⁻¹). This can be explained by the addition of nitromethane in high concentration changed the polarity of the reaction mixture due to its low log *P* of -0.24. Thus, the water entrapped in celite-GtHNL-3V diffused into the reaction mixture. This changed the water activity in celite-GtHNL-3V with its consequent deactivation. The development of a 50/50% biphasic system resulted in higher yield during the first 30 minutes but the system was not stable over time. The leaching of the enzyme in the biphasic system may explain the instability. In general, the HNL catalysed synthesis of β -nitro alcohols requires more water for optimal enzymatic activity. A potential solution can be the development of a continuous

biphasic system to keep the enzyme constantly hydrated. For this, the enzyme has to be immobilised by a different method where the enzyme is bound more tightly to the carrier (i.e covalent immobilisation).

A new non-natural activity for HNLs was introduced into *Gt*HNL. The mutation H96A opened an additional binding site of the substrate to the catalytic manganese cofactor and created more space in the active site in *Gt*HNL. Remarkably, this enabled the oxidative cleavage of a range of styrene derivatives. Electron paramagnetic resonance (EPR) studies did not provide evidence of a Mn(III) species that was anticipated. The reaction was suppressed in the presence of a radical scavenger. This suggests a radical mechanism for this reaction. The introduction of this novel activity in *Gt*HNL represents a starting point for its further improvement and shows the potential of protein engineering and rational design for the exploration and development of new biocatalysts.

In conclusion, this thesis was dedicated to demonstrate the potential of flow biocatalysis and immobilisation to achieve process intensification, straightforward reuse of the biocatalyst and high enzyme stability. Moreover, the use of buffer saturated organic solvent as reaction medium allowed high substrate loading and facilitates the downstream processing. The successful implementation of flow biocatalysis is dependent of the properties of the immobilised enzyme and its interaction with the reaction medium. The continuous application of these techniques will help to develop more efficient, safe and environmentally friendly processes for the synthesis of valuable pharmaceutical and chemical products.

8

Acknowledgements

My doctoral studies and also my time in The Netherlands are coming to their end. This has been an extraordinary experience. It has transformed me as a scientist but also as a person. I met many people during this journey and now I would like to express my gratitude for them.

I am profoundly grateful to my promotor Prof. Dr. Ulf Hanefeld for giving me the opportunity to join his research group. I recognise you as a true scientist who guided me over the years. Thanks for sharing your knowledge and specially for being always honest, positive, respectful and supportive.

My sincere thanks to my daily supervisor Dr. ir. Peter-Leon Hagedoorn for your insightful comments, corrections and suggestions during my research. You greatly contributed to improve the quality of our manuscripts. Thanks for finding the time to help me.

I would like to thank to Dr. Yann Guiavarc'h. I was very lucky that you chose TUDelft for your sabbatic year. You spent a lot of time helping me during my initial weeks or months when I was introduced to the project and the lab techniques. I really appreciate your patience and willingness to help me when I needed it the most.

Special thanks to my office mates Luuk, Fabio, Eman, Natalia, Hanna and Stefan. I enjoyed sharing the office and lunches with you. You were always very kind sharing your knowledge and expertise in biocatalysis. It was a real pleasure to share the office with you. Jisk van der Meer and Wouter Kools, thanks for translating the summary and propositions from English to Dutch for me.

My sincere thanks to the team of technicians. Lloyd, Marc, Laura, Remco and Stephen, thanks for being always ready to help me when it was needed.

Special thanks to Mieke van der Kooij for helping me with all the paperwork during the last 4 years.

Furthermore, a special thank to all my students Muhammad, Tim L, Suzanne, Tim W, Lidwien, Jens, Annemiek, Merle, Niva and Linn. I had the privilege of supervising your bachelor or master projects. I learnt a lot from you. Your enthusiasm and hard work is really appreciated. Thank you.

I would also like to thank the Secretary of Higher Education, Science and Technology from Ecuador for funding this research. The support of the Lay University Eloy Alfaro of Manabi is also acknowledged.

Lastly, I want to thank the most important persons in my life, my beloved wife and sons. Karina, thanks for leaving your comfort zone in Ecuador and starting this new adventure together. You believed in me even when I was doubting about my own capabilities. Thanks for being the best wife I can have and being with me always. Matias and Jorgito, my two wonderful big boys, I am sure you will never forget these years in The Netherlands. Thanks for being very brave during your first months in a new school, new language, new culture, etc. I am very proud of you. Finally, my little boy Jose Adrian. I did not know that my life could be better until you came to my life. Thanks for making me happier.

9

***Curriculum vitae* and list of publications**

Curriculum vitae

Name: Jose Luis Coloma Hurel
Date of Birth: 06.10.1981
Place of Birth: Guayaquil, Ecuador



Education

05/2000 – 02/2005 **Food Engineer**
Escuela Superior Politecnica del Litoral, Ecuador
10/2012 – 09/2014 **Master Programme in Food Processing**
Universidad Agraria del Ecuador, Ecuador
06/2018 – 06/2022 **PhD candidate**
Institute of Biotechnology, Delft University of Technology,
The Netherlands

List of publications

1. 'Probing batch and continuous flow reactions in organic solvents: *Granulicella tundricola* hydroxynitrile lyase (GtHNL)'
Coloma, J.; Guiavarc'h, Y.; Hagedoorn, P. L.; and Hanefeld, U. *Catal. Sci. Technol.*, **2020**, 10, 3613–3621. DOI: 10.1039/d0cy00604a
2. 'Immobilisation of *Arabidopsis thaliana* hydroxynitrile lyase (AtHNL) on EziG Opal'
Coloma, J.; Lugtenburg, T.; Afendi, M.; Lazzarotto, M., Bracco, P.; Hagedoorn, P. L.; Gardossi, L.; and Hanefeld. U. *Catalysts*, **2020**, 10, 899. DOI:10.3390/catal10080899
3. 'Immobilisation and flow chemistry: tools for implementing biocatalysis'
Coloma, J.; Guiavarc'h, Y.; Hagedoorn, P. L.; and Hanefeld, U. *Chem. Commun.*, **2021**, 57, 11416–11428. DOI: 10.1039/d1cc04315c
4. 'Batch and flow nitroaldol synthesis catalysed by *Granulicella tundricola* hydroxynitrile lyase immobilised on Celite R-633'
Coloma, J., Teeuwisse, L.; Afendi, M.; Hagedoorn, P. L.; and Hanefeld, U. *Catalysts*, **2022**, 12, 161. DOI:10.3390/catal12020161
5. 'Continuous flow for enantioselective cyanohydrin synthesis'
Stradomska, D.; **Coloma, J.**; Hanefeld, U.; Szymańska, K. *Catal. Sci. Technol.*, **2022**. DOI: 10.1039/d2cy00054g